LEABHARLANN CHOLÁISTE NA TRÍONÓIDE, BAILE ÁTHA CLIATH | TRINITY COLLEGE LIBRARY DUBLIN
Ollscoil Átha Cliath | The University of Dublin

Terms and Conditions of Use of Digitised Theses from Trinity College Library Dublin

Copyright statement

All material supplied by Trinity College Library is protected by copyright (under the Copyright and Related Rights Act, 2000 as amended) and other relevant Intellectual Property Rights. By accessing and using a Digitised Thesis from Trinity College Library you acknowledge that all Intellectual Property Rights in any Works supplied are the sole and exclusive property of the copyright and/or other IPR holder. Specific copyright holders may not be explicitly identified. Use of materials from other sources within a thesis should not be construed as a claim over them.

A non-exclusive, non-transferable licence is hereby granted to those using or reproducing, in whole or in part, the material for valid purposes, providing the copyright owners are acknowledged using the normal conventions. Where specific permission to use material is required, this is identified and such permission must be sought from the copyright holder or agency cited.

Liability statement

By using a Digitised Thesis, I accept that Trinity College Dublin bears no legal responsibility for the accuracy, legality or comprehensiveness of materials contained within the thesis, and that Trinity College Dublin accepts no liability for indirect, consequential, or incidental, damages or losses arising from use of the thesis for whatever reason. Information located in a thesis may be subject to specific use constraints, details of which may not be explicitly described. It is the responsibility of potential and actual users to be aware of such constraints and to abide by them. By making use of material from a digitised thesis, you accept these copyright and disclaimer provisions. Where it is brought to the attention of Trinity College Library that there may be a breach of copyright or other restraint, it is the policy to withdraw or take down access to a thesis while the issue is being resolved.

Access Agreement

By using a Digitised Thesis from Trinity College Library you are bound by the following Terms & Conditions. Please read them carefully.

I have read and I understand the following statement: All material supplied via a Digitised Thesis from Trinity College Library is protected by copyright and other intellectual property rights, and duplication or sale of all or part of any of a thesis is not permitted, except that material may be duplicated by you for your research use or for educational purposes in electronic or print form providing the copyright owners are acknowledged using the normal conventions. You must obtain permission for any other use. Electronic or print copies may not be offered, whether for sale or otherwise to anyone. This copy has been supplied on the understanding that it is copyright material and that no quotation from the thesis may be published without proper acknowledgement.

Trinity College/ University of Dublin

School of Natural Sciences

Zoology Department

Expression Analysis of Inhibitor of Apoptosis Proteins (IAPs) and Caspases in Chick (*Gallus gallus*) Neural Retina Embryonic Development

Aisha Abdullah Alrofidi

Thesis submitted to Trinity College/ University of Dublin

as a partial fulfilment for the degree of

Doctor in Philosophy (Ph.D.)

2016

Supervisor

Dr. Michael A. Wride

External Examiner

Prof. Thomas Cotter

(University College Cork)

Internal Examiner

Dr. Paula Murphy

TRINITY LIBRARY
27 JUL 2016
DUBLIN
Thesis 11004

Declaration

I declare that this thesis is submitted by the undersigned for the degree of Doctor in Philosophy at the University of Dublin, Trinity College Dublin and had not been submitted to any other as an exercise for a degree and it is entirely my own work.

I agree to deposit this thesis in the University's open access institutional repository or allow the library to do so on my behalf, subject to Irish copyright legislation and Trinity College Library conditions of use and acknowledgment

I Summary

Programmed cell death occurs naturally in developing neural tissues to regulate cell population, neural circuit connection and refined tissue structure. Caspases and inhibitor of apoptosis proteins (IAPs) are believed to contribute to the regulation of developmental cell death mechanisms by activating or inhibiting apoptosis. The molecular mechanism of apoptosis is still largely unidentified. This work aimed to characterise the temporal and spatial patterns of expression for all known embryonic chicken (*Gallus gallus*) IAP and caspase genes in the developing neural retina at both transcript and protein levels. In the developing retina of a chick embryo, two waves of cell death were reported by earlier studies between E4 and E16; early and late. Ten developmental stages ranging for early (embryonic day (E4) to late stage (E16) were investigated. Gene expression analysis was performed using PCR techniques. Subsequently, Western blotting (WB) and ELISA were used for investigation of protein temporal and spatial expression.

Relative gene expression data for all chicken known chicken IAPs (five) and caspases (ten) genes using PCR techniques. Whereas for the protein expression study, only two IAP (Birc-4 (XIAP) and Birc-5 (Survivin)) and two caspase (Casp-3 and Casp-7) were analysed based on their transcript-level data where these four factors showed patterns that corresponded to waves of apoptotic cell death in the developing retina, reported in previous studies. In this study, some IAP expression patterns –at the transcript level- revealed an anti-apoptotic pattern, i.e. downregulated at the two developmental cell-death stages. In contrast, some caspases were upregulated during these two proposed cell-death waves. Three out of the five chicken IAP genes; namely; Birc-4 (XIAP), Birc-5 (Survivin) and Birc-7, were found to be downregulated during the two cell death waves. On the other hand, apoptotic caspases 2, 3, 7, 8 and 10 were found to be upregulated during the two cell death waves to different extents. These findings suggest that these enzymes play a role in the developmental apoptotic cell death of the developing chick retina.

From protein analyses data with Western blotting (WB) and ELISA, it is shown that Birc-4 (XIAP) and Birc-5 (Survivin) protein expression is significantly lower at the

early and late developmental stages than at the middle stage, and the exact opposite pattern was obtained for Casp-3 and Casp-7. This expression pattern for the four enzymes reflects the transcript expression pattern.

IHC was run for the same four factors *in situ* in combination with immunostaining with the Islet1 neuronal marker and revealed the same temporal expression trend obtained with WB and ELISA for the two IAPs and two caspases. Spatial expression of the four enzymes validated occurrence of protein expression within the neuroretina with the aid of co-localisation of target enzymes with the Islet1 neuromarker that specifically stained the neuroretina and not surrounding non-neuronal tissues. TUNEL assay was run as well for early, intermediate and late stages to investigate the occurrence of apoptosis during these three developmental stages and for correlation of apoptosis onset with the expression of four enzymes. Apoptosis was detected at the early and late stages coinciding with the upregulation of caspases and downregulation of IAPs.

More work needs to be performed to complete the spatial gene expression pattern of all 15 genes, and for the spatio-temporal protein expression profile for the rest of IAPs and caspases. These studies pave the way for further functional studies both *in vitro* and *in ovo* involving manipulation of IAP and caspase expression.

II Acknowledgment

All praise and thanks be to Almighty Allah. Then I would like to acknowledge my parents, Abdullah and Fatima, whose prayers and encouragement accompanied me in each step of my life. Thanks to my first mentor uncle Ali Alrofaidi, to Aunt Saleha and uncle Saleh for helping me launching my academic journey. My deepest gratitude to my husband Ali and four children, Abdullah, Amr, Princess Mai and Abdulmalek for their love and belief in me.

I need to sincerely thank my supervisor Dr. Michael Wride for his support and guidance throughout the period of my PhD study. I also would like to thank Dr. Paula Murphy for her expertise and valuable assistance as my research advisor. My appreciation is also extended to Prof. Yvonne Buckley, the chair of Zoology for her genuine care and support when I mostly needed it.

I also need to especially thank Dr. Fiona Mansergh for her generous assistance with my project when I needed an expert advice. My thanks extend to Dr. Andrew Jackson and Dr. Ken Irvine for assisting in co-ordinating my project committee meetings.

This project would not have been possible without the support of the technical and administrative staff in the Department of Zoology, Dr. Martyn Linnie, Mr. Peter Stafford, Ms. Fiona Moloney, Ms. Alison Boyce and Mr. Richard Hollinshead. Their dedication and commitment to helping graduate students in the department is extraordinary.

"The soul, fortunately, has an interpreter - often an unconscious but still a faithful interpreter - in the eye."

Charlotte Brontë, *Jane Eyre*

III Table of Contents

Summary i

Acknowledgment iii

Table of contents v

List of Figures x

List of Tables xii

Abbreviations xiv

Chapter 1. General Introduction

1.1. Introduction 1

1.2. Eye anatomy and development 2

1.2.1. Formation of the eye and eye field 2

1.2.2. Retinal neurogenesis 3

1.2.2.1. Retinal ganglion cell neurogenesis: morphological and physiological characteristics 4

1.2.2.2. Role of neurotrophins and growth factors in retina neuronal development 6

1.3. Cell death 8

1.3.1. Types of cell death 8

1.4. Regulators of apoptosis in the developing retina 10

1.4.1. Caspases as apoptosis promoters 10

1.4.1.1. Bcl-2 involvement in retina neuronal cell death 15

1.4.1.2. The extrinsic apoptosis pathway 16

1.4.1.3. The intrinsic apoptosis pathway 16

1.4.1.4. Cytotoxic lymphocyte-initiated granzyme B pathway 17

1.4.2. Inhibitors of apoptosis proteins (IAPs) 17

1.4.3. Role of other proteolytic enzymes 21

1.5. Cell death in the developing retina 22

1.5.1. Cell death waves in chick developing retina....23
1.5.2. Cell differentiation in the chick developing retina....26
1.5.3. Factors regulating cell death in the retina....27
1.6. Biological significance of utilising chick embryos as model for studying role of IAPs on RGCs....28
1.7. Hypothesis and aims....29
1.7.1. Hypothesis....29
1.7.2. Aims....30

2. General Materials and Methods

2.1. Chick embryos....31
2.2. Microdissection and retina extraction....31
2.3. RNA extraction and integrity check....32
2.4. Conventional semi-quantitative PCR....34
2.4.1. Principle....34
2.4.2. Primer design....35
2.4.2.1. Procedure....35
2.4.3. cDNA synthesis....39
2.4.4. Semi-quantitative PCR procedure....40
2.4.4.1. Quantification of conventional PCR bands....41
2.5. RT-qPCR....42
2.5.1. Principle....42
2.5.2. Procedure....42
2.5.3. RT-qPCR data analysis....43
2.5.3.1. RT-qPCR statistical analysis....43
2.6. Western blotting (WB)....43
2.6.1. Principle....43

2.6.2. Protein extraction and quantification 44
2.6.3. Western blotting procedure 44
2.6.3.1. Principle 44
2.6.3.2 Primary and secondary antibodies 44
2.6.3.3. WB procedure 45
2.6.3.4. Membrane stripping for reprobing 49
2.6.3.5. Quantification of protein expression 49
2.6.3.6. Statistical analysis 49
2.7. ELISA 50
2.7.1. Principle 50
2.7.2. Procedure 50
2.7.3. Statistical analysis 52
2.8. Immunohistochemistry (IHC) and immunofluorescence (IF) 52
2.8.1. Principle 52
2.8.2. Tissue wax-embedding for H&E staining 53
2.8.3. Tissue processing for cryosectioning 53
2.8.4. Cryostat sectioning 54
2.8.5. H&E staining 54
2.8.6. Staining nuclei with Cytox Green 54
2.8.7. TUNEL staining for apoptotic activity analysis 55
2.8.8. Immunohistochemistry (IHC) and immunofluorescence (IF) 56
2.8.9. Image analysis 56

Chapter 3. Gene Expression for IAPs and Caspases

3.1. Introduction 59
3.2. Aim 60

3.3. Experimental design 61
3.4. Results 61
3.4.1. RNA integrity 61
3.4.2. PCR ptimisation and housekeeping gene consistency evaluation 62
3.4.3. Semi-quantitative PCR 64
3.4.3.1. IAPs and caspases gene expression 64
3.4.4. Real-Time quantitative PCR (RT-qPCR) 66
3.4.4.1. IAPs gene expression 66
3.4.4.2. Caspases gene expression 69
3.4.4.3. Correlation of IAPs and caspases temporal gene expression 72
3.5. Discussion 72
3.5.1 RNA purity and integrity 73
3.5.2. Semi-quantitative vs. quantitative PCR results 73
3.5.3. Five IAPs gene expression 76
3.5.4. Ten caspases gene expression 77
3.5.4.1. Non-apoptotic caspases gene expression 77
3.5.4.2. Apoptotic caspases gene expression 79
3.5.4.3. Correlation between anti-apoptotic IAPs and pro-apoptotic caspases 81

Chapter 4. Protein Expression of IAPs and Caspases

4.1. Introduction 83
4.2. Aims 84
4.3. Experimental design 85
4.4. Results 85

4.4.1. WB protein expression profile for Birc-4 (XIAP), Birc-5 (Survivin) and Casp-3. 86
4.4.2. Enzyme detection by ELISA..... .....88.

4.5. Discussion.....90

4.5.1. WB vs. ELISA.....91

4.5.2. Protein expression profile for Birc-4 (XIAP) and Birc-5 (Survivin).91

4.5.3. Protein expression profile for Casp-3 and Casp-7.....92

4.5.4. Correlation between gene and protein expression.....95

Chapter 5. Immunohistochemistry (IHC) Analysis for IAPs and Caspases

5.1. Introduction.....101

5.2. Aims.....103

5.3. Experimental design.....103

5.4. Results.....104

5.4.1. Retina morphology analysis by Hematoxylin and Eosin staining (H&E) and Cytox Green nuclei staining.....104

5.4.2. Immunohistochemistry (IHC) and Immunofluorescence (IF).....106

5.4.2.1. TUNEL apoptosis assay.....107

5.4.2.2. Spatiotemporal analysis of IAPs and Islet-1 with double-staining IHC.....109

5.4.2.3. Spatiotemporal analysis of caspases and Islet-1 with double-staining IHC.....112

5.5. Discussion.....115

5.5.1. Morphological retinal structure staining.....115

5.5.2. Assessment of apoptosis by TUNEL assay.....116

5.5.3. Apoptotic enzymes expression assessment.....116

5.5.3.1. Birc-4 (XIAP) and Birc-5 (Survivin) downregulation during cell death waves in the developing retina.....117

5.5.3.2. Casp-3 and Casp-7 upregulation coincides with cell death waves in

the developing retina.....s.....117

5.5.4. Conclusion.....118

Chapter 6. Final Discussion and Conclusion

6.1. General discussion and conclusion.....121

6.1.1. Gene (Transcript) expression analyses for IAPs and caspases.....122

6.1.2. Protein expression analyses for Birc-4 (XIAP), Birc-5 (Survivin), Casp-3 and Casp-7.....127

6.1.3. IHC analysis for Birc-4 (XIAP), Birc-5 (Survivin), Casp-3 and Casp-7.....130

6.2. Future directions.....131

References.....**I**

Appendices.....**a**

Appendix 1.....b

Appendix 2.....b

Appendix 3.....f

Appendix 4.....g

IV List of Figures

Chapter 1

Figure 1.1. Structure and components of the mature higher vertebrate eye 2

Figure 1.2. Retinal neurogenesis 4

Figure 1.3. Trk receptors and p75NTR mediate differentiation and survival signalling 7

Figure 1.4. Morphological structural appearance of cells undergoing apoptosis by electron microscopy 9

Figure 1.5. Chicken (*Gallus gallus*) ten caspases structure 11

Figure 1.6. Caspase-mediated apoptotic pathways 14

Figure 1.7. Chicken five IAPs structure 18

Figure 1.8. Temporal pattern of naturally dying, and proliferating cells in the early embryonic central retina 23

Chapter 2

Figure 2.1. Schematic diagram of neural retina extraction by microdissection 32

Figure 2.2. ELISA assay procedure summary 51

Figure 2.3. TUNEL assay procedure summary 55

Chapter 3

Figure 3.1. Total RNA integrity test using non-denaturing agaros gel electrophoresis 62

Figure 3.2. β -actin control gene expression for all ten embryonic stages with semi-quantitative PCR analysis 63

Figure 3.3. Semi-quantitative PCR data of IAPs in the neural retina during development 64

Figure 3.4. Semi-quantitative PCR data of caspases in the neural retina during development 65-66

Figure 3.5. RT-qPCR analysis data of IAPs genetic expression 67

Figure 3.6. RT-qPCR analysis data of caspases genetic expression 69-70

Figure 3.7. Inverse correlation of the temporal expression of Birc-4 and Birc-5 (IAPs) with selected caspases expression 72

Chapter 4

Figure 4.1. Differential expression of Birc-4, -5 and Casp-3 from Western blotting analysis 87

Figure 4.2. ELISA analysis for Birc-4, Birc-5, Casp-3 and Casp-7 90

Figure 4.3. Correlation of gene and protein expression for Birc-4, Birc-5, Casp-3 and Casp-7 96-97

Figure 4.4. Correlation coefficient blot for relationship between gene (mRNA) and protein expression Birc-4, Birc-5, Casp-3 and Casp-7 99-100

Chapter 5

Figure 5.1. H&E and Cytox Green staining of chick embryo developing retina 105

Figure 5.2. Neural retina structure and orientation in the eye 106

Figure 5.3. TUNEL assay for developing retina 108

Figure 5.4. Spatiotemporal expression pattern for Islet-1 and Birc-4 (XIAP) 110

Figure 5.5. Spatiotemporal expression pattern for Islet-1 and Birc-5 (Survivin) 111

Figure 5.6. Spatiotemporal expression pattern for Islet-1 and Casp-3 113

Figure 5.6. Spatiotemporal expression pattern for Islet-1 and Casp-7 114

V List of Tables

Chapter 1

Table 1.1. Listing and properties of the ten caspases of this study 13

Table 1.2. The five chicken IAPs 20

Table 1.3. Programmed cell death waves in the neuronal retina in developing chick embryo 25

Chapter 2

Table 2.1. Primers of this study, nucleotide sequence, predicted product size and optimum PCR conditions 37-38

Table 2.2. Comparison of three cDNA synthesis protocols 40

Table 2.3. List of antibodies used in Western blotting 47-48

Table 2.4. List of Cusabio ELISA kits used in this study 52

Table 2.5. List of primary and secondary antibodies used in Immunohistochemistry 57

Chapter 3

Table 3.1. Fold change difference for the five IAPs 68

Table 3.2. Fold change difference of the ten chicken caspases 70

Table 3.3. The five categories of gene expression patterns for ten chicken caspases form RT-qPCR analysis 71

Table 3.4. Comparison between IAPs expression with two PCR techniques 74

Table 3.5. Comparison between caspases expression with two PCR techniques 75

Chapter 4

Table 4.1. Fold change of Birc-4 (XIAP), Birc-5 (Survivin) and Casp-3 expression obtained from Western blotting 88

Table 4.2. Comarison of WB and ELISA analysis data for IAPs (Birc-4 and Birc-5) and caspases (Casp-3 and Casp-7) expression trend 91

Abbreviations

β	Beta
Bcl-2	B-cell lymphoma 2
BIR	Baculovirus IAP repeat domain
Birc	Baculoviral IAP repeat-containing protein
BLAST	*Basic Local Alignment Search Tool*
BrdU	Bromodeoxyuridine (5-bromo-2'-deoxyuridine)
bP	Base pair
°C	Degree Celsius
Casp	Caspase
cDNA	Complementary DNA
cIAP	Cellular IAP
CNS	Central nervous system
ΔΔCt	Delta delta Ct
dH_2O	Distilled water
DAPI	4',6-diamidino-2-phenylindole
DNA	Deoxyribonucleic acid
DNase	Deoxyribonuclease
E	Embryonic day
ELISA	Enzyme-linked immunosorbent assay
g	Gravity force
GCL	Ganglion cell layer
HH	Hamburger and Hamilton
HRP	Horseradish peroxidase
IAPs	Inhibitor of apoptosis proteins

IHC	Immunohistochemistry
INL	Inner nuclear lamina
kb	Kilobase
µg	Microgram
µl	Microlitre
µM	Micromolar
mL	Millilitre
mRNA	Messenger RNA
NE	Neural retina
PBS	Phosphate-buffered saline
PBST	Phosphate-buffered saline-Tween20
PBS-Tr	Phosphate-buffered saline-Triton
PCD	Programmed cell death
PCR	Polymerase chain reaction
PFA	*Paraformaldehyde*
PVDF	Polyvinylidene difluoride
r	Correlation coefficient
RGCs	Retinal ganglion cells
RIPA	Radio-immunoprecipitation assay
RNA	Ribonucleic acid
RNase	Ribonuclease
RPE	Retinal pigmented epithelium
RQ	Relative quantification
RT-qPCR	Real time quantitative PCR
SD	Standard deviation
SDS-PAGE	Sodium dodecyl sulphate- polyacrylamide gel electrophoresis

SEM	Standard error of the mean
TBS	Tris-buffered saline
TBST	Tris-buffered saline-Tween20
TUNEL	Terminal deoxynucleotidyl transferase dUTP nick end labelling
V	Volts
WB	Western blotting
XIAP	X-linked inhibitor of apoptosis protein

Chapter 1

General Introduction

1.1. Introduction

Cell death has been studied intensively as a relevant process in the physiology and pathology of the developing eye and other tissues (Glucksmann, 1965); however, the current knowledge of the dynamic morphological and molecular modification that occur during embryonic development still have to be fully understood. Retinal embryonic development and developmental programmed cell death received particular interest in biomedical research in an attempt to comprehend the mechanism of retinal cells death. Understanding cell death in embryonic life and in inappropriate pathogenic cell death in some eye neurodegenerative diseases in adult life, such as glaucoma, might shed a light on how cells die and help develop preventive measures for eye degenerative disorders of cell-death origin. Retina neuronal programmed cell death (PCD) during development was reported to contribute to the generation of the final complex cytoarchitecture of the retina and to define the pattern of interneuronal connection, neurons number and their spatial distribution and dendritic synaptogenesis (Bunt and Lund, 1981, Linden and Perry, 1982, Young, 1984). However, accidental neuronal cell death that occurs in adult life is not homeostatic or programmed (Buss *et al.*, 2006) and is considered to be a pathological condition due to the fact that mature neurons have a very small capacity of regeneration, if none at all, throughout adult life.

Cell death occurring in the developing vertebrate retina appears to be mediated by caspase-dependent apoptosis (Mayordomo *et al.*, 2003); one form of programmed cell death. Key regulators of apoptosis include two groups of proteins: caspases (pro-apoptotic) and inhibitors of apoptosis (IAPs) (anti-apoptotic) amongst others factors. However, caspase-independent photoreceptor apoptosis has been reported in the developing retina (Donovan and Cotter, 2002) and in the retinal ganglion cells under certain conditions (Spalding *et al.*, 2005). Developmental cell death affects neural precursors, newly born and immature, proliferating and differentiated neurons (Varela-Nieto *et al.*, 2003). The survival/death mechanism during development of retinal neurons is also influenced by a number of factors such as neurotrophic factors (Wiese *et al.*, 1999, Agarwal *et al.*, 2007).

1.2. Eye anatomy and development

The mature eye is a complex organ comprising of a variety of specialised tissues (Figure 1.1). During embryogenesis, the eye is derived from different precursor tissues. The ectoderm gives rise to both retina and lens (Wong, 2006). The sclera is derived from mesenchymal cells of neural crest origin, which also migrate to the cornea. The optic vesicles are connected to the developing central nervous system (CNS) by a stalk that later becomes the optic nerve.

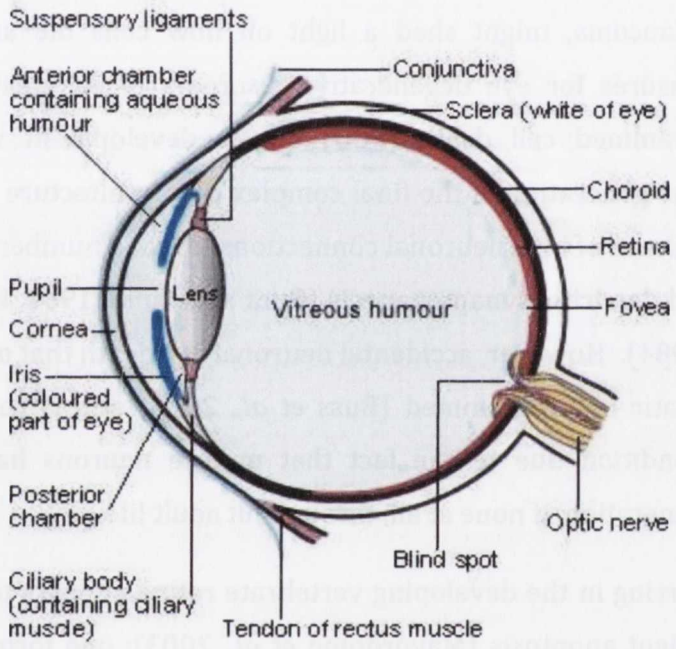

Figure 1.1. Structure and components of the mature higher vertebrate eye. (From Wong, 2006)

1.2.1. Formation of the eye and eye field

Vertebrate eye origin can be traced back to the 32-cell-stage blastula to a single region of neuroectodermal cells called the eye field (Zuber, 2006). A highly conserved set of transcription factors, collectively referred to as eye field transcription factors (EFTFs), is required for normal eye formation. Recent experiments point to a more complex mechanism in which these genes act synergistically in a self-regulating feed-back network to convert a region of the

neural plate into the eye field, and appear to be conserved among all vertebrate species. However, potential differences still exist between the diverse models of vertebrate eye-field specification.

In humans, eye development begins at around 22 days of development and, like most higher vertebrates, is not completed until several months after birth (Wong, 2006). In the chick embryo (*Gallus gallus*) the primary optic vesicles are firstly present at Hamburger and Hamilton chick embryo stage (HH)-9 (29-33 hrs) (Hamburger and Hamilton, 1992).

1.2.2. Retinal neurogenesis

The retina is a light-sensitive neuroepithelial tissue, an accessible part of the brain that displays a laminar cytoarchitecture. The vertebrate retina develops from a single layer of undifferentiated neuroepithelial cells into a multilayered structure of terminally differentiated neurons (Guerin *et al.*, 2006). In the developing chick, neurogenesis of the retina starts at E2 (Prada *et al.*, 1991) and terminates at E18 (Doh *et al.*, 2010). Multipotent retinal stem/progenitor cells undergo successive processes of proliferation, differentiation, cell migration, axonal and dendritic growth as well as navigation (Valenciano *et al.*, 2009), which overlaps spatially and temporally (Chavarria *et al.*, 2013). Seven cell types (six neurons and one glia) are confined to one of three laminae (Rapaport, 2006). These include photoreceptors (rods and cones), in the outer nuclear layer (ONL), short projection neurons (bipolar cells), local circuit neurons (horizontal and amacrine cells) and glial (Müeller cells) in the inner nuclear layer (INL) and long projection neurons (or retinal ganglion cells (RGC)) in the ganglion cell layer (GCL) (Figure 1.2).

The ultimate aim of retinal development is to produce the right cell type in the right quantity at the right time and in the right place to allow formation of functional retinal circuits. Furthermore, the sequence of cell genesis in the vertebrate retina is highly conserved. After the generation of different retinal cells, the sequence of developmental events converges to the building and maintaining of connections between the retina cellular components and between the retina and its targets in the brain.

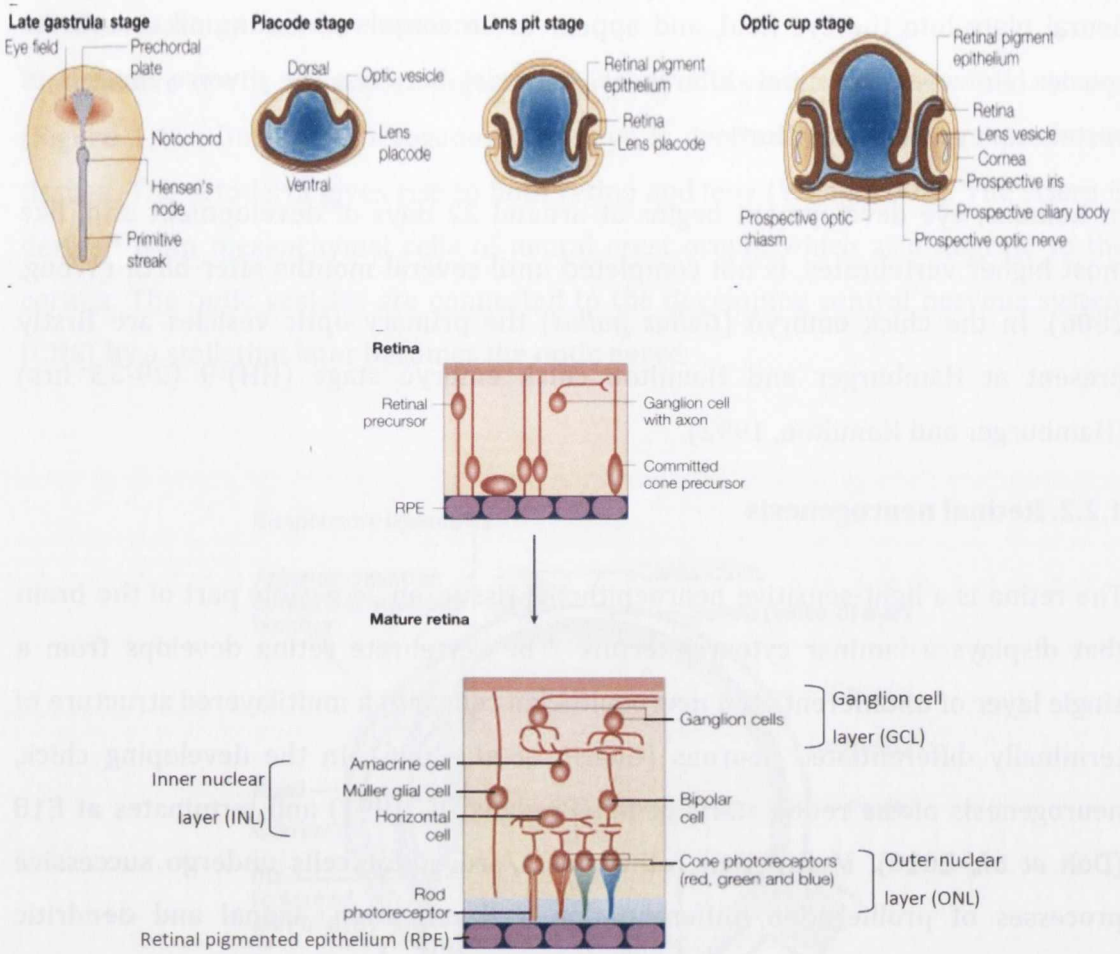

Figure 1.2. Retinal neurogenesis from neural tube of ectodermal origin, the evagination of optic vesicle, formation of optic cup and the differentiation of distinct retinal different types of cells and their connections. Modified from Graw (2003).

1.2.2.1. Retinal ganglion cell neurogenesis: morphological and physiological characteristics

RGCs, like other projection CNS neurons, are the first to be born in the inner nuclear lamina (INL) in the chick embryo (Prada *et al.*, 1991) and other species such as the rat (Rapaport *et al.*, 2004). Within the population of RGCs, several functional sub-types have been distinguished and appear to differ in their location and time of genesis. Approximately between 10-15 types of RGCs have been characterised in the mammalian retina (Masland, 2001). Retrograde labelling studies indicated that RGCs project to the parvocellular layers of the dorsal lateral geniculate nucleus (LGNd)

and are located vitreal to those terminating in the magnocellular layer. The axons of these cells are unmyelinated within the ocular globe and have recently been shown to have varicosities that are rich in mitochondria (Nucci, 2008). These varicosities have been interpreted as functional sites with local high-energy demand, possibly relevant for signal transmission.

RGCs and horizontal cells are the largest in the retina (Rapaport, 2006). Somata of some RGCs are displaced from the ganglion cell layer (GCL) to the INL. Conversely, up to 50% of the cells within the GCL are not RGCs, but may be amacrine cells, which are interneurons that modulate the majority of the output to the RGCs (Guerin *et al.*, 2006). In the avian retina, RGCs leave the cell cycle early (E3), and their neurogenesis terminates at E8.

In vitro, RGCs can be identified by specific markers as macroneurons with long processes (Brocco and Panzetta, 1997). In fact, the axons are cut off when the retina is dissected for culturing its cells. In the vertebrate retina, Thy-1 is an exceptional marker for ganglion cells. Thy-1 is a phosphatidylinositol anchored glycoprotein that is expressed on the plasma membrane of several cell types including neurons. The disposition of this molecule on RGCs allows for the separation of these cells from others by the panning purification using immobilized antibodies to Thy-1 (Brocco and Panzetta, 1997). *Brn-3a* and gamma-synuclein (*Sncg*) mRNAs are expressed specifically and highly in human and adult mouse RGCs, and both have been used as specific markers for RGC (Surgucheva et al., 2008, Sanders et al., 2009b) Other gene expression pattern including Math5, Brn3b, Islet-1 and Thy-2 are found in the progenitors of retinal ganglion cell line that can be also used as markers for RGC (Zuber *et al.*, 2003, Mu *et al.*, 2005, Chen *et al.*, 2010).

1.2.2.2. Role of neurotrophins and growth factors in retina neuronal development

During development, up to 50% of neurons die by apoptosis soon after the formation of synaptic connections with their target field (Raff *et al.*, 1993). Early studies have demonstrated that the growth and survival of developing neurons are regulated by target-derived molecules. These molecules are collectively termed neurotrophic factors (NTFs) (Campenot, 1977) (Edgar, 1985). The neurotrophic theory stated that competition for a limited amounts of trophic factors match the

innervating neurons to target cells (Oppenheim, 1991). The survival signals are thought to operate by suppressing the intrinsic (intracellular) apoptotic pathway (Raff *et al.*, 1993). By using *in vivo* administration of nerve growth factor (NGF), Hamburger *et al.* (1981) demonstrated the significance of this naturally produced trophic maintenance agent for embryonic sensory neurons. NGF promotes neuron survival at exactly the same time they would have died without NGF supplementation. However, in the absence of tyrosine kinase receptor A (TrkA), NGF promotes neuronal cell death via activation of transcription factor nuclear factor kappa B (NF-kappa B) in rat (Carter *et al.*, 1996). In another rescue experiment, both *in vivo* and *in vitro* administration of brain-derived neurotrophic factor (BDNF) reduce neuronal cell death (Hofer *et al.*, 1990).

Neurotrophin-3 (NT-3) is important in early retinal development at the time most retinal neurons are being generated (Bovolenta *et al.*, 1996). When NT-3 is neutralized, evident decrease of neuronal numbers and abnormal retinal organization were observed. This is specifically important for RGCs where anterograde transport of endogenous NT3 along their axons was documented at late stages of chick embryo development (von Bartheld and Butowt, 2000).

Recently, the neurotrophism concept has expanded to include the trophic dependence of neurons, and glial cells, at different developmental stages on various survival signals. These signals are comprised of the classical neurotrophic factors, growth factors and many others (de la Rosa and de Pablo, 2000). Many studies have investigated the effect of administration of survival factors on the neuronal number/death during development. The neural retina was found to be a site for production and action of growth hormone (GH) in the earlier stages of development, where it plays an important neuroprotective role (Harvey *et al.*, 2009). GH is found in the early chick embryo prior to the ontogeny of the pituitary gland, associated with the presence of GH receptor (GHR) and GHR mRNA (Harvey *et al.*, 2003) (Baudet *et al.*, 2003), and has proven to have anti-apoptotic role in embryonic retinal ganglion cell differentiation (Sanders *et al.*, 2005). Also, it has found that GH promotes survival in adult human RGCs (Sanders et al., 2009b).

The neuronal response to neurotrophins is mediated via two types of receptors; tyrosine kinase receptors (Trk) and p75 neurotrophin receptor (p75NTR) (Kaplan and Miller, 2000). The functions of the neurotrophin receptors vary markedly, from shaping the developing nervous system to the regeneration of injured neurons (Figure 1.3). While Trk receptors mediate positive signals such as enhanced survival and growth, p75NTR transmits both positive and negative signals. These receptors can either collaborate with or inhibit each other's actions to mediate neurotrophin effects.

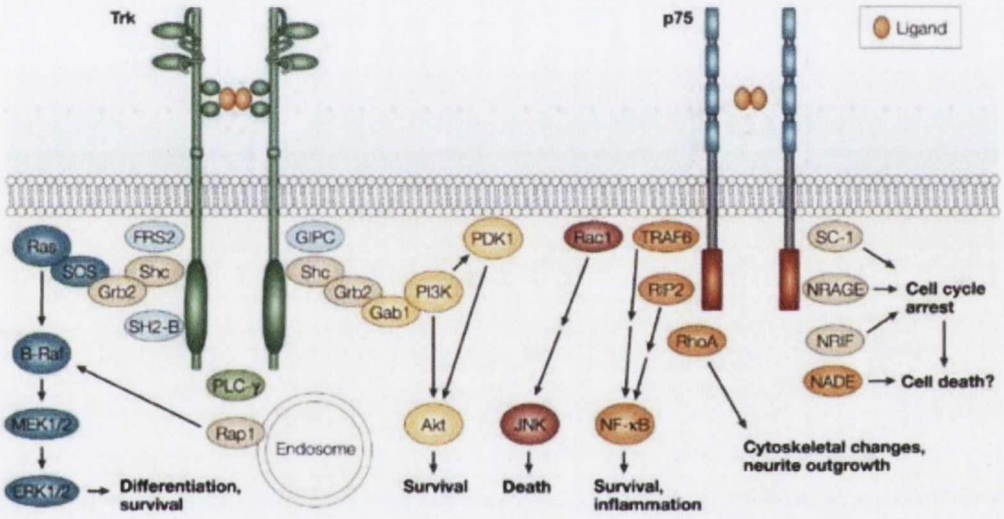

Figure 1.3. The targets of PI-3K Trk receptors and p75NTR mediate differentiation and survival signalling. Trk family members induce the phosphorylation of adaptor protein, which leads to activation of PI3K and ERK. PI-3K activity stimulates the activation of Akt. The targets of PI-3K. From Chao (2003)

1.3. Cell death

Cell death can be either genetically programmed or due to a traumatic cellular injury. Apoptosis and autophagy are prominent varieties of programmed, intracellularly mediated cell death. Necrosis, on the other hand, mostly occurs due to traumatic external factors, which are induced by pathological stimuli.

1.3.1. Types of cell death

Different cell death types are characterised mainly by morphological criteria (Kroemer *et al.*, 2005).

Apoptosis is the most recognized form of PCD. The name was proposed by Kerr (1972) (from Greek, meaning "falling off") to describe the active, energy-dependent process of naturally-occurring cell death. Apoptosis is accompanied by distinct morphological characteristics observed as cells are eliminated during embryonic development and in normal adult tissues. Apoptotic cellular changes include plasma membrane blebbing, reduction of cellular volume (pyknosis), fragmentation of the nucleus (karyorhexis) and chromatin condensation within the nucleus (Figure 1.4).

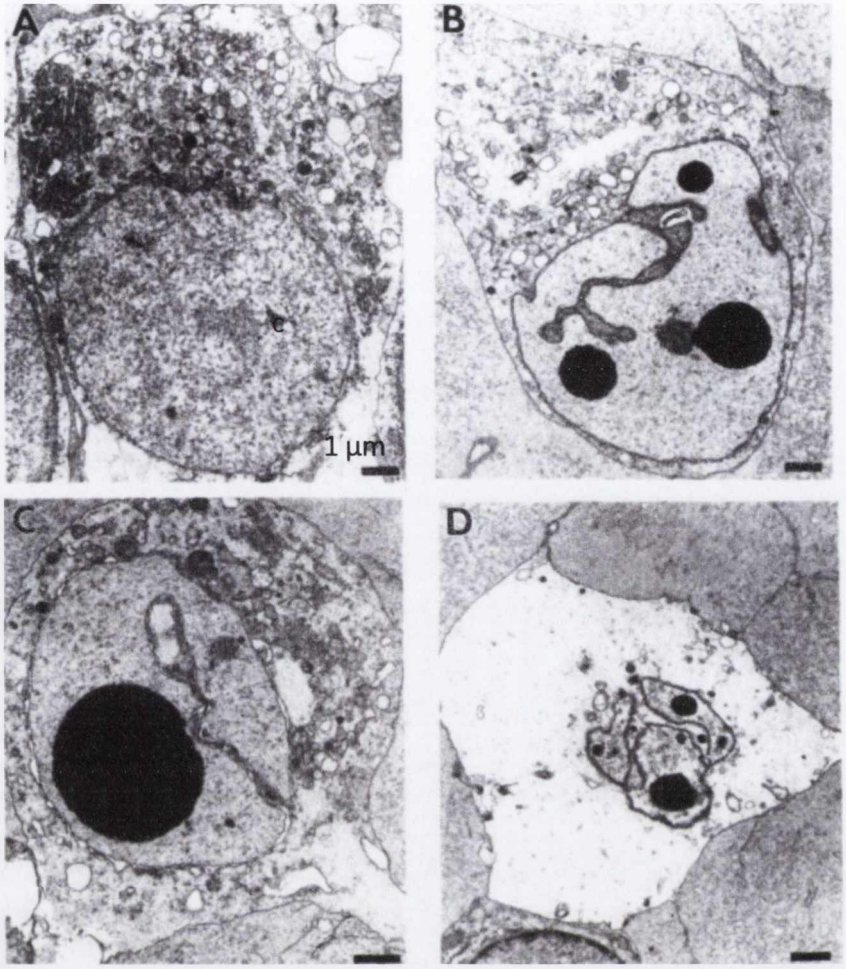

Figure 1.4. Morphological structural appearance of cells undergoing apoptosis by electron microscopy from a normal rabbit retinal ganglion cell (RGC) (A). Cell exhibits apoptotic morphology characteristic: shrinkage of cell, aggregation of organelles with undefined cytoplasm on the peripheral area, high condensation of chromatin in nucleus (B) and (C) formation of apoptotic bodies. (D) Late stage of apoptosis where chromatin concentrates of in the centre of the nucleus. Abundant degradative autophagic vacuoles in the cytoplasm are observed. (Quigley *et al.*, 1995).

Other cell death types have been described. Autophagic cell death (or autophagocytosis) was morphologically defined as a type of PCD that occurs independent of chromatin condensation (Kroemer *et al.*, 2005) and considered to be a basic catabolic mechanism that involves the action of lysosomes (Lin *et al.*, 2013). Necrosis is cell death characterised by loss of cytoplasmic integrity, release of cellular components to the intracellular space (Proskuryakov *et al.*, 2003), as well as less defined chromatin condensation (Kroemer *et al.*, 2005). Excitotoxicity is also a type of pathological cell death specific to neurons where excitatory neurotransmitters, lead to the opening of calcium channels, with subsequent rise of

cytosolic calcium and ultimately neuronal cell death (Manev *et al.*, 1989). Glutamate is the main excitatory neurotransmitter that brings about excitotoxicity.

1.4. Regulators of apoptosis in the developing retina

Over the last few decades, genetic studies have focused on elucidating the role of apoptosis regulators in controlling survival and death decisions in the nervous system. The physiological role of apoptosis during retinal development particularly has improved immensely (Ahmed *et al.*, 1998, Linden *et al.*, 1999, Donovan and Cotter, 2002, Pequignot *et al.*, 2003, Pequignot *et al.*, 2011, Braunger *et al.*, 2014). However, more work is still has to be carried out to further illustrate the exact role of apoptosis and related processes such as autophagy and other forms of cell death in refining the final structure of the vertebrate retina.

1.4.1. Caspases as apoptosis promoters

Caspases are a family of cysteine aspartic acid proteases, which orderly digest the apoptotic cells and appear to be major executioners of cell death in the developing nervous system (Mayordomo *et al.*, 2003). Caspase-3 and caspase-9 knockout mice suffer from tumours in the developing brain and die perinatally, which highlights their physiological significance in developmental PCD (Kuida *et al.*, 1998, Kuida *et al.*, 1996). Up until now, 14 caspases have been identified, 12 in human (Qu *et al.*, 2010, http://www.genenames.org/, 2014).

In 1993, Robert Horvitz first established the importance of caspases in apoptosis. Along with his colleagues, he found that the protein encoded by the *ced-3* gene in the nematode *C. elegans* was most abundant during embryogenesis, where most cell death occurs (Yuan *et al.*, 1993). This protein was a cysteine protease with similar properties to the mammalian interleukin-1-beta converting enzyme (ICE), which was the only known caspase, at the time. Now, ICE is known as caspase-1. Caspases-2, -3, -6, -7, -8, -9, -10, -12 and -14 are centrally involved in apoptosis, while caspases-1, -4, -5 and -11 are known to play roles in inflammation in human (Qu *et al.*, 2010). Caspases are synthesised as inactive single-chain zymogens that become activated into dimeric molecules by scaffold-mediated transactivation or by cleavage via upstream proteases in an intracellular cascade (Earnshaw *et al.*,

1999). Each pro-caspase is composed of a large subunit preceded by N-terminal pro-domain, and a small subunit (Park, 2012) (Figure 1.5). Additional domains; namely, death effector domain (DED) and caspase recruitment domain (CARD) can be found in some caspases but not others. DED is important for interaction with signalling adaptor proteins such as apoptosis mediating receptor Fas-associated protein with death domain (FADD) and tumour necrosis factor receptor type 1-associated death domain protein (TRADD) adaptor protein. CARD, on the other hand, facilitates the interaction between different caspases and between caspases and their regulatory adapting proteins (Chinnaiyan *et al.*, 1995, Hofmann *et al.*, 1997, Earnshaw *et al.*, 1999, Degterev *et al.*, 2003).

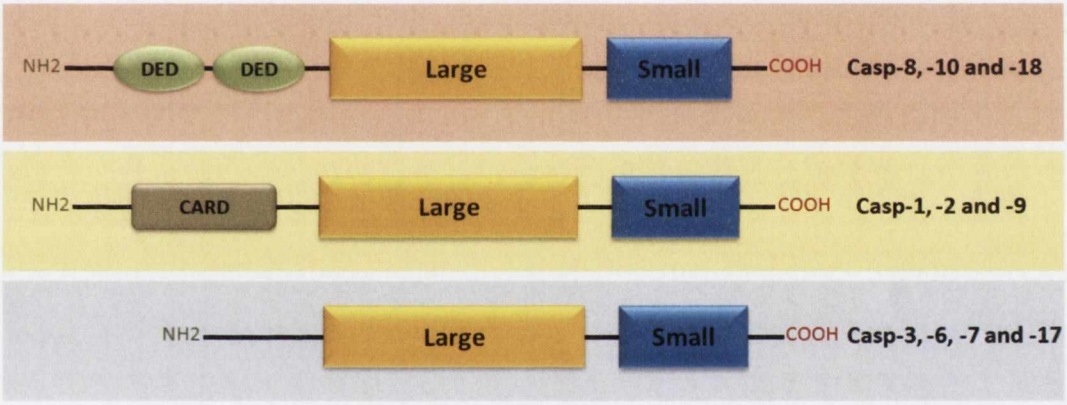

Figure 1.5. Chicken (*Gallus gallus*) ten caspases structure. All caspases are characterised by an N-terminal pro-domain of variable length, a catalytic domain that gives rise to large and small subunits upon processing. Pro-domain segment contains specific protein-protein interaction domains (death effector domain; DED or caspases recruitment domain; CARD) that are involved in the recruitment of caspases in apoptosis in inflammation responses.

Activation of caspases proceeds through three principal pathways. The receptor-mediated extrinsic (extracellular pathway), and mitochondria-mediated (intrinsic pathway) and the granzyme B pathways, which reunite at the final phase of apoptosis through activation of caspase-3. Once activated, caspases induce cell death by cleaving cytoskeletal proteins including kinases, members of the Bcl- 2 family of apoptosis-related proteins and DNA repair enzymes as well as by indirect activation of chromosomal endonucleases (Guerin *et al.*, 2006). Activated caspase-8 can cleave

BH3 interacting-domain death agonist (BID). Truncated BID is detected in glaucomatous eyes in a rat experimental glaucoma model, and once cleaved; BID is translocated from the cytoplasm to the mitochondria and promotes the release of cytochrome c, leading to apoptosome complex formation and activation of caspase-9, triggering the activation of downstream caspases as in the intrinsic pathway. Furthermore, the mitochondria can be involved in the extrinsic caspase cascade, which was considered to be mitochondrial- independent (Qu *et al.*, 2010). It is important to emphasise that not all caspases have lethal effects on cells when activated.

Table 1.1 lists the ten chicken (*Gallus gallus*) caspases studied here and some of their properties. In neuronal cells, apoptotic caspases -2, -8, -9 and -10 are considered to be initiators that respond to pro-apoptotic signals and activate the downstream executioner caspases; caspases -3, -6 and -7 (Philchenkov, 2004). Although general structural features are shared between the initiator and the effector caspases, their activation, inhibition and release of inhibition are differentially regulated (Riedl and Shi, 2004).

Table 1.1. Listing and properties of the ten caspases of this study

Caspase			Role in Apoptosis
Apoptotic	Initiators	Casp-2	Direct effector of the mitochondrial apoptotic pathway (Guo *et al.*, 2002). Also a pro-survival factor (Shi *et al.*, 2009)
		Casp-8	Activation of pro-caspase-3 independently of mitochondrial apoptotic pathway (extrinsic) (Stennicke *et al.*, 1998).
		Casp-9	Activation of pro-caspase-3 through mitochondrial pathway (intrinsic) (Hakem *et al.*, 1998).
		Casp-10	Processing of Casp-3 and -7 upon death-receptor activation (Kischkel *et al.*, 2001).
	Effectors	Casp-3	Disintegration of nuclear matrix (Kivinen *et al.*, 2005), axonal degeneration (Kuida *et al.*, 1996).
		Casp-6	Degradation of nuclear and cytoskeletal components (Inoue, 2009).
		Casp-7	Microfilament reorganisation (Sgorbissa *et al.*, 1999).
Non-apoptotic		Casp-1 a.k.a. ICE	Casp1; Immune system maturation and inflammatory response (Quesada *et al.*, 2010, Wilson *et al.*, 1994). Casp14/17 also has a role in epithelial tissues differentiation (Eckhart *et al.*, 2000) (Al-Shabrawey *et al.*, 2012)
		Casp14/ 17	
		Casp-18	

Caspase-associated apoptosis can be mediated via either of three major pathways: the extrinsic (death receptor) (Adams, 2003), intrinsic (apoptosome-mediated) (Adams, 2003, Kroemer *et al.*, 2007) or cytotoxic lymphocyte-initiated granzyme B pathways (Cullen and Martin, 2009) (Figure 1.6).

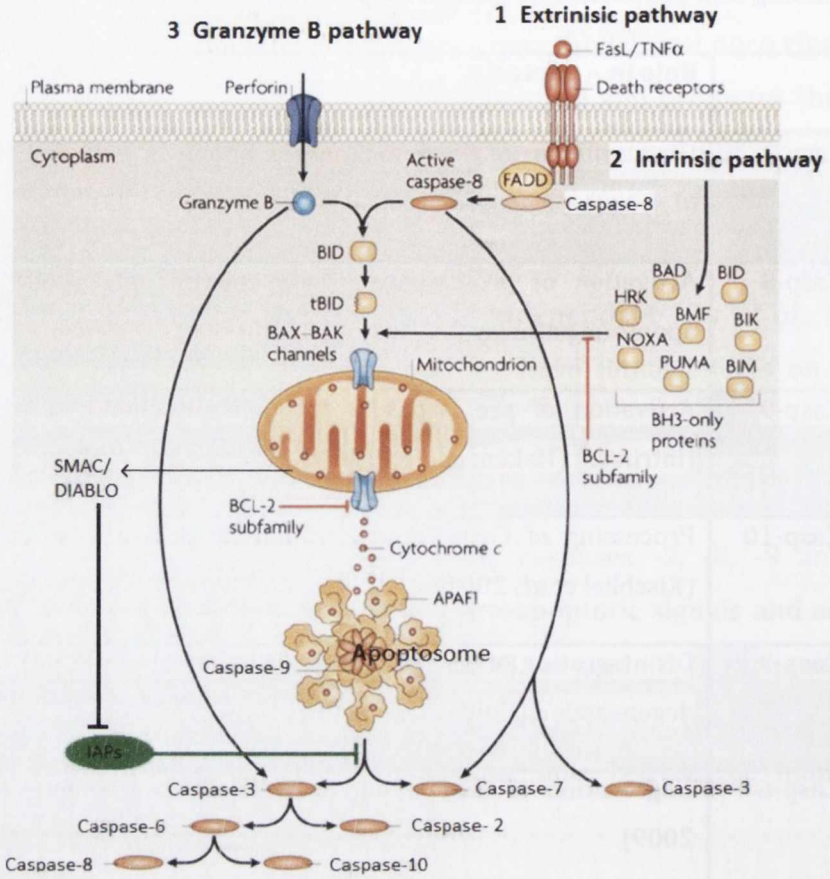

Figure 1.6. The caspase-mediated apoptotic pathways. 1. Caspase activation extrinsic pathway is initiated when extracellular death ligands, such as Fas and tumour necrosis factor-α (TNF- α), binds to their cell membrane death receptors, which leads to recruitment of adaptor protein Fas-associated death domain protein (FADD) and trigger the aggregation of several initiator caspase-8 molecules, which leads to its activation. In turn, activation of caspase-8 proteolytically activates effector caspase-3 and -7 to provoke downstream apoptotic degradation of cellular components leading eventually to cell death. In some cases, extrinsic and intrinsic pathways can crosstalk through activated caspase-8-mediated proteolysis of BH3-only protein BID, which causes cytochrome c release from the mitochondria and formation of the apoptosome. 2. The intrinsic pathway involves the action of multiple cell stress stimuli that in turn activate one or more of the BH-3 only proteins that can promote mitochondrial transmembrane BAK-BAX assembly oligomers; which permits the efflux of cytochrome c into the cytosol. BH-3 protein activation has to reach a threshold that can overcome the inhibitory effect of anti-apoptotic Bcl-2 factors. Cytosolic cytochrome c seeds apoptosome complex formation with activated caspase-9 molecules and this complex initiate a propagated cascade of further caspase proteolysis/activation. 3. The granzyme B-dependent pathway to caspase activation begins with the delivery of this enzyme from cytotoxic T lymphocytes (CTL) or natural killer (NK) cells through perforin pore-forming protein. Granzyme B then activates BID, caspase-3 and caspase-7 and leads to apoptotic cell death. Modified from (Taylor *et al.*, 2008).

1.4.1.1. Bcl-2 involvement in retina neuronal cell death

The *Bcl-2* family of proteins makes the critical decision of life-or-death in response to neuronal stress and injury (Bonfanti *et al.*, 1996, Yang *et al.*, 1997, Nir *et al.*, 2000, Pequignot *et al.*, 2003, Hahn *et al.*, 2003, Donovan *et al.*, 2006, Qu *et al.*, 2010). Apoptosis in the CNS is tightly regulated by alterations in the levels of pro-apoptotic (e.g., Bax, Bad, BID, Bcl-xS) and anti-apoptotic (e.g., Bcl-2, Bcl-xL) members of the Bcl-2 family, whose expression varies and can be regulated at the transcriptional level (Merry and Korsmeyer, 1997). Blocking the pro-apoptotic factors and promoting the anti-apoptotic factors has been proven neuroprotective upon RGC injury. *Bax*$^{-}$/$^{-}$ mice exhibit complete abrogation of RGC soma death after optic nerve crush, and in a chronic glaucoma model. However, mutation of the *Bax* gene does not prevent optic nerve damage. Overexpression of Bcl-2 prolongs RGC survival after optic nerve lesions, and excess Bcl-x has been demonstrated to prevent RGC loss in rat axotomy models (Qu *et al.*, 2010).

Bcl-2 family proteins can be categorised according to their physiological role in the cell in modulating mitochondrial function and integrity, such as Bcl-2 and Bcl-xL (Sattler *et al.*, 1997). These two factors, along with the pro-apoptotic proteins BAX, BAK and BIM, promote the release of cytochrome c from the mitochondrion into the cytosol (Green and Reed, 1998, Gross *et al.*, 1999). Another anti-apoptotic group of proteins, such as FLIP inhibit pro-apoptotic caspases by blocking their activation (Kataoka *et al.*, 1998, Safa *et al.*, 2008).

Attempts to modulate apoptotic pathways for therapeutic prevention of a number of diseases have recently received much attention. For example, small molecule inhibitors of BCL-2 or mimetics of Smac/DIABLO (second mitochondria-derived activator of caspases/ direct IAP binding with low pl) oppose the actions of XIAP, a potent anti-apoptotic enzyme, have recently been shown to promote the antineoplastic activity of conventional cytotoxic agents. It is expected that an improved understanding of apoptosis regulation will provide important leads for the development of novel anti-tumour strategies (Harada and Grant, 2003). This notion is based on the belief that defects in apoptotic signalling can disturb the balance between cell proliferation and cell death. Overexpression of antiapoptotic

proteins is associated with numerous forms of human cancers. As such, the development of therapies that induce apoptosis is a promising strategy for treating cancerous tumours (Dubrez *et al.*, 2013, Hennessy *et al.*, 2013, Bai *et al.*, 2014, Perez *et al.*, 2015).

1.4.1.2. The extrinsic apoptosis pathway

The extrinsic caspase pathway, also known as the death receptor pathway, is initiated by ligation of tumour necrosis factor-α (TNF-α) or Fas ligand (FasL) to their receptors (*i.e.* TNFR, FasR, respectively) on the cytoplasmic membrane (Krammer *et al.*, 1994) (Figure 1.6). The death domain of the death receptors form clusters with procaspase-8 via adaptor proteins (Qu *et al.*, 2010). The death-inducing signaling complex (DISC) is formed and cleaves caspase-8 to activate it, which in turn can activate caspase-3 and -7. Caspase-3 then activates caspase-6 and -2, and caspase-6 in turn activates caspases-8 and -10, both containing death effector domains (DEDs) for auto-activation of the initiator caspase (Lendeckel *et al.*, 2005). TNF also activates survival pathways through nuclear transcription factor kappa B (NFkB), which is known to have an antiapoptotic role (Wajant *et al.*, 2003) The activation of TNF- α promotes degradation of NFkB inhibiting protein; nuclear factor of kappa light polypeptide gene enhancer in B-cells inhibitor alpha (IκBα), thus releasing NF-κB.

1.4.1.3. The intrinsic apoptosis pathway

The intrinsic caspase cascade is triggered by mitochondria that receive apoptotic stimuli, such as neurotrophin deprivation and oxidative stress (Qu *et al.*, 2010). Although the initial steps of the intrinsic pathways are not clear, they all eventually converge onto the mitochondrion, which in turn releases cytochrome c from the intermembrane space into the cytosol (Figure 1.6). Cytochrome c binds to the apoptotic protease activating factor-1 (Apaf-1), which has CARD domains (Lendeckel *et al.*, 2005). Apaf-1 recruits procaspase-9 through CARDs leading to autoactivation of caspase-9, which then converts procaspase-3 into its active form. The release of cytochrome c is regulated by the *Bcl-2* family members (Qu *et al.*, 2010), and cytochrome c then binds to Apaf-1 and in the presence of dATP/ATP promotes assembly of the apoptosome (Acehan *et al.*, 2002). This large protein

complex then binds and activates procaspase-9. Activated caspase-9 also activates caspase-7, triggering the same downstream caspase cascade as caspase-8 does in the extrinsic pathway (Qu, *et al*, 2010).

1.4.1.4. Cytotoxic lymphocyte-initiated granzyme B pathway

Immune system cytotoxic T lymphocyte (CTL) and natural killer (NK) cells can induce apoptosis through granule formation within the lymphocyte and release into the target cell where perforin protein perforin polymerises at the cell membrane and form a non-specific ion pores on the cell membrane (Shi *et al.*, 1997). The granules also contain granzyme B, a serine protease that enters the cell through perforin channels (Shi *et al.*, 1996).

1.4.2. Inhibitors of apoptosis proteins (IAPs)

IAPs are a family of functionally- and structurally- related catalytic enzymes, which serve as endogenous inhibitors of apoptosis through modulating the activity of caspases (Altieri, 2010). There are eight conserved mammalian IAPs (Prunell and Troy, 2004), namely, Birc2/cellular IAP-1 (cIAP-1), Birc3/cIAP-2, Birc4/X-chromosome-linked IAP (XIAP), Birc5/Survivin, Birc6/Bruce/Apollon, Birc7/Livin/melanoma IAP (ML-IAP), testis-specific IAP (Ts-IAP)/ILP2 and neuronal IAP (NIAP) (See table 1.2 for chicken IAP list and properties). IAPs are characterised by the presence of one or more 70–80 amino-acid baculovirus IAP repeat (BIR) domains (Miller, 1999, Vaux and Silke, 2005) of either type I or II. Only type II BIR domains; namely, BIR 2 and BIR 3 possess peptide-binding groove (Hinds *et al.*, 1999). Some IAPs contain a carboxy-terminal really interesting new gene (RING)-zinc finger domain, which employs E3 ubiquitin ligase activity and enables IAP to catalyse ubiquitination (Joazeiro and Weissman, 2000). Caspase activation and recruitment domains (CARD) also can be found in some IAPs and allows for homotypic protein-protein interaction (Liston *et al.*, 2003; Kisiswa *et al.*, 2010) (Figure 1.7).

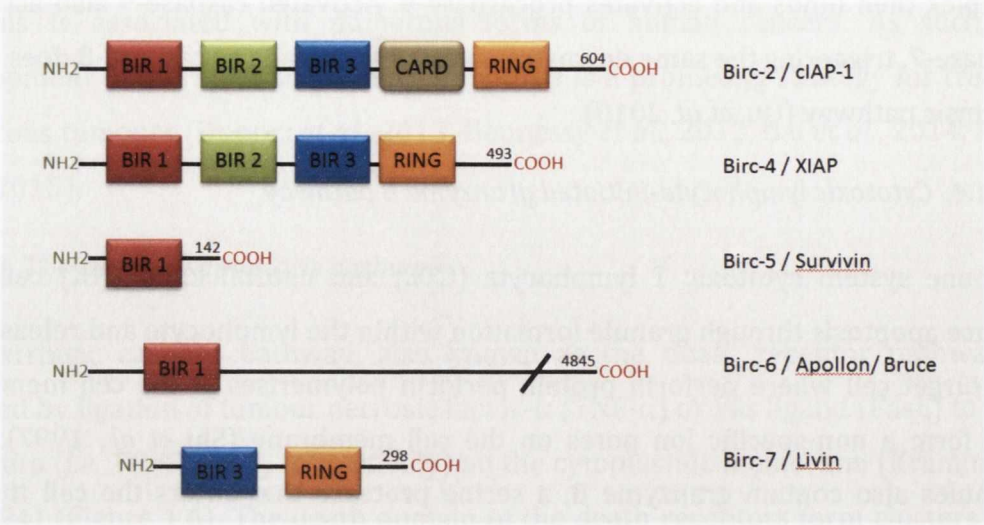

Figure 1.7. Structure of the five chicken IAPs. Each IAP contains one or more baculovirus IAP repeat; BIR domain of type I (BIR 1) or II (BIR 2 and 3). Some IAPs contain RING zinc-finger domain located at the extreme carboxyl terminus, which enables IAPs to catalyse ubiquitination of substrates. Only BIRC-2 includes caspase activation and recruitment domain; CARD that allows for protein-protein interaction. Figure adapted from Kisiswa *et al.* (2009).

IAPs can also be divided into two distinct groups according to their caspase-inhibition properties. Birc-2, -3, -4, -7 and -8 efficiently bind to and inhibit caspase-3, -7 and -9 and function as potent apoptosis inhibitors (Dai *et al.*, 2009), while Birc-5 (Survivin) and -6 do not bind to caspases or inhibit apoptosis directly (O'Riordan *et al.*, 2008). However, they both have a role in cell cycle regulation and are essential for cell viability. See Table 2 for listing and properties of the five IAPs in this study.

IAPs function by inhibiting the executioners of cell death, or by blocking the pathways that activate them. Additionally, IAPs can promote the transfer of ubiquitin to themselves through adaptor proteins, and balance between substrate and autoubiquitination is crucial for their physiological roles (Mace *et al.*, 2010).

Upon activation, Birc-4 (XIAP) suppresses the activities of caspase-3 and caspase-9 (Eckelman *et al.*, 2006). Activity of Birc-4 (XIAP) is blocked by binding to Smac/Diablo and Omi serine protease/Htr2A (high temperature requirement protein 2A) proteins released from mitochondria after pro-apoptotic stimuli (Yang *et al.*, 2000, Gray *et al.*, 2000, Verhagen *et al.*, 2002). Smac/Diablo is also released by

mitochondria along with cytochrome c. This protein neutralizes a set of endogenous inhibitor of apoptosis proteins (IAPs) that suppress the activities of caspase-3 and caspase-9. Moreover, X-linked IAP-associated factor I (XAFI), a nuclear protein, was identified as a potent Birc-4 (XIAP) antagonist (Liston *et al.*, 2001). IAPs, IAPs antagonists and caspases are the three main factors regulating the apoptotic cascade progress in many species (Wei *et al.*, 2008).

Table 1.2. The five chicken (*Gallus gallus*) IAPs of this study, and their properties

IAP	Other names	Biological role	Caspase-specificity	Endogenous inhibitors
Birc-2	cIAP-1; IAP-1; ITA	TNF-mediated signalling (Rothe *et al.*, 1995). Targeting caspases for ubiquitination (O'Riordan *et al.*, 2008)	Casp-3, -7, and -9	Smac/DIABLO (Verhagen *et al.*, 2000, Song *et al.*, 2003)
Birc-4	**XIAP**; IAP-3; ILP1	Directly inhibits apoptosis (Eckelman *et al.*, 2006)	Casp-3, -7 and -9 (Deveraux *et al.*, 1997)	Omi/Htr2A (Verhagen *et al.*, 2002)
Birc-5	**Survivin**	Apoptotic indirect inhibition (Ambrosini *et al.*, 1997), Embryonic development and mitotic regulation (Delvaeye *et al.*, 2009)	Casp-3 and -7	
Birc-6	Apollon; Bruce	Cell cycle regulation and embryonic development (Pohl and Jentsch, 2008) Regulates p53 and the mitochondrial pathway of apoptosis (Ren *et al.*, 2005)	Casp-3 and -9 (Ren *et al.*, 2005)	
Birc-7	Livin	Inhibits Apoptosis directly. Found in developing tissues and several tumour cell lines (Crnkovic-Mertens *et al.*, 2003).	Casp-3, -7 and -9 (Kasof and Gomes, 2001)	

1.4.3. Role of other proteolytic enzymes

Other enzymes in CNS, such as calpains, cathepsins and metalloproteinases (Chan and Mattson, 1999, Wride *et al.*, 2006, Lopatniuk and Witkowski, 2011, Yang *et al.*, 2011, Chakraborti *et al.*, 2012). Calpains are ubiquitous intracellular Ca^{2+}-dependent cystein proteases that are expressed in retinal neurons and the nerve fiber layer (Qu *et al.*, 2010). Cell culture models have confirmed that overactivation of calpains contributes to apoptosis in neurons. Overactivation of calpains is also known to be responsible for neurodegeneration in the animal models of CNS injuries such as spinal cord injury, and traumatic brain injury. Moreover, the inhibition of calpains and cleavage of calpains substrates both significantly protect the neurons in GCL from apoptosis following calcium ionophore treatment (McKernan and Cotter, 2007). It is strongly suggested that synergistic activation of calpains and caspase-3 for mediation of apoptosis is required (Sanders *et al.*, 2009a). The calpain pathway, as well as extrinsic and intrinsic caspase cascades ultimately converges to activate caspase-3 for mediation of apoptosis. Therefore, it is hypothesized that inhibition of one target preceding caspase-3 in apoptotic pathway may not provide enough neuroprotection. Additionally, inhibition of caspase-3 itself can provide sufficient neuroprotection in degenerative neuropathies.

The cathepsin family of proteolytic enzymes is involved in PCD of developing neurons (Uchiyama, 2001, Yamashima and Oikawa, 2009, Repnik *et al.*, 2012). Cathepsins, are among the most abundant lysosomal proteases. Proteases of the endosomal-lysosomal system degrade many proteins and cellular components as part of normal turnover, and the endosomal-lysosomal dysregulation is associated with pathological neural degeneration and aging.

Calcineurin is a Ca^{2+} calmodulin-dependent serine-threonine phosphatase (Wang *et al.*, 1999) (Qu *et al.*, 2010). It acts on Bad, a Bcl-2 member, which in turn dissociates and is translocated to the mitochondrial membrane where it binds to the anti-apoptotic Bcl-2 or Bcl-xL and promotes release of cytochrome c (Shou *et al.*, 2004). Calcineurin is expressed in RGC somas in rat, bovine and human retinas. Its role in the RGC death was detected in experimental glaucoma (Huang *et al.*, 2005).

It has been hypothesized that calpain may act through calcineurin to promote cell death in glaucoma. Cathepsin substrates in the CNS include myelin basic protein, neurofilaments, pro-forms of several hormones and neuropeptides (Liuzzo *et al.*, 1999). In contrast to caspases and calpains, cathepsin proteolysis is aimed at terminal protein degradation, rather than cleavage to modulate substrate activity, although there are exceptions to this generalization. In addition, cathepsins are optimally active in the relatively acidic environment of lysosomes (particularly cathepsin D), even though some retain activity in neutral biological conditions (cathepsin B). Cathepsins have been linked to early stages of caspase-dependent and caspase-independent cell death pathways in non-neural cells. Since a variety of cell types utilize cathepsin in apoptotic pathways, it is likely that they may contribute to apoptosis in neurons as well (Nakanishi, 2003, Mutka *et al.*, 2010).

1.5. Cell death in the developing retina

Retinal neurons, like in most other neural tissues, are produced in excess during neurogenesis, and then partially eliminated by a series of apoptotic waves, before finally achieving final mature, post-developmental state (Young, 1984, Sanders and Wride, 1995, Papermaster, 1997, Frade *et al.*, 1997, Cook *et al.*, 1998, Blaschke *et al.*, 1998, Clarke *et al.*, 1998, de la Rosa and de Pablo, 2000, Vecino *et al.*, 2004, Guerin *et al.*, 2006, Valenciano *et al.*, 2009). Indeed, it has been reported that up to 90% of neurons in RGL undergo PCD during the retinal development of rat (Galli-Resta and Ensini, 1996). Counts of axons within the optic nerve at progressive developmental stages have suggested massive RGC death during development (Linden, 2006). In the chick, for example, nearly four million axons are present at the peak (E10-11) (Rager and Rager, 1978), plummeting to about two and a half million eight days later. Nevertheless, the relative frequency of dying cells, based on TUNEL-positive profiles, in the different layers of the retina has raised the possibility that naturally occurring cell death may affect different cell types to markedly different extents. In Mayordomo *et al.* (2003) study, the spatial distribution of TUNEL-stained cells did not correlate with the proliferating

neuroepithelial cells, as detected by BrdU immunostaining, in the central retina (Figure 1.8). Apoptotic cells were detected as early as E2 in association with the optic stalk, and the peak period of cell death was at E4.

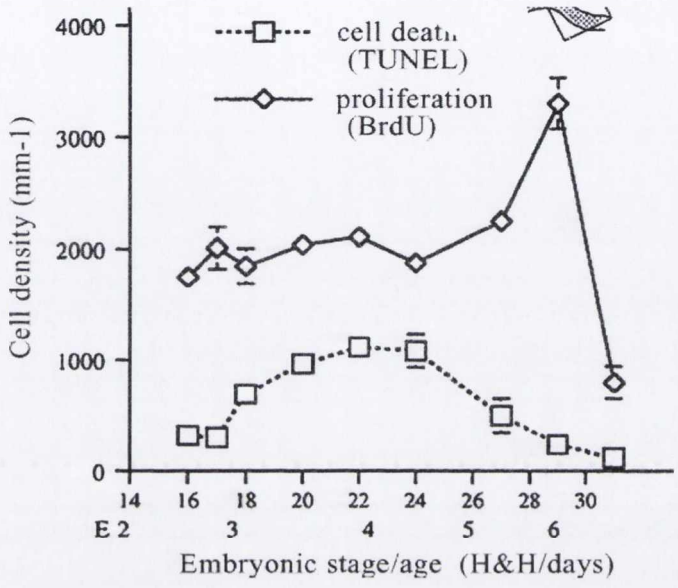

Figure 1.8. Temporal pattern of naturally dying, and proliferating cells in the early embryonic central chick retina. Apoptotic cells were detected by TUNEL-staining, and proliferation by BrdU immunostaining. From Mayordomo *et al.* (2003)

It is well established that apoptosis is involved in the embryonic development of the brain (Yoshida *et al.*, 1998) and that PCD affects neural stem cells, proliferating progenitors, projecting neurons as well as other types of differentiated neurons and glia. (de la Rosa and de Pablo, 2000, Boya and de la Rosa, 2005, Chavarria *et al.*, 2013). If RGC axonal projection fails to properly innervate its target, it suffers deprivation of trophic factors and undergoes death.

1.5.1. Cell death waves in the developing chick retina

Neuronal retinal cells undergo several developmental stages of death (See Table 1.3). PCD in the vertebrate retina has been categorized by Valenciano *et al.* (2009) according to the developmental phases in which they occur into three phases; morphogenic cell death that is related to optic vesicle invagination, optic cup invagination and closure of the optic fissure; early neural cell death, affecting

proliferating neuroepithelial cells and recently born neuronal cells; and the well characterized neurotrophic cell death, which affects differentiated neurons (Valenciano *et al.*, 2009). In the chick embryo, the first wave of cell death occurs as early as E 2.5 determined by the presence of pyknotic nuclei in the neuroretina (Cuadros and Rios, 1988, Martin-Partido *et al.*, 1988, Trousse *et al.*, 2001). Early neural cell death takes place between E2.5 - 6 (HH17 - 25 or 26) (Frade *et al.*, 1997, Diaz *et al.*, 2000, Mayordomo *et al.*, 2003). Finally, the last wave of cell death, or the neurotrophic cell death phase, occurs during neurons maturation and synaptogenesis between E10 - 14 (HH36 - 40) after neurons form synaptic connection with their brain targets (Rager, 1980, Cook *et al.*, 1998, Chavarria *et al.*, 2007). Autophagy was reported to be vital for proper retinal neurogenesis (Boya *et al.*, 2008), particularly at the early phase associated with morphogenesis and RGC generation (Mellen *et al.*, 2009).

Table 1.3. Programmed cell death waves in the neuronal retina in developing chick (*Gallus gallus*) embryo

Cell death wave	Embryonic stage (age)	Technique	Specialised tissue/cells	Reference
(1)Morphogenetic	E2(HH12) - E2.5(HH17)(peak HH 15) E2.5-E4(HH23)	Quantitative microscopy In vivo BrdU incorporation and TUNEL	Ventral retina Neuroretina	(Cuadros and Rios, 1988) (Martin-Partido *et al.*, 1988) (Chavarria *et al.*, 2013)
(2) Early	E4-E6(HH28,29) E3(HH18)-E4.5 (HH24)	Release of free Nucleosomes or TUNEL TUNEL	Central retina	(Frade *et al.*, 1997, Diaz *et al.*, 2000) (Mayordomo *et al.*, 2003)
(3) Neurotrophic (Late)	E10(HH36)-E14(HH40) E7(HH30,31)-E18(HH44) (peak E13(HH39))	Quantitative electron microscopy Propodium iodide or TUNEL	RGCs GCL	(Rager and Rager, 1979) (Cook *et al.*, 1998)

Cell death in the embryonic chick retina was reported to be reduced to up to 50% as a result of *in vivo* treatment with caspase inhibitors z-DEVD-fmk and Boc-D-fmk within 6 hours, and evident increase in the number of RGCs was detected as well. Morphological abnormalities of these treated retinas at this early period of development were shown, resulting in slight retinal widening due to the enlargement of the GCL (Mayordomo et al., 2003). An inhibitor of other proteases other than caspases had been used as control. Leupeptin, the proteases inhibitor, did not affect the number of TUNEL. This finding supports the notion that the RGC generation is modulated by caspase-dependent cell death. However, it has been shown that the ganglion cell axon growth and navigation towards the optic fissure was not affected (Mayordomo *et al.*, 2003).

The exact role of cell death in retinal formation remains largely speculative (Mayordomo *et al.*, 2003). Since 1988, Cuadros and Ríos suggested that early cell death in the central retina may have a role in navigation and exit of RGCs axons from the eyeball to the optic stalk. Early cell death in the vertebrate retina is concentrated in the central optic disc region, which further supports the former hypothesis. However, de la Rosa and de Pablo (2000) discussed a complementary role for early cell death in the retina, its involvement in the control of neurogenesis. Moreover, de la Rosa suggested the role of target-derived neurotrophic factors in the protection of projecting neurons from PCD. The neurotrophic theory has expanded to include the trophic dependence of different types of neurons and glia at early and late developmental stages (de la Rosa and de Pablo, 2000).

1.5.2. Cell differentiation in the chick developing retina

Retinal cell differentiation has been widely studied in several species including the chick embryo (Prada *et al.*, 1991, Harris, 1997, Hicks, 1998, Reh and Levine, 1998, Cepko, 1999, Adler, 2000). These studies have shown that there are important similarities, but also many differences in retinal cells differentiation among various species. A simple, morphologically homogenous neuroepithelial cell layers of the optic cup proliferate into a diverse cell types, both neuronal and glial, and becomes arranged into an orderly laminar pattern and selectively interconnected with each other.

Retinal cell differentiation tractability studies using tritiated-thymidine (^{3}H-TdR) or 5'-bromo-2'deoxy-uridine (BrdU) labelling methods and have been employed along with terminal deoxynucleotide-transferase mediated nick end labelling (TUNEL) and in combination with cell-specific markers to investigate the neurogenesis and cell death of each cell type (Bruhn and Cepko, 1996, Belecky-Adams *et al.*, 1996, Liu *et al.*, 2000, Chavarria *et al.*, 2013). Proliferation, differentiation and cell death progression coincide with overlapping distribution patterns of proliferation, differentiation and cell death (Adler, 2000, Chavarria *et al.*, 2013).

A number of DNA-binding transcriptional factors are reported to be involved in controlling the differentiation of the different retinal cell types (Toy *et al.*, 2002). Candidate factors identified in the chick retina include Eya2, GH6, NeuroD, NeuroM, SOHo and otx2 (Stadler and Solursh, 1994, Deitcher *et al.*, 1994, Bovolenta *et al.*, 1997, Roztocil *et al.*, 1997, Yan and Wang, 1998, Mishima and Tomarev, 1998).

In vivo, neuronal differentiation of retinal precursor cells precedes the differentiation of the photoreceptors (Austin *et al.*, 1995), in contrary to the case *in vitro* where these progenitor cell differentiate into photoreceptors first. It was proposed that absence of neurons-induced signals is the reason for this variation (Ballios, 2012, Adler and Hatlee, 1989). Moreover, the developmental potential of the pigmented epithelial (PE) cells is not completely restricted to generate PE cells only. Until embryonic day 4.5 in chick embryos, cells are able to switch their phenotype and differentiate into neural retinal progenitors when treated with fibroblast growth factors (FGF) (Pittack *et al.*, 1991). However, this transdifferentiation of retinal pigmented epithelium (RPE) seems to be a distinct feature for some species but not others. It has been reported during development of amphibians, such as frog, and the chick embryo (Reh *et al.*, 1991).

1.5.3. Factors regulating cell death in the retina

A number of factors ranging from trophic factors to growth hormones, as well as neurotransmitters and the electrical activity of neighbouring neurons have been shown to affect cell death of retinal cell.

Growth factors play important role in earlier stages of neurons development in the retina, *i.e.* proliferation and differentiation (Lewin and Barde, 1996). NT-3 regulates neuron differentiation and survival of retinal cells (Bovolenta *et al.*, 1996). BDNF acts as survival factors in the newly born RGCs (Frade *et al.*, 1997). Also endogenous NGF induces cell death of retinal neurons via p75 receptor (Frade *et al.*, 1996). Similarly, Proinsulin mRNA and proinsulin/insulin immunoreactivity were detected in the developing retina, and were found to possess a survival effects in rat (Valenciano *et al.*, 2009) and chicken (Waldbillig *et al.*, 1991, Hernandez-Sanchez *et al.*, 1995, Chavarria *et al.*, 2007). It was suggested that these effects are achieved by interfering with the action of cell death executors, namely, caspases and cathepsins. Another emerging neuroprotective factor is Neuropeptide Y (NPY) that has been shown to induce proliferation and to exert a neuroprotective effect on rat and other non-mammalian species retinal neurons (Santos-Carvalho *et al.*, 2013, Santos-Carvalho *et al.*, 2014). Furthermore, anti-apoptotic factors are being investigated as potentially therapeutic targets for pathologies of retinal degenerative disorders, such as glaucoma and diabetic retinopathy as well as different cancerous conditions (Doonan and Cotter, 2004, Hiss and Gabriels, 2009, Doonan *et al.*, 2012, Fulda and Vucic, 2012, Hensley *et al.*, 2013, Hassan *et al.*, 2014, Chinskey *et al.*, 2014).

1.6. Biological significance of utilising chick embryos as a model for studying the role of IAPs on RGCs

The embryonic avian retina is a classical vertebrate CNS model for the study of neurogenesis (Prada *et al.*, 1991, Adler, 2000). The relatively large size of the eye and the embryo as a whole, the accessibility for visualization, availability of eggs all year-round, its rapid development and the ease of manipulating precise stages of embryogenesis, make the chick embryo a favourable model for studying the early development of the eye and CNS in general (Lemmon and Gottlieb, 1982, Belecky-Adams, 2008). The eye develops entirely within a relatively short period of embryogenesis, and manipulating the retina within the egg is made possible by many techniques, such as *in ovo* electroporation (Dezawa *et al.*, 2002) with its application of reporter gene assay, gene over-expression and gene knock down. The

chick embryo resemble the human embryo at the anatomical and molecular levels making it a significantly important model organism (Vergara and Canto-Soler, 2012).

Hamburger and Hamilton (1951) specified the chick embryonic development stages (HH), a series of 46 chronological stages in chick development, starting from laying of the egg and ending with the hatching of the chick. Each embryonic age denoted by embryonic day (ED or E) is a series of normal stages of development (denoted by a number from 1 to 46) . A number of factors including: normal genetic variations amongst individual embryos, seasonal differences in the viability, freshness and size of egg and the type of used incubator can cause the inconsistency of the correlation between chronological and structural age (Hamburger and Hamilton, 1951).

Moreover, the chicken genome sequencing was completed in 2004 (Stern, 2005). Many useful chick resources online are now available such as National Center for Biotechnology information (NCBI) Genome database (http://www.ncbi.nlm.nih.gov/genome/guide/chicken), Ensmbl (http://www.ensembl.org/) and ChickEST Database- UMIST (http://www.chick.manchester.ac.uk/). The application of chicken genetic and genomic tools is made possible and allows for robust molecular analysis of a wide variety of cellular signalling and pathways.

1.7. Hypothesis and aims

1.7.1. Hypothesis

IAPs and caspases are differentially expressed, at the genetic and proteomic level, in the developing neural retina of the chick (*Gallus gallus*) embryo. These two groups of enzymes, or at least some of them, have a regulatory role in the programmed apoptotic cell deletion mechanism of the neural retinal tissue during normal embryonic development. Lastly, temporal and spatial gene and corresponding protein expression of these regulatory enzymes (IAPs and caspases) are directly correlated.

1.7.2. Aims

1 - To test whether or not chicken IAPs and caspases genes and proteins are expressed during embryonic development of the neural retina of the chick embryo.

2 - To characterise the temporal pattern of expression of IAPs and caspases in chick retina development *in vivo* throughout early and late developmental stages (from E4 to E16). Both gene and protein relative expression levels are the aim of this study.
3 - To correlate temporal gene and corresponding protein expression of selected IAPs and caspases throughout the embryonic development.

4 - To localise selected enzymes in the whole neural retinal tissue by means of immunohistochemical analysis (IHC) and to relate this to programmed cell death in the developing retina identified using the TUNEL technique.

2.1. Chick embryos

Fertilised Ross 1A hens eggs (Enfield Broiler Breeders Ltd., Co. Kildare) were labeled and incubated in a humidified incubator at 38.4°C for the ten designated ages (Embryonic day (E) 4, E5, E6, E7, E8, E9, E10, E12, E14, E16). Unhatched early stages embryos (E4-E7) were anesthetised by hypothermia and removed from the egg and staged according to Hamburger and Hamilton (H and H) (1951) through the 24-hours increment of development (see appendix I for H & H stages corresponding to the ten embryonic days time points). Staging in 24 hour time points is denoted by embryonic days (E). Each embryonic age includes a series of normal stages based on the length of time of incubation. Embryos were decapitated and dissected to isolate the eyes in ice cold phosphate buffered saline (PBS) (see appendix III). Older embryos (E8-E16) were immediately decapitated upon removal from incubator and out of the egg, and then staged according to H and H (See Appendix I(A) for embryo staging).

2.2. Microdissection and retina extraction

Whole neural retinal tissues were obtained from embryos eyes by microdissection using N° 5 Watchmaker's forceps in ice cold Tyrode's solution (see Appendix III). The neural retina was separated from the retinal pigmented epithelium (RPE) to extract the translucent neural retina (Figure 2.1) and immediately stored in RNA*later*® (Ambion- Life Technologies, Carlsbad, CA, USA) or in TRIzol® Reagent (Ambion) for storage and direct RNA extraction. Different pools of neural retina samples were obtained for each of the ten designated ages (See Appendix I(B) for number of retinal tissue samples per each sample pool).

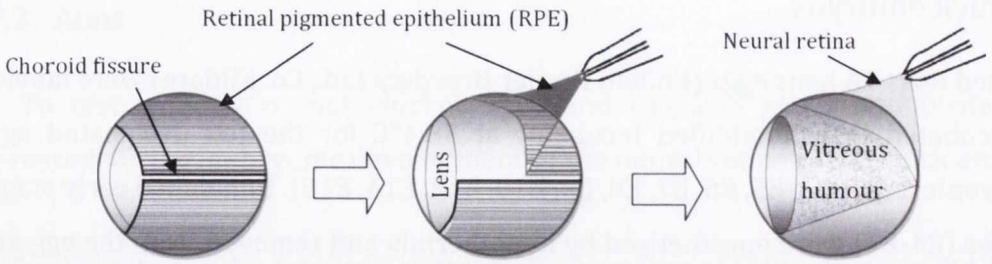

Figure 2.1. Schematic diagram of neural retina extraction by microdissection. The pigmented epithelium is peeled off the eye globe starting from the choroid fissure where it is less intact revealing the translucent neural retina directly surrounding the jelly-like vitreous humour globe. The neural retina is extracted using microdissection forceps.

2.3. RNA extraction and integrity check

TRIzol® Reagent (Ambion), or GenElute™ Mammalian Total RNA Miniprep Kit (Sigma Aldrich, Gillingham, UK) were used to extract total retinal RNA at the different stages of development as per manufacturer's protocol. GenElute combine the advantages of a silica-based microspin system, elimination of alcohol precipitation and the harmful organic compounds; phenol and chloroform.

TRIzol Reagent (Ambion) was used to extract total retinal RNA at the different stages of development as per manufacturer's protocol. Briefly, neural retina tissues were homogenised in TRIzol in 1:10 volume ratio in 1 ml glass tissue grinder (Wheaton, Millville (NJ), USA) for at least 1 minute and then transferred to a 2 ml RNase-free centrifuge tube and left to incubate at room temperature for 5 minutes. Chloroform was added to the homogenised sample with vigorous shaking then incubated for further 2 minutes prior to centrifugation (ALC International S.r.l., Cologno Monzese (MI), Italy) at 12'000 g (12'000 rpm for 7.5 cm rotor radius) for 15 minutes at 4 °C. The upper aqueous solution containing RNA is transferred into a new 2 ml Eppendorf tubes. 0.5 ml of 100% isopropanol (2-propanol or isopropyl alcohol) for each 1 ml TRIzol is added and the mixture was allowed to incubate for 10 minutes then centrifuged again for 10 minutes. The white pellet formed was washed with 75% ethanol and centrifuged at 6500 g for 5 minutes, the wash was discarded and the RNA was resuspended in RNase-free water. RNA samples were stored at -80 °C for long term storage, or at -20 °C.

Chapter 2

General Materials and Methods

When GenElute™ Mammalian Total RNA Miniprep Kit (Sigma Aldrich) was used for RNA extraction, retinal tissue was lysed and homogenized in guanidine thiocyanate to release RNA and 2-mercaptoethanol (2-ME) that inactivates RNases. A lysis mixture was prepared according to the manufacturer's instructions by mixing 10 µl of 2-ME for each 1 ml of Lysis Solution. Neural retina tissues were transferred very quickly from RNA*later* solution to the lysis solution/2-ME mixture, quick transfer was essential to minimise RNA degradation. Early stages retina tissue samples were very delicate and loose and were difficult to weigh, so an estimated amount of 20 mg was lysed in 250 µl of lysis mixture. For older embryo retina samples were tissues are harder and easier to handle, about 40 mg of tissue were lysed in 500 µl of lysis mixture. Samples in lysis mixture were immediately homogenised in 1 ml glass tissue grinder for 1 minute then tissue homogenate were pipetted into the provided 2 ml filtration column and centrifuged at maximum speed (12'000 g) for 2 minutes. A filtration column with 250 or 500 µl of 70% ethanol solution was added into each filtered lysate for the binding step, according to the starting lysis mixture volume. Lysate/ethanol mixture was pipetted into provided 2 ml binding columns, centrifuged at maximum speed for 15 seconds and the flow-through liquid was discarded. The collection tube with the filtered sample was kept and used for On-Column DNase I Digestion (Sigma-Aldrich) prior to washing steps. For each preparation 10 µl of DNase I was mixed with 70 µl of DNase Digest Buffer and the mixture was directly added onto the filtered sample in the binding column and allowed to incubate at room temperature for 15 minutes. 250 µl of provided Wash solution 1 was pipetted into each column and centrifuged at maximum speed for 15 seconds. The binding columns were transferred to a fresh 2 ml collection tubes. Another wash were applied with 500 µl of Wash solution 2. A third wash with 500 µl of Wash solution 2 followed by centrifugation for 2 minutes resulted in drying the binding tube. Elution final step involved transferring the binding column after the third wash into a fresh 2 ml collection tube and addition of 25-50 µl Elution solution into the binding columns then centrifugation at maximum speed for 1 minute. Aqueous flow-through eluates containing purified RNA were collected and stored at -80°C or used immediately for detection of RNA concentration and integrity check and cDNA synthesis. RNA yield was quantified with *Qubit*® fluorometric quantitation (Invitrogen, Paisley, UK) using 1 µl of RNA sample for each measurement as per the

provider's protocol. Subsequently, RNA quality was assessed by non-denaturing 1% agarose gel electrophoresis. Fresh 1% agarose gel was prepared using 1x Tris-Borate-EDTA (TBE) buffer (Sigma-Aldrich) and GelRed nucleic acid stain (Biotium, Inc., Hayward, CA, USA), 5 µl of RNA sample (between 0.2 and 7 µg/µl) was mixed with 1 µl gel loading solution (Sigma-Aldrich), heated RNA sample aliquots at 70 °C for 1 minute and placed on ice before loading the total volume into the gel and running electrophoresis at 100 volts (V) (10V/cm) for 40 minutes. RNA sampled integrity ranged from intact to degraded. Intact RNA gave two distinct bands, 28S ribosomal RNA (rRNA) and lighter 18S rRNA with the ratio 2:1 (28S:18S). Only intact and partially degraded RNA samples were used for downstream cDNA synthesis. Partially degraded RNA is assessed in the gel by means of detecting a smearing along the sample lane instead of the two distinct two rRNA subunits bands, while completely degraded RNA is indicated by a low molecular weight smear below the 18S rRNA band. Gels were visualised by VWR GenoPlex gel doc system (VWR) and images were captured using GenoCapture 7.01 software (VWR).

2.4. Conventional semi-quantitative PCR

2.4.1. Principle

Developed in 1983 by Kary Mullis, Polymerase chain reaction (PCR) is the technique utilising *Taq* DNA polymerase enzyme, from heat-resistant *Thermis aquaticus* bacteria, to amplify target DNA template exponentially *in vitro* allowing for detection of the accumulated amplified product (about 10^5 copies of the starting target sequence) to quantify gene expression. This technique also utilises gene-specific up- and down-stream oligonucleotide primers optimised conditions for the amplification.

Essentially, three thermal steps repeating cycles (20-35 cycles) are taking place, where two template DNA strands are denatured at 95 °C by non-enzymatic disruption of hydrogen bonds resulting in single stranded DNA. Optimal cell cycle number has to be determined through trial to eliminate false non-specific signal during cDNA amplification. The next step is annealing where the primers tag the two ends of the target gene segment by ionic bonds at an optimised temperature for the

primers annealing (T_a) (usually between 55 and 72°C depending on primers structure and length determined by their design). The extension step at 70°C is where polymerase enzyme attaches to the newly formed short segment of double stranded chain to facilitate the formation of complement structure to the longest segment of DNA (template) utilising the four nucleotide mix; dNTPs (deoxynucleotide triphosphates). The annealing temperature is typically 5 °C below the primer's calculated melting temperature (T_m), which is the temperature at which 50% of the primers and their complementary structure are in formation.

Post-amplification detection is required to visualize the PCR amplicon bands through agarose gel by running electrophoresis. This detection is an end-point and therefore the optimised number of cycles for each target gene has to be reached. Another limitation to this technique is the possibility of cross-contamination of the PCR product samples during the post-amplification detection step.

2.4.2. Primer design

PCR primers are single-stranded oligonucleotide chains used to identify and hybridise to the beginning (forward or upstream) and the end (reverse or downstream) of the target gene. PCR primers optimal length is between 18 and 30 base pairs (bp) to ensure enough length for adequate specificity but short enough to bind easily to the template at the annealing step. The Basic Local Alignment Search Tool (BLAST), a powerful bioinformatic tool, uses an algorithm to compare the high scoring sequence alignment of a query sequence against the basic biological sequence library of genes and proteins of interest for potential targets. Nowadays, BLAST is used in combination with the Primer3 program (Rozen and Skaletsky, 1998) for straightforward and more sensitive design of new target-specific PCR primers using primer-BLAST software (Ye *et al.*, 2012). 15 target genes (five IAPs and ten caspases) and the house-keeping gene β-actin were designed for this study

2.4.2.1. Procedure

Sequences for all 15 target genes and β-Actin control gene were obtained from NCBI , and primers were designed across exon-intron boundaries near the 3^{l} prime end of the gene by using primer-BLAST tool (http://www.ncbi.nlm.nih.gov/tools/primer-

blast/) based on their nucleotide sequence obtained from NCBI gene database (http://www.ncbi.nlm.nih.gov/nucleotide) (Table 2.1.) with limiting the product size to 100-150 bp, melting temperature between 61.5 and 66.5 °C and the primers with least percentage GC value were selected.

Primers (Sigma Aldrich) for the following 16 genes were designed; β-actin (endogenous endogenous control gene), Birc-2 (a.k.a.cIAP-1), Birc-4 (X-chromosome linked IAP; XIAP), Birc-5 (Survivin), Birc-6 (Apollon/Bruce), Birc-7 (Livin), Caspase-1, Caspase-2, Caspase-3, Caspase-6, Caspase-7, Caspase-8, Caspase-9, Caspase-10, Caspase-17 and Caspase-18.

Table 2.1. Primers of this study, nucleotide sequence, predicted product size and optimum PCR conditions

Gene Name	Primer Sequence	T_m (°C)	Ta	Number of Cycles	Product Size
Birc-2 (cIAP-1)	F AGCATGAAGTATGTTCCCACAG	52.5	56	32	136
	R AGTGCCCACACGGAATAAAA	51.8	56		
Birc-4 (XIAP)	F AAAGGGAGAACCACCAAAAG	49.8	56	34	138
	R TGACCACAGGGAATGAGGA	51.5	56		
Birc-5 (Survivin)	F CTGGATAAAAAGCGGACCAA	50.2	57	28	263
	R CACCGTAGACCCAGAGGAAC	53.6	57		
Birc-6 (Bruce)	F AGGCAGAACTATGTCCCATCA	52.5	58	30	130
	R ACTGCATTTTTCCACGGAGT	52.1	58		
Birc-7 (Livin)	F TGCCAAATGGTATCCAAGGT	51.1	56	35	132
	R CGTCGGAGCTGTTCTTCTGT	54.3	56		
Casp-1	F CGGATGGCTGGAGATGTGT	53.6	60	30	127
	R GAACCTTCTGTGGGGCTTCT	53.6	60		
Casp-2	F GGGACACTCATGTGGCTGA	53.4	60	28	128
	R CACGCCTGTGAGAACAGAAA	52.7	60		
Casp -3	F GGTATTGAAGCAGACAGTGGA	51.8	58	30	146
	R CACAGAGACTGAATAAACCAGGA	51.9	58		
Casp -6	F GGCAGACAGAAACAATCTGAAA	51.3	58	28	146
	R CACAAACAAAGCAGTCAGCA	51.7	58		
Casp -7	F GGAAACAGATGCCAATCCT	49.3	60	32	130
	R GCACAGAGACTGCACAAACC	54.0	60		

Casp-8	F TGTCTCCTACAGAAGCCCAAG	53.1	60	30	138
	R TCAATCTTGCTGCTCACCTC	52.1	60		
Casp -9	F ACCTTGGACAGCGTACTGGA	54.9	58	30	103
	R TCTGCTTGTACCTCCCCTTG	53.1	58		
Casp -10	F GGCATGTTCAGGAGGGTACTT	53.7	60	32	140
	R TGTCCCATAACGGTCAACAC	52.0	60		
Casp -17	F CGCGGAGAGACCCAAAGT	53.6	58	32	128
	R CACAAACACCCCCTGGTC	52.0	58		
Casp -18	F TGGCATGGCTACTGTGGA	52.3	58	35	150
	R CCCACTTCCTTGTTCACTTCT	51.9	58		
β-Actin	F GCTACAGCTTCACCACCACA	54.4	62	22	119
	R CAGGGAAGAGCTAGAGGCAG	53.4			

2.4.3. cDNA synthesis

cDNAs for each embryonic age were selectively made from mRNA template isolated from the appropriate embryonic age and amplified for all the 15 target genes for semi-quantitative and quantitative estimation of the target genes expression levels using β-actin as house-keeping gene.

Total RNA was treated with DNA-*free*™ DNase Treatment and Removal Reagent (Ambion) to eliminate any DNA trace contamination from RNA samples by means of utilising recombinant DNase I (rDNase I) enzyme, which is subsequently removed from the reaction medium by an inactivation reagent. The first step included the addition of 1 µl DNase I in 1X DNase I buffer in a 25 µl final reaction volume. Samples were incubated at 37° C for 30 minutes. Then 2.5 µl volume of resuspended DNase Deactivation reagent was added and allowed to incubate at room temperature with occasional mixing. Tubes were centrifuged at 8'000 **g** for 2 minutes. Finally, RNase ONE™ Ribonuclease (Promega, Southampton, UK) digestion of RNA for cDNA samples purification according to the manufactures protocol was carried out as a final step. 0.5 µl of ribonuclease enzyme was added to each aliquot of cDNA samples and allowed to incubate at 37° C for 20 minutes.

Three commercially available cDNA synthesis kits were used in this study. Either of GoScript Reverse Transcription System (Promega), iScript™ cDNA synthesis kit (Bio-Rad, Hamel Hempstead, UK) or Tetro cDNA synthesis kit (Bioline, Taunton (MA), USA) was used for cDNA synthesis from the total RNA samples Table 2.2 compares the three kits protocol.

Each cDNA synthesis reaction utilised dNTPs, oligo(dT) primer, random primers in an optimised buffer and Moloney Murine Leukemia Virus reverse transcriptase (MMLV-RT), which is an RNA-dependent DNA polymerase that can be used for cDNA synthesis with long messenger (m)RNA templates (>5 kb). No-RT-control samples (No-RT) were run in parallel.

Table 2.2. Comparison of three cDNA synthesis protocols.

GoScript	iScript	Tetro cDNA synthesis kit
Step (1) 300 ng- 1 µg RNA-containing sample volume was mixed with Oligo(dT) and random primers (0.1 µg/reaction) and nuclease-free water up to 5 µl final volume. (2) The mixture was heated at 70° C for 5 minutes, then chilled in ice for another 5 minutes and centrifuged for 10 seconds. (3) 15 µl Reverse transcription mix/reaction was made by adding 4 µl 5X buffer with 2.4 µl $MgCl_2$, 1 µl 0.5 mM of each dNTP, 1 µl reverse transcriptase and 6.5 µl nuclease-free water. (4) 15 µl RT mix was added to 5 µl sample mix. Thermocycler RT reaction as follows: 25° C for 5 minutes 42° C 5 minutes (5) Reverse transcriptase enzyme was inactivated by incubation at 70° C for 15 minutes.	(1) RNA sample was added to 4 µl 5X reaction mix, 1 µl reverse transcriptase and water to bring final reaction volume to 20 µl. (2) RT reaction carried out in a thermocycler as follows: 25° C for 5 minutes 42° C 30 minutes 85° C 5 minutes	(1) RNA samples were added to 0.5 µM Oligo(dT) and 2 µM random hexamer primers and brought up to 12 µl total volume with molecular grade water. (2) Mixture was incubated at 70° C for 5 minutes then chilled on ice. (3) 1 µl of 10mM dNTP mix (2.5mM each) were added to the mix along with 4 µl of 5X buffer, 1 µl transcriptase and bring up to final volume of 20 µl. (4) Incubation at 42°C for 30 min. F) The reaction was stopped by heating at 95°C for 5 minutes.

No-RT-control samples were run in parallel with each cDNA synthesis by running at the same conditions excluding the reverse transcriptase enzyme.

2.4.4. Semi-quantitative PCR procedure

GoTaq® Flexi DNA Polymerase (Promega, Southampton, UK) for cDNA amplification was carried out to optimise PCR conditions to ensure highest yield and reducing amplification of non-specific products (See appendix III(A) for PCR reaction

conditions). Optimisation of PCR conditions facilitated setting the parameters for the following RT-qPCR validation analysis.

Semi-quantitative PCR was performed in triplicate using 1 µl cDNA in 20 µl final reaction volume. Green GoTaq® Flexi buffer was used to aid monitoring the migration progress during electrophoresis and increase sample density without adding other loading buffer. A mixture of dNTPs, 10 µM of each of the forward and reverse primers and DNA polymerase are added to the reaction and conditions were optimised in Biometra TProfessional Basic thermocycler (Biometra GmbH, Goettingen, Germany). Annealing temperature (Ta) for each primer pair was optimised by running PCR and running electrophoresis gel. Reaction products were analysed on 2% agarose gel containing 1X GelRed nucleic acid gel stain (Biotium) and run on electrophoresis with 1 kb Plus DNA Ladder (Invitrogen) at 100 V for 40-55 minutes.

2.4.4.1. Quantification of conventional PCR bands

ImageJ 1.45s (http://rsbweb.nih.gov/ij/) was used to determine gene specific bands intensity by means of measuring pixel size, and readings were exported to an Excel spreadsheet for further analyses. Relative expression levels were estimated for all 15 target genes normalised to the β-Actin control gene. Each individual band reading for each of the ten ages was normalised to its corresponding β-actin band reading for correction of variation in sample size, RNA quality and quantity and reverse transcription (RT) efficiency (Thal *et al.*, 2008). Semi-quantitative PCR was performed in triplicate to initially determine the expression pattern for each of the 15 enzymes. Annealing temperature for each pair of primers and the duration of product elongation were also assessed and optimized.

Standard statistical analyses for comparing means were run using IBM SPSS 21 software and Excel statistical functions.

2.5. RT-qPCR

2.5.1. Principle

Fluorescence-based real-time quantitative PCR (RT-qPCR) is the most recent commonly used technology to quantify DNA and RNA products for gene expression evaluation. The validity of RT-qPCR studies depend on adequate handling of experimental settings, choice of appropriate reference (control) gene and statistical analysis of generated data.

2.5.2. Procedure

QuantiTect SYBR Green PCR Kit (Qiagen, Crawley, UK) was used for two-step RT-qPCR. For each reaction approximately 0.02 µg cDNA were amplified in 14 µl reaction volume by HotStarTaq DNA Polymerase using the same primers used for semi-quantitative PCR (Table 2.1). In a 96 wells optical microplate (Fischer Scientific, Loughborough, UK), 4 µl of cDNA sample was pipetted into 7 µl 2X SYBR Green PCR master mix, 0.75 µl of each primer and 1.5 H_2O. Microplates were sealed and mixed by tapping the microplate on a levelled surface for few seconds. In each microplate run, two genes were run with β-actin simultaneously for automatic normalisation, and assays were carried out in triplicate for each data point. Microplates were loaded to the Applied Biosystems 7500 Real-Time PCR system (See appendix III(B) for RT-qPCR conditions) running 7500 Real-Time PCR SDS v1.4.1 software.

QuantiTect SYBR Green PCR kit contains an optimized, ready-to-use 2X master mix with the fluorescent dye SYBR Green I, a balanced combination of K^+ and NH_4^+ions in the PCR buffer, HotStarTaq DNA Polymerase and 2′-deoxyuridine, 5′-triphosphate (dUTP) to prevent carryover from previous amplification amplicons.

SYBR Green I dye binds to double-stranded DNA and detect uracil-containing PCR amplicons, as it accumulate during PCR cycles. QuantiTect SYBR Green PCR master mix contains 2′-Deoxyuridine, 5′-Triphosphate (dUTP), which enable pretreatment of newly formed PCR product with uracil-N-glycosylase (UNG) in each cycle.

Melting curve analysis was performed for primers specificity analysis, and fluorescence specificity for target genes and β-actin was confirmed.

2.5.3. RT-qPCR data analysis

Relative quantification (RQ) in gene expression was determined using the $2^{-\Delta\Delta Ct}$ method (Livak and Schmittgen, 2001), and melting curve analysis was performed to confirm primers specificity. Fold changes were obtained for gene expression normalised to β-Actin control gene, and relative to E9 (internal calibrator).

2.5.3.1. RT-qPCR statistical analysis

Relative expression for target transcripts was represented as increased or decreased fold change normalised to the β-Actin control gene, and relative to E9 (internal calibrator). E9 was used as the calibrator as it resides in the middle of the embryonic ages selected and is at a stage were developmental apoptotic cell death is much reduced compared to the reported early and late waves of developmental cell death. Additionally, E9 represents the median value of the embryonic days. Mean data between two groups (target and calibrator) were assessed using two-way independent t-test or two-way ANOVA as appropriate, and significance was set at 95% confidence. IBM SPSS 21 software and Excel statistical functions were used for statistical analysis.

2.6. Western blotting (WB)

2.6.1. Principle

Also known as immunoblot, WB was first introduced by (Towbin *et al.*, 1979) is a routine analytical technique used to detect protein of interest in a tissue extract. By using sodium dodecyl sulphate-polyacrylamide gel electrophoresis (SDS-PAGE), native proteins are separated by 3-D structure or denatured proteins by the length of the negatively charged polypeptide, then transferred to a positively charged membrane and selective primary antibodies are applied in a diluted solution of blocking buffer. The membrane used for protein blotting is usually either a nitrocellulose or polyvinylidene difluoride (PVDF) transfer membrane resulting in the same imprint of proteins as the gel. Secondary antibody that is species-specific to the primary antibody is added where it is typically linked to a reporter enzyme such as horseradish peroxidase which has the ability to cleave chemiluminescent

agent. The reaction product produces luminescence in proportion to the amount of protein and bands image can be photographed.

2.6.2. Protein extraction and quantification

Eggs were incubated and retinae were dissected from eyes for the ten embryonic ages as described in 2.1 and 2.2. Whole neural retinas were collected for different embryonic ages. Pools of neural retina samples were processed for protein lysis with radio-immunoprecipitation assay (RIPA) buffer (Upstate (Merk Millipore), Darmastadt, Germany), containing Complete Protease Inhibitor Cocktail (Roche, Welwyn Garden City, UK) to eliminate activity of a multitude of protease classes including serine proteases, cysteine proteases, and metalloproteases. Samples then were incubated at 4°C with agitation for 30 min then centrifuged at 9,000 g for 30 min at 4°C. The supernatant was aliquoted and stored at -80°C for later analysis. Finally, Protein samples concentration was measured using *Qubit*® fluorometric quantitation according to the manufacturing protocol.

2.6.3. Western blotting procedure

2.6.3.1. Principle

Denatured proteins were separated by the length of the negatively charged polypeptide, and then transferred to a positively charged PVDF. Selective primary antibodies were applied for detection of target enzymes in the protein lysate sample solution. Species–specific secondary antibody linked to HRP was used for chemiluminescent detection.

2.6.3.2. Primary and secondary antibodies

Primary antibodies for recognition of target protein, Birc-4 (XIAP), Birc-5 (Survivin), Casp-3 and Casp-7 were chosen according to species-species amino acid sequence homology testing between chicken and other vertebrate species (see appendix IV for homology testing). Chicken antibodies for proteins of this study were not found by commercial providers. However, cross-species antibodies that react with chicken antigens were ordered (see Table 2.3 for list of primary antibodies from providers). Choice of primary antibody was based on the higher percentage of homology to

either human (*Homo sapiens*), mouse (*Mus musculus)* or rat (*Rattus norvegicus)*. All primary antibodies were raised in rabbit.
The secondary antibody was chosen to be against rabbit. HRP-labelled goat anti-rabbit was used (see table 2.3).

2.6.3.3. WB procedure

For separation of proteins, 12% SDS-PAGE was used, where 10 µg of total protein i for each of the ten developmental ages was loaded to each well. Electrophoresis was run for 90 minutes at 100 V using Bio-Rad Mini-Protean® 3 cell system in a standard Tris-glycine running (migration) buffer (See appendix II for composition of buffers).

Samples were loaded in a 30 µl final volume with Laemmli loading buffer after heating in 95°C for a few minutes. 15 µL protein marker (ColorBurst™ Electrophoresis Marker, Sigma-Aldrich) was loaded as reference for molecular weight, with unoccupied wells are loaded with 1X Laemmli buffer for better running.

After running, stacking gel was removed and running gel was stained with Commassie blue protein dye (Brilliant Blue R Concentrate- Sigma-Aldrich) for 4 hours at room temperature on agitation to fix and stain proteins, then washed in a mixture of 67% dH_2O, 8% acetic acid and 25% methanol solution to wash away excess dye from the gel and visualise separated proteins. Gels were destained by rinsing in dH_2O and used for transfer.

Either polyvinylidene difluoride (PVDF) or nitrocellulose membrane is widely used. These membranes are synthetic and available in different pore sizes. In this work, PVDF Hybond™-P transfer membrane (Amersham, Buckinghamshire, UK) was used and activated by incubating in methanol for 10 minutes and transfer cell was assembled were the gel is in direct contact with PVDF membrane for a proper and complete transfer of separated proteins from gel to the synthetic membrane. The gel is detected for traces of untransferred proteins using Coomassie stain and Proteins are visualised on the membrane using Ponceau S stain (Sigma-Aldrich). The membranes are thoroughly washed with tris saline buffer (TSB) containing 0.1% Tween20 (PBST) to remove Ponceau stain before probing with antibody.

Prior to incubation with primary antibody, blocking of the membrane is necessary. The membranes are blocked with 5% non-fat milk in PBST for 1 hour in room temperature with agitation before washing with TBST and incubation with primary antibodies diluted in 3% non-fat milk/TBST at 4°C with agitation overnight. All primary antibodies used in this work were raised in rabbit (List and dilutions of primary antibodies in table 2.3). Species cross-reactivity for each primary antibody was tested using the two-protein BLAST analysis tool (http://blast.ncbi.nlm.nih.gov). Analysis was run between chicken (*Gallus gallus*) and the species to which the primary antibody is raised against. Species-species homology ≥58% was considered acceptable and then the primary antibody was chosen to work with the chick embryo retina samples (see Appendix IV).

Following three washes wit TBST, membranes were incubated in anti-rabbit secondary antibody (see Table 2.3) for one hour with agitation before detection with enzyme chemiluminescence (ECL) (ECL Plus Western Blotting Detection Reagents, Amersham, UK), then blot bands were visualised with LAS-3000 system (Prof. Ramaswami lab. - Trinity College Institute of Neuroscience (TCIN), Lloyd Building, TCD) at different exposure times ranging from 30 seconds to 4 minutes. Detection with ECL was performed to visualise the blot bands and band pixel intensity measurements were taken and normalised to the endogenous control protein.

Table 2.3. List of antibodies used in Western blotting (WB) and their dilution.

Protein		Antibody (cat. #)	Type	Company	Quantity	Dilution
Endogenous control	β-Actin	Human* Actin antibody (1-19) (sc-1616)	Rabbit poly-clonal	Santa Cruz Biotechnology, Inc.	200 µg In 1 mL PBS	1:1000
IAPs	Birc-4/ XIAP	Rat* anti-XIAP antibody (ab21278)	Rabbit poly-clonal	Abcam	100 µg at 1mg/ mL PBS	1:750
	Birc-5/ Survivin	Human* Survivin antibody (sc-10811)	Rabbit poly-clonal	Santa Cruz	200 µg at 1mg/ mL PBS	1:500
Caspases	Caspase-3	Rat* Caspase-3 antibody (H-277) (sc-7148)	Rabbit poly-clonal	Santa Cruz	200 µg at 1mg/ mL PBS	1:500

	Caspase-7	Mouse* Caspase-7 antibody (ab25900)	Rabbit Poly-clonal	Abcam	100 µg at 1mg/ mL PBS	1:500
Secondary antibody	Goat anti-rabbit	Goat anti-rabbit IgG-HRP (sc-2004)	HRP-conjugate	Santa Cruz	200 µg in 0.5 ml volume	1:1000

* Cross-species homology is based on BLAST-protein (http://blast.ncbi.nlm.nih.gov) analysis (see appendix IV).

Dot blot analysis was done for all primary antibodies to assess the efficiency of the primary antibody specificity and the detection system. A strip of PVDF was used and 10 µL of different concentrations of protein cell lysate (2, 1, 0.5 and 0.2 µg/µL were blotted onto the membrane. 10 µL of primary antibody (100 µg/mL) was blotted alongside protein sample. Membrane was incubated for one hour at room temperature. The whole membrane was then blocked with 5% dry milk in PBST for one hour at room temperature. After removing blocking solution, the membrane was incubated with the primary antibody (1:200 in 1% PBS-Tr) for one hour. Membrane was washes 3x 10 minutes with PBS-Tr and incubated with secondary antibody (1:500 goat anti-rabbit IgG-HRP) for one hour and then washed 3x 10 minutes. Detection with ECL was performed to visualise the blot dots and results were recorded.

2.6.3.4. Membrane stripping for reprobing

The blotting membrane sometimes needed to be stripped from both primary and secondary antibodies for further usage with new antibodies. Advantages of membrane stripping include saving protein samples, assay material and time. However, some protein might be lost as well during stripping. Each blotting membrane was used two or three times. After each protein detection, the membrane was stripped from both primary and secondary antibodies, allowing for probing with a different primary antibody. The procedure was carried out by incubating the membrane in stripping buffer (see appendix II) at 65 °C with agitation for 30 minutes, and then washed with plenty of water then TBST for at least 5 minutes. Washing was repeated 3 times for 15 minutes in large volume of TBST followed by blocking with 5% non-fat milk in TBST overnight at 4 °C and reprobed the next day as previously.

2.6.3.5. Quantification of protein expression

As performed for conventional PCR results, ImageJ 1.45s (http://rsbweb.nih.gov/ij/) was used for measuring WB band intensity by means of pixel density. Target protein band density was normalised to the corresponding β-actin protein control.

2.6.3.6. Statistical analysis

Relative expression for target enzymes was represented as an increased or decreased fold change normalised to the β-Actin control protein, and relative to E9 (internal calibrator). Mean data between two groups (target and calibrator) was assessed using two-way independent t-test or two-way ANOVA as appropriate, and significance was set at 95% confidence. IBM SPSS 21 software and Excel statistical functions were used.

2.7. ELISA

2.7.1. Principle

Enzyme-linked immunosorbent assay (ELISA) is a popular analytic assay for quantification of target antigens in an aqueous solution. ELISA employs the quantitative sandwich enzyme immunoassay technique on ready-made microplates. Protein concentration can be determined in the cell lysate by utilising specific antibody that has pre-coated on a microplate. Colour development due to an enzymatic reaction was measured by means of spectrophotometry using a plate reader.

2.7.2. Procedure

Cusabio® (Wuhan, Hubei Province, P.R.China) ELISA kits for the four proteins: XIAP, Survivin, Casp-3 and Casp-7 were used as a validation check for WB results. The kit components and experimental flow is illustrated in Figure 2.2.

Cusabio Human anti-survivin (Surv) antibody ELISA kit, rat baculoviral IAP repeat-containing protein 4 (XIAP), rat Caspase 3 (Casp-3) and mouse Caspase 7 (Casp-7) ELISA kits were used as a quantitative determination of target enzymes in retinal tissue lysate. Standards and samples were loaded in pre-coated microplates with specific antibodies for the target proteins and handled as per manufacturer protocol. The concentration of total protein in retinal tissue protein lysate was 1 µg/mL of sample diluents provided with the kit. After removing unbound proteins, a specific biotin-conjugate antibody was added to the wells. After washing, avidin conjugated Horseraddish Peroxidase (HRP) was added. Following washing, a chromogenic substrate solution; 3,3',5,5'-Tetramethylbenzidine (TMB). Colour was developed in proportion to the amount of the target enzyme, and the reaction terminated by adding the stop solution provided with the kit. Finally, colour intensity was measured using TriStar LB 941 Multimode Reader (Berthold Technologies GmbH and Co. KG, Bad Wildbad, Germany).

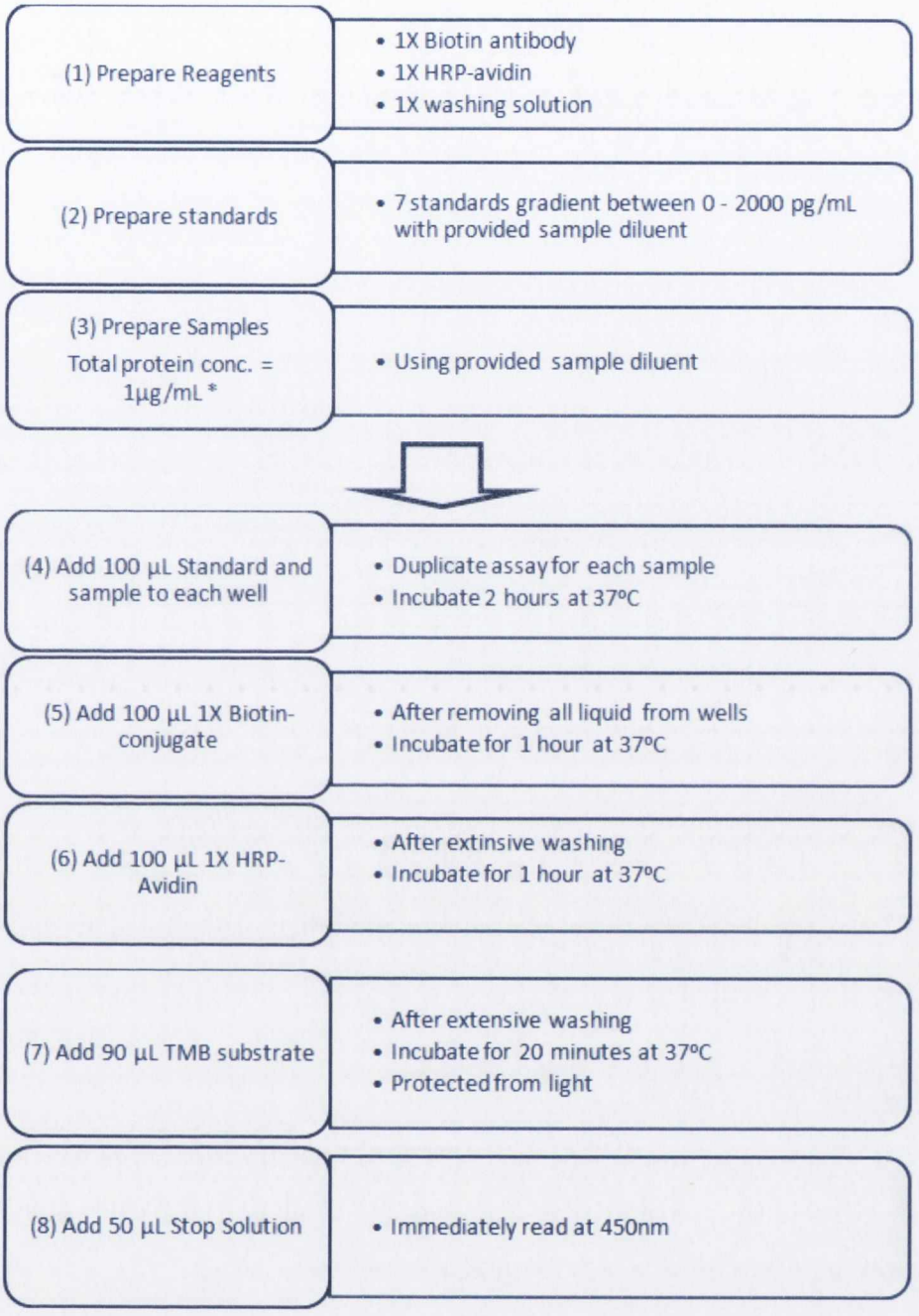

Figure 2.2. ELISA assay procedure summary.

Antibody species choice was based on the homology between chicken and the species of choice that were available from the provider. Table 2.4. lists the four ELISA kits, their antibody specificity and homology to the chicken enzymes based on BLAST two sequences check. See Appendix IV for BLAST analysis results.

Table 2.4. List of Cusabio ELISA kits used in this stud and their properties

ELISA kit	Species	Homology to Chicken*	Sensitivity range (ng/mL)
Birc-4 (XIAP)	Rat	58%	0.02 - 1.5
Birc-5 (Survivin)	Human	61%	0.625 - 40
Casp-3	Rat	67%	0.3 - 20
Casp-7	Mouse	68%	0.03 - 2

* Based on BLAST-protein (http://blast.ncbi.nlm.nih.gov) analysis (see appendix IV).

2.7.3. Statistical analysis

ELISA data for each protein was normalised to E9 calibrator stage. Since each data point represent the concentration (in either mg or pg per mL), calibrator value was not 1, rather it was the actual protein concentration.

2.8. Immunohistochemistry (IHC) and immunofluorescence (IF)

2.8.1. Principle

Immunohistochemistry (IHC) allows for qualitative detection of proteins within a tissue section by using antigen- specific antibodies. Subsequently, a visualisation of antigen-antibody interaction can be achieved by a fluorophore-tagged species-

specific secondary antibody and detected by a fluorescent microscopy. Fluorescent microscopy uses a high intensity light source than visible light. A fluorescent substance (fluorophore) within the sample is excited by this light and, in turn, a lower energy light of a longer wavelength is emitted. Emitted light can be separated from surrounding radiation with filters that are specific for designated wavelengths. The different fluorescent filters are used for a distinction to be made between the nucleic acid stained DAPI images and the fluorophore-stained secondary antibody Alexa Fluor images. Ultraviolet (UV) filter (excitation at 360 -370 nm and emission > 420 nm) was used to detect blue DAPI fluorescence (of nuclei). Blue excitation filter (Excitation at 470 - 490 nm and emission > 515 nm) was used for Alexa Fluor 488 (green). Finally, Green excitation filter (Excitation at 530 - 550 nm and emission > 590 nm) was used for Alexa Fluor 594 (red) samples.

Standard Hematoxylin and Eosin staining (H&E) was performed with wax-embedded eye tissue to show the laminar and cellular structure of the retina during these developmental stages.

2.8.1. Tissue wax-embedding for H&E staining

Eggs were incubated to the designated embryonic ages and then embryos were removed from eggs and placed in ice cold 1X PBS. Embryos heads (E4 and E5) and eyes (E8.5, 14 and 16) were dissected as described in 2.2. Tissues were fixed in 4% paraformaldehyde (PFA) for 24 hours at 4° C, then washed 2× 30 min in PBS, dehydrated through a graded series of ethanol and cleared in 50:50 ethanol:xylene for 30 minutes and then in 100% xylene for 3 min. Retinas were infiltrated with paraffin wax and embedded in molds according to the standard procedure. Whole eye samples were sectioned sagittally parallel to the optic nerve on a microtome (~ 10 μm) and serial sections were mounted on glass slides.

2.8.3. Tissue processing for cryosectioning

Chicken embryos heads and eyes were dissected in Tyrode's solution then placed in ice cold 1X PBS for storage. Tissues were then fixed 4% PFA at 4° C, then washed for 15 minutes in PBS and saturated with a sucrose gradient (10%, 20% at room temperature and 30% at 4° C) for variant periods of time (15, 30 minutes and overnight; respectively) and stored in 30% sucrose solution at 4° C.

2.8.4. Cryostat sectioning

Frozen sectioning of chick embryo heads or eyes was performed using a Leica CM1850 cryostat (Leica Microsystems, Wetzlar, Germany). Settings were adjusted to ensure the main cryostat chamber was -30° C and section thickness was adjusted to 8 μm. The angle of the blade was adjusted to 15°. The samples were removed from sucrose fixing medium and placed on a bed of OCT (Optimal Cutting Temperature) compound (Jung's Tissue Freezing Medium, Leica Microsystems) on a frozen specimen holder. More OCT compound was added onto the sample until it was completely embedded, frozen and ready for sectioning. Whole eye were serially sectioned sagittally parallel to the optic nerve and frozen sections were collected by adhering to the Superfrost Plus microscope slides (Thermo Fisher Scientific, Waltham, Massachusetts, USA), Superfrost slides are specially treated to carry a charge, which allows tissues to attach to the slide and prevent loss of tissue from subsequent treatments. The slides were stored at -20° C in slide boxes (Fischer-Scientific Inc).

2.8.5. H&E staining

Wax-embedded sections were dewaxed by immersing slides in Histo-Clear solution (National Diagnostics, Atlanta, GA, USA) for 10 minutes. Hydration of sections was performed in descending ethanol gradient (absolute, 90 and 70% ethanol). After a brief wash of slides with tap water for a few seconds, slides were immersed in Hematoxylin for 5 minutes, then washed briefly and immersed in Scott's tap water (see appendix II for composition) as a bluing reagent for Hematoxylin stain. Slides then were stained with Eosin solution for 1 minute and dehydrated in ascending alcohol gradient (70, 90 and 100%). Lastly, slides were cleared in Histo-Clear for 2 minutes, then mounted with DPX mounting medium (Fischer Scientific) and examined under the light microscopy.

2.8.6. Staining nuclei with Cytox Green

Cryosections were incubated with 0.05% PBS-Tr for 30 minutes to permeabilise the cells then incubated with Cytox Green nuclei dye (Life Technologies) for 15 minutes at room temperature. Sections were then washed for 2x 5 minutes and slides were mounted using Mowiol mounting media. Mowiol solution was made by adding 2.4 g

of Mowiol granules to 6 g glycerol (Sigma- Aldrich) and mixed. 6 mL dH_2O was added and the mixture left for 3 hours at room temperature with occasional stirring. 12 mL of 0.2 M Tris solution in dH_2O (pH 8.6) was added to the Mowiol/glycerol mixture and put in a 50° C water bath for 6 hours with stirring every hour. The mixture then was centrifuges at 5,000 g for 15 minutes to remove any undissolved solids. Supernatant was drawn and aliquoted into 1ml aliquots in eppendorf tubes then used as mounting medium or stored at -20° C. Finally, 1,4-Diazabicyclo[2.2.2]octane solution (DABCO) at 2.5 % concentration was added to Mowiol solution as an anti-fading reagent for fluorescence dyes. Stained sections were observed and captured under the fluorescent microscopy using Olympus BX40 Fluorescent microscope (Olympus, Center Valley, PA, USA) connected to a computer running cellSens 1.9 Digital Imaging Software (Olympus).

2.8.7. TUNEL staining for apoptotic activity analysis

The Promega DeadEnd TUNEL *in situ* fluorometric was used according to manufacturer's protocol (Figure 2.3).

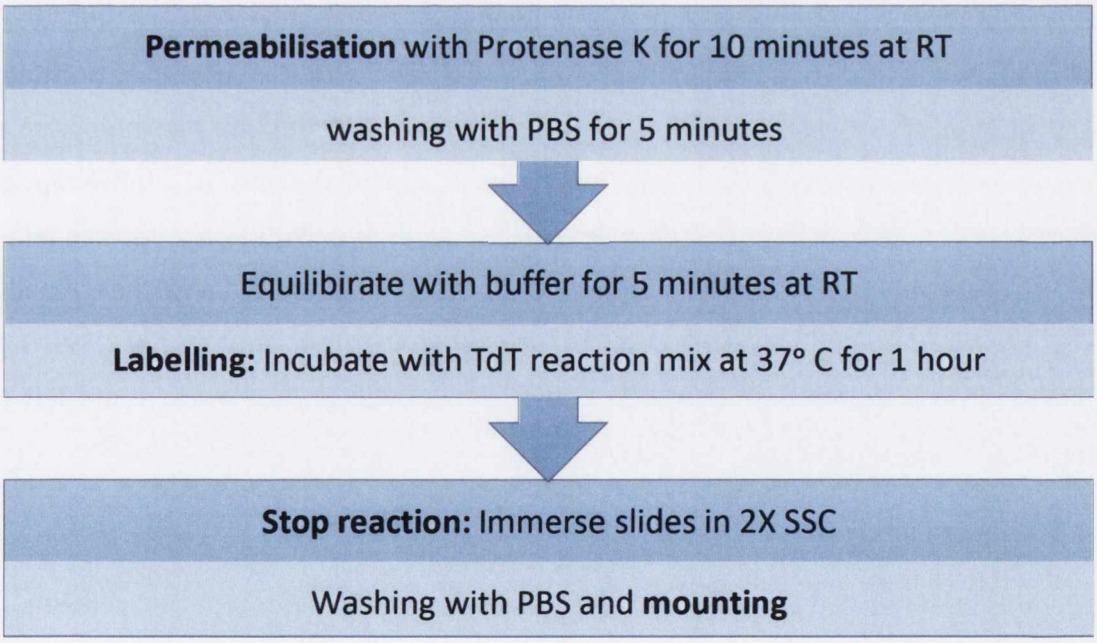

Figure 2.3. Flow of TUNEL technique experiment using Paraformaldehyde-fixed retinal tissue cryosections and Promega's DeadEnd Tunel assay kit.

2.8.8. Immunohistochemistry (IHC) and immunofluorescence (IF)

Slides were removed from the freezer and placed at room temperature overnight in a humid slide tray chamber to facilitate the adherence of the tissues to the slides before processing slides for IHC. The next day, slides were washed very gently to avoid loss of sections in 0.05% PBS-Triton (PBS-Tr) by incubating the sections in PBS-Tr for 30 minutes. Triton detergent improves the permeability of cells for antibodies staining. Each section was marked with a water-repellent PAP pen (Sigma-Aldrich), which allowed a hydrophobic barrier to be drawn around sections to be stained, minimizing the volume of antibody and other reagents used in the IHC process. Reagents were dropped onto the sections with a wide bore Pasteur pipette (Fisher-Scientific) and removed with fine pipettes, with great care taken to avoid damaging the tissue sections. The sections were then incubated for 30 minutes in 5% goat serum in PBS-Tr for blocking non-specific binding sites. Primary antibodies (see listing and details in Table 2.5) were diluted at 1:50 and 1:100 in 1% goat serum/PBS-Tr and sections were incubated with the antibodies for 24 hours at 4°C. For negative control, sections on separate slide were incubated with 1% goat serum PBS-Tr without the antibody at the same conditions. The following day, slides were washed 3x 5 minutes in PBS and were then incubated with the secondary antibody (Alexa Fluor 488 Goat Anti-Rabbit IgG green-fluorescent dye; Life Technologies) at 1:200 in 1% goat serum/PBS-Tr for two hours at 4° C at the dark in a foil-wrapped slide tray chamber. Slides then were washed 3x 5 minutes with PBS with care taken to avoid damaging or drying out sample tissues between and after washes. Finally, sections were mounted using Mowiol mounting medium containing 2.5% 1,4-diazabicyclo-[2,2,2]-octane (DABCO) then covered with glass coverslip and left to harden for 15 minutes.

2.8.9. Image analysis

Sections were viewed and analysed using the fluorescent microscope and cellSens Software package. Localisation of target proteins: Birc-4 (XIAP), Birc-5 (Survivin), Caspase-3 and Caspase-7 was visualised by means of fluorescence emission measurement. Appropriate filters for each fluorophore were used allowing for distinction to be made between fluorophore stained Alexa Fluor counterstaining.

Table 2.5. List of primary and secondary antibodies used in Immunohistochemistry (IHC) and their dilutions

Protein		Antibody (cat. #)	Type	Company	Quantity	Dilution
IAPs	Birc-4/ XIAP	Anti-XIAP antibody (ab21278)	Rabbit poly-clonal	Abcam	100 µg at 1mg/ mL PBS	1:100
	Birc-5/ Survivin	Survivin antibody (sc-10811)	Rabbit poly-clonal	Santa Cruz	200 µg at 1mg/ mL PBS	1:100
Caspases	Caspase-3	Caspase-3 (H-277) (sc-7148)	Rabbit poly-clonal	Santa Cruz	200 µg at 1mg/ mL PBS	1:100
	Caspase-7	Anti-Caspase 7 (ab25900)	Rabbit poly-clonal	Abcam	100 µg at 1mg/ mL PBS	1:100
Neuronal marker	Islet1	Islet-1 (K-20) (sc-23590)	Goat poly-clonal	Santa Cruz	200 µg in 1 mL volume	1:200
Secondary antibody	Alexa Fluor 594 Goat anti-rabbit (Red)	Alexa Fluor 488 Goat Anti-rabbit IgG (A-11008)	———	Life-technologies	200 µg in 0.5 mL volume	1:250
	Alexa Fluor 488 donkey anti-goat (Green)	Alexa Fluor 488 Goat Anti-rabbit IgG (A-11008)	———	Life-technologies	200 µg in 0.5 mL volume	1:400

Chapter 3

Gene Expression for IAPs and Caspases

3.1. Introduction

To date, five IAPs and ten caspases have been identified in the chicken (*Gallus gallus*). Gene sequences were obtained from (http://www.ncbi.nlm.nih.gov/gene/). Enzymes of each category are given the same nomenclature; *i.e.* IAP and caspase, due to chemical composition and structural similarity when first identified. However, each individual enzyme is unique in its functional properties and activity during multiple biological pathways. In fact, not all IAPs are inhibitors of caspases (O'Riordan *et al.*, 2008), neither do all caspases bring about apoptotic cell death; but rather have other non-apoptotic functions such as the inflammation response (Quesada *et al.*, 2010) and contribute to synaptic plasticity in neurons (Chan and Mattson, 1999).

In general, survival of neurons during development is a tight balance between pro-survival and pro-death factors. In the normal context of retinal neurogenesis, cell death magnitude exceeded that of neuronal differentiation amongst the newly born precursor cells (Chavarria *et al.*, 2013) and up to 50% of differentiated neurons die by apoptosis soon after the formation of synaptic connections with their target field (Raff *et al.*, 1993). PCD in the developing neuroretina was categorised into three phases or waves; the morphogenetic (between E2 and E4) (Cuadros and Rios, 1988, Trousse *et al.*, 2001), early (between E2.5 – 4.5) (Martin-Partido *et al.*, 1988, Mayordomo *et al.*, 2003), and the late (or neurotrophic) cell death wave (between E10 and E14) (Rager, 1980, Chavarria *et al.*, 2007) after neurons form their synaptic connections with their brain targets.

Genetic expression investigation can be achieved by a number of techniques including Northern blotting, *in situ* hybridisation, microarray and PCR. For quantitative analyses, particularly when the gene of interest is scarcely expressed, PCR is the technique of choice due to its sensitivity and controlled specificity (Murphy *et al.*, 1990). Quantitative estimation of target gene expression can be assessed indirectly through creation of complementary DNA (cDNA) transcripts from total RNA (Freeman *et al.*, 1999) by reverse transcription followed by the PCR technique to estimate the level of gene expression. Wong *et al.*, 1994 were the first to describe examining mRNA expression by the PCR technique, which was referred to as the "primer-dropping" method (Wong *et al.*, 1994) and where change in gene

expression were demonstrated from as low as two fold and up to 75 fold. Conventional PCR allows for measuring of the end-point concentration of amplified expressed gene semi-quantitatively (Gottwald *et al.*, 2001) by means of measuring the intensity of the resulting band from gel electrophoresis.

RT-qPCR is one of PCR variants and the most cutting edge and popular techniques for quantitative analysis of mRNA expression levels (Livak and Schmittgen, 2001) in real time as the reaction progresses. The reliability of any gene quantification analysis depends mainly on data normalisation by including a housekeeping gene (reference or endogenous control) (Bustin, 2002). The housekeeping gene allows for the normalisation of sample-to-sample and run-to-run variations and sample quantification inaccuracies in PCR assays. RNA integrity, reverse transcriptase (RT) efficiency and cDNA sample loading variations are some of many other factors that affect the reliability of PCR assays, especially when samples are obtained from different individuals and/or different time courses (Pfaffl, 2001, Bustin, 2002, Stahlberg *et al.*, 2004). Normalisation carried out against an unregulated endogenous control gene transcript has proven to be the most dependable method of normalisation over that against total cellular DNA or RNA content (Huggett *et al.*, 2005). RT-qPCR can be run by one of two common chemical principles; SYBR GreenI or fluorogenic probe. SYBR GreenI fluorescent dye is non-specific and intercalates with any double-stranded DNA (dsDNA), whereas sequence-specific probes labelled with fluorescent reporters allows for detection of hybridised probes only after binding to their complementary sequence within the reaction mixture.

3.2. Aim

Characterisation of the temporal pattern of expression of chicken IAPs and caspases is important for ascertaining the correlation between the gene expression pattern and that of the known developmental cell death exhibited at multiple stages in the chick retina. Such identification will help in gaining further understanding of the precise role of each of the 15 enzymes in developmental cell death and survival mechanisms throughout the developmental course of the retina.

3.3. Experimental design

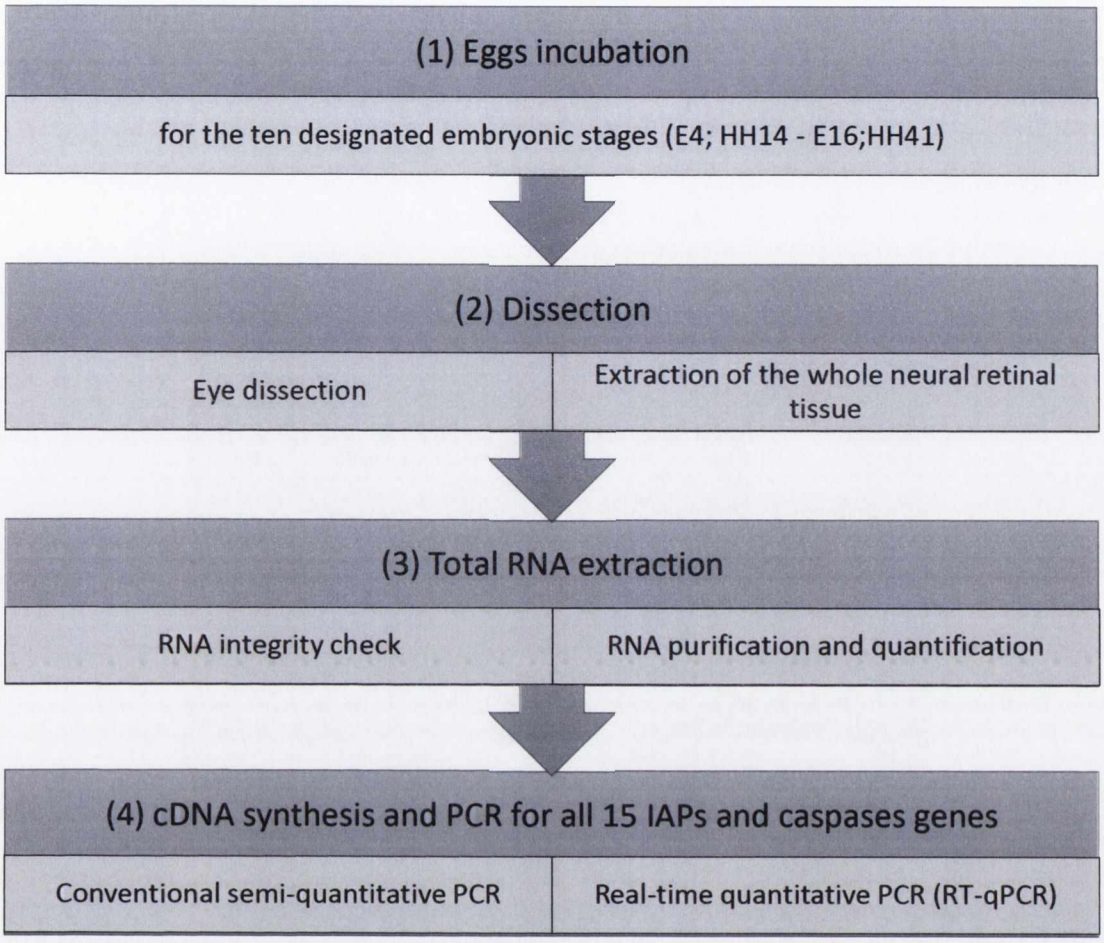

3.4. Results

3.4.1. RNA integrity

Purity and integrity of RNA are crucial for the overall efficiency of RNA-based analyses. Extracted RNA was quantified and evaluated for purity. Following isolation, total RNA concentration was assessed by means of fluorometric quantitation, and then checked on non-denaturing agaros gel electrophoresis for the distinct two 28S and 18S rRNA bands. Figure 3.1 represents three states of RNA integrity where E14 and E16 samples were partially degraded, where the two rRNA bands were faint, a smear is showing along the lane and degraded RNA bands were accumulate at the bottom of the lane (05S). Lane 4 had E5 RNA that seemed to be at very low concentration and degraded as well. E6 RNA sample at lane 5 exhibited the

two rRNA bands at the appropriate ratio, which indicated its integrity and viability as cDNA synthesis template. However, even partially degraded RNA samples were used in this project for making cDNA and subsequently proceeding to PCR owing to the difficulty of obtaining and scarcity of samples.

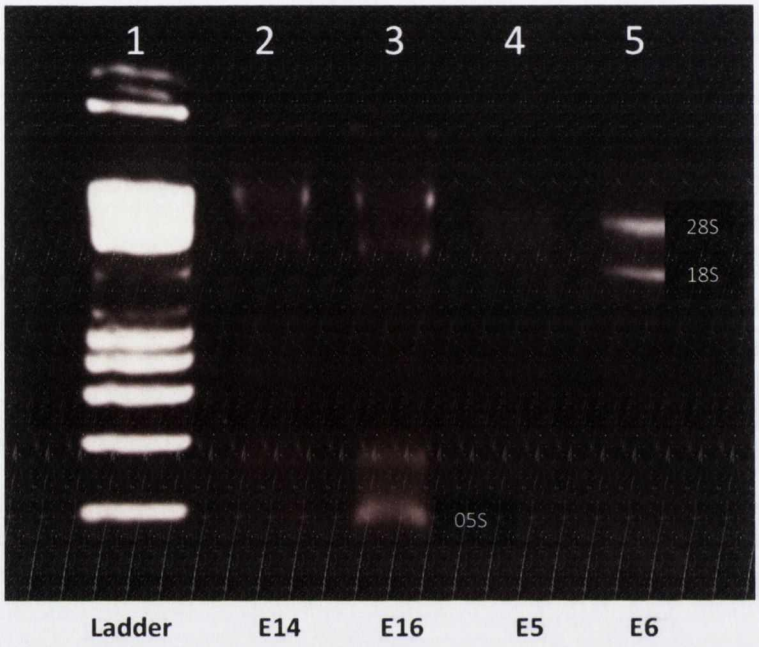

Figure 3.1. Total RNA integrity test using non-denaturing agarose gel electrophoresis. E14 and E16 RNA (in lanes 2 and 3) were partially degraded. E6 RNA (lane 5) showed the distinct two 28S and 18S subunits bands with appropriate ratio (about 2:1) indicating a relative integrity of this sample with smaller fragmented RNA (05S). E5 sample (lane4) did not represent good quality RNA; it was degraded, and the concentration seemed to be very low.

3.4.2. PCR optimisation and housekeeping gene consistency evaluation

Following primer choice and design, semi-quantitative PCR was run on 2% agarose gel electrophoresis for checking primers viability, optimal concentration and optimal annealing temperature.

β-actin was chosen as the endogenous control gene and was run alongside all the 15 genes for both semi-quantitative and quantitative PCR. The same concentration and sample volume of all ten embryonic stages were loaded for the PCR reaction with 10mM of each forward and reverse β-actin primers (Figure 3.2).

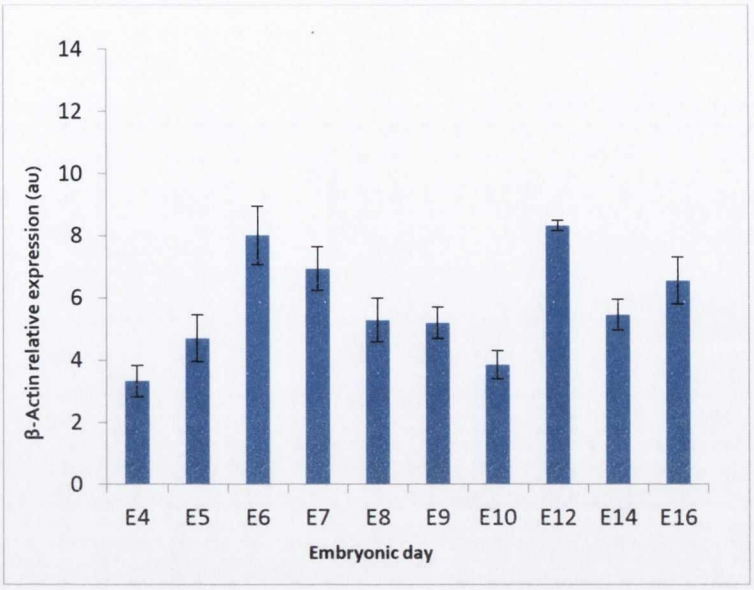

Figure 3.2. β-actin control gene expression for all ten embryonic stages with semi-quantitative PCR analysis. (au): arbitrary units. Each column represents the mean of at least three experiments ± 0.5 SD.

Relative expression levels were estimated for all 15 genes normalised to the β-Actin control gene and are represented in Figures 3.3(B) and 3.4(B) as the mean value ± 0.5 SD.

Inherent variations were considered by pooling samples in different tubes with each tube containing at least three retinae (see appendix I(B)). PCR experiments were then repeated at least three times with the same sample for each embryonic age to account for the technical variation. Although each time (age) point for each transcript expression was run using the same sample pool (tube), but for different transcript (different IAPs and caspases), different tubes were used. The difference in expression results are attributed to inevitable random fluctuation in biological systems rather than actual biological difference within sample source.

3.4.3. Semi-quantitative PCR

3.4.3.1. IAPs and caspases gene expression

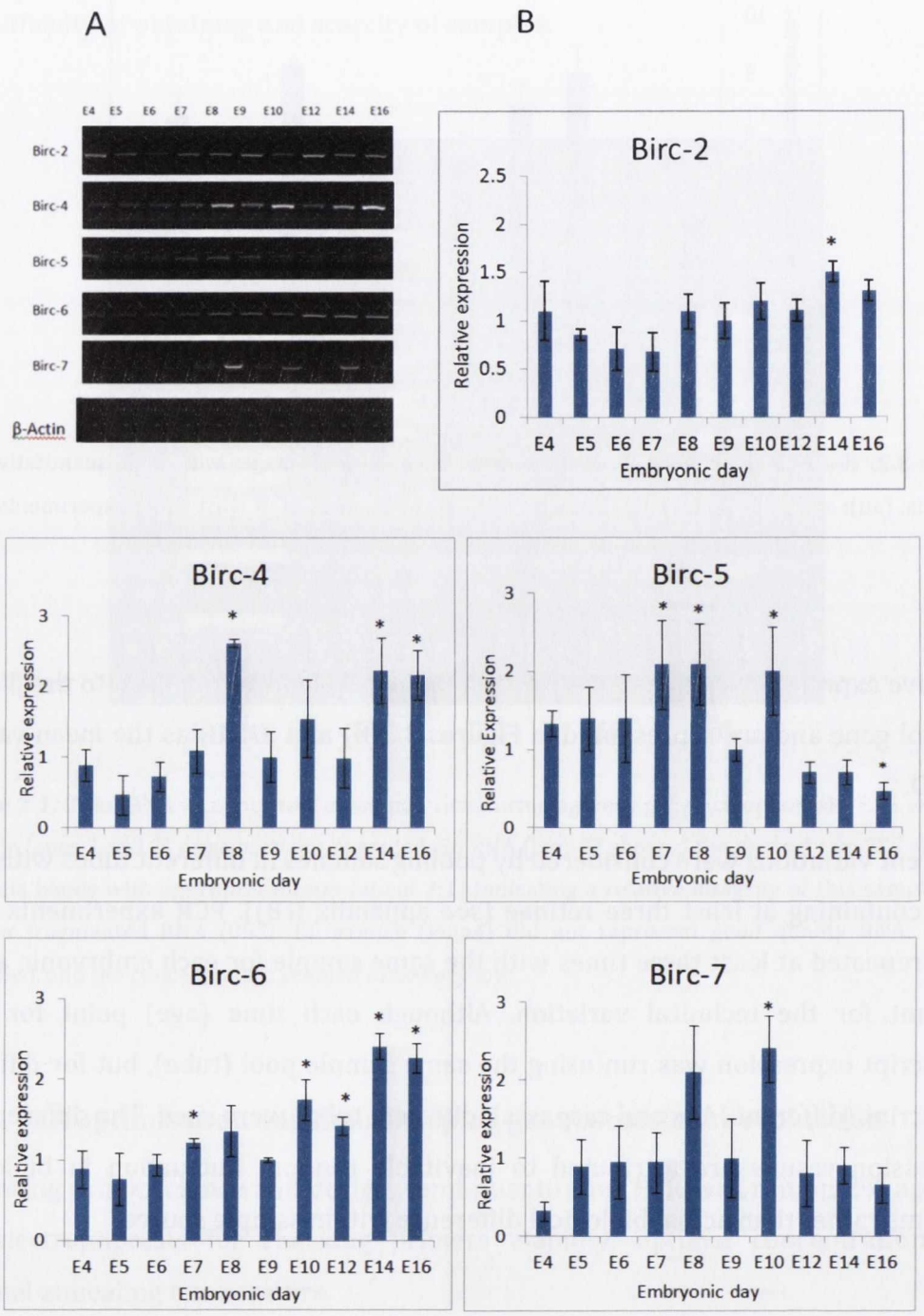

Figure 3.3. IAPs are expressed differentially in the whole retina during development. The expression profile of the five IAPs in the developing chick retinal embryonic between E4 and E16 with semi-quantitative PCR normalised to β-actin control gene. Bar values represent the mean densitometry of triplicate experimental data for ±SEM. Statistically significance difference between the expression level of each transcript at all stages compared to E9 (calibrator) is denoted by * (*=p<0.05; n=3).

A

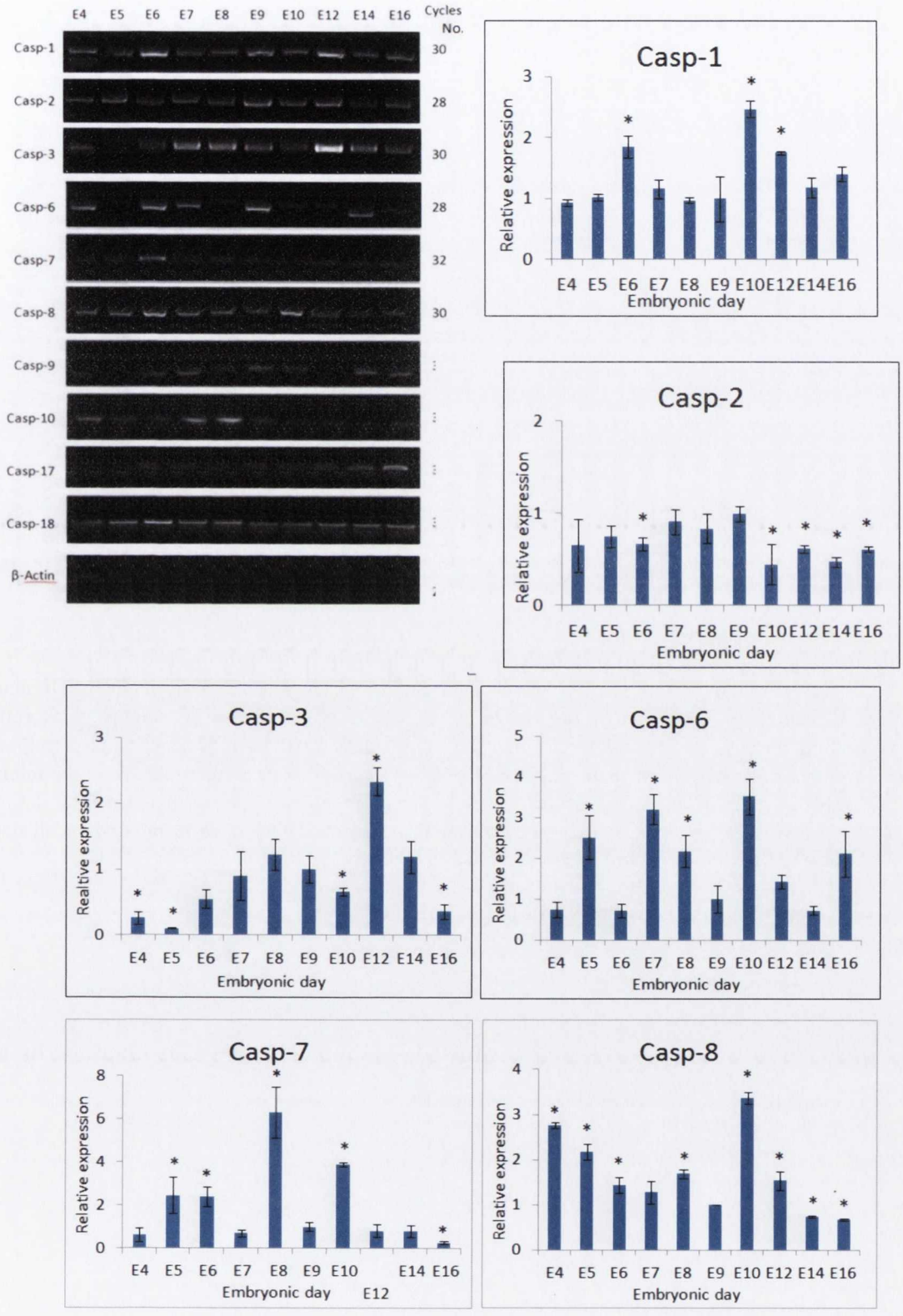
E4 E5 E6 E7 E8 E9 E10 E12 E14 E16 Cycles No.
Casp-1 30
Casp-2 28
Casp-3 30
Casp-6 28
Casp-7 32
Casp-8 30
Casp-9
Casp-10
Casp-17
Casp-18
β-Actin
Casp-1
Relative expression
Embryonic day
Casp-2
Relative expression
Embryonic day
Casp-3
Realtive expression
Embryonic day
Casp-6
Relative expression
Embryonic day
Casp-7
Relative expression
Embryonic day
Casp-8
Relative expression
Embryonic day

B

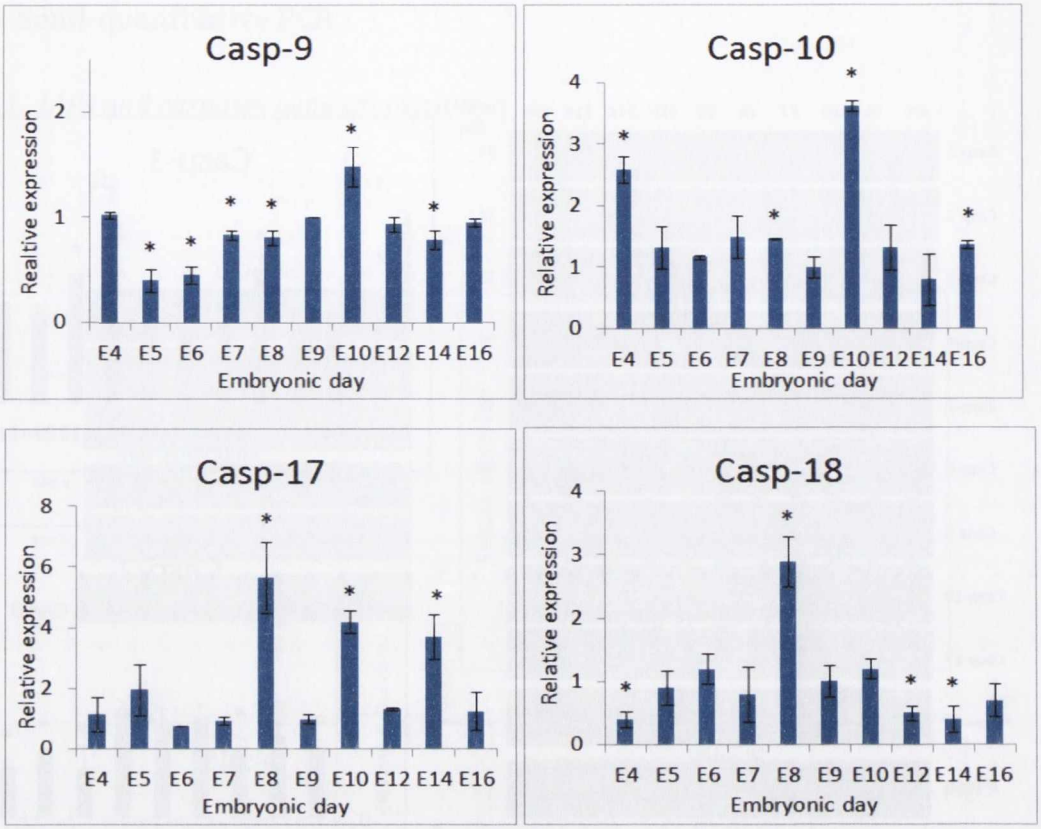

Figure 3.4. Semi-quantitative PCR data of differentially expressed caspases in the whole neural retina during development. (A) Gel image of the ten caspases in the developing chick retinal embryonic were analysed between E4 and E16 with semi-quantitative PCR normalised to β-actin control gene. (B) Bar graph representation of relative expression of caspases to E9 as the internal calibrator stage. Bar values represent the mean densitometry of triplicate experimental data for ±SEM. Statistically significance difference between the expression level of each transcript at all stages compared to E9 (calibrator) is denoted by * (*=p<0.05; n=3).

3.4.4. Real-Time quantitative PCR (RT-qPCR)

3.4.4.1. IAPs gene expression

Figure 3.5 represents bar graphs for the RQ of the five IAPs genes obtained by RT-qPCR and used to interpret the study results.

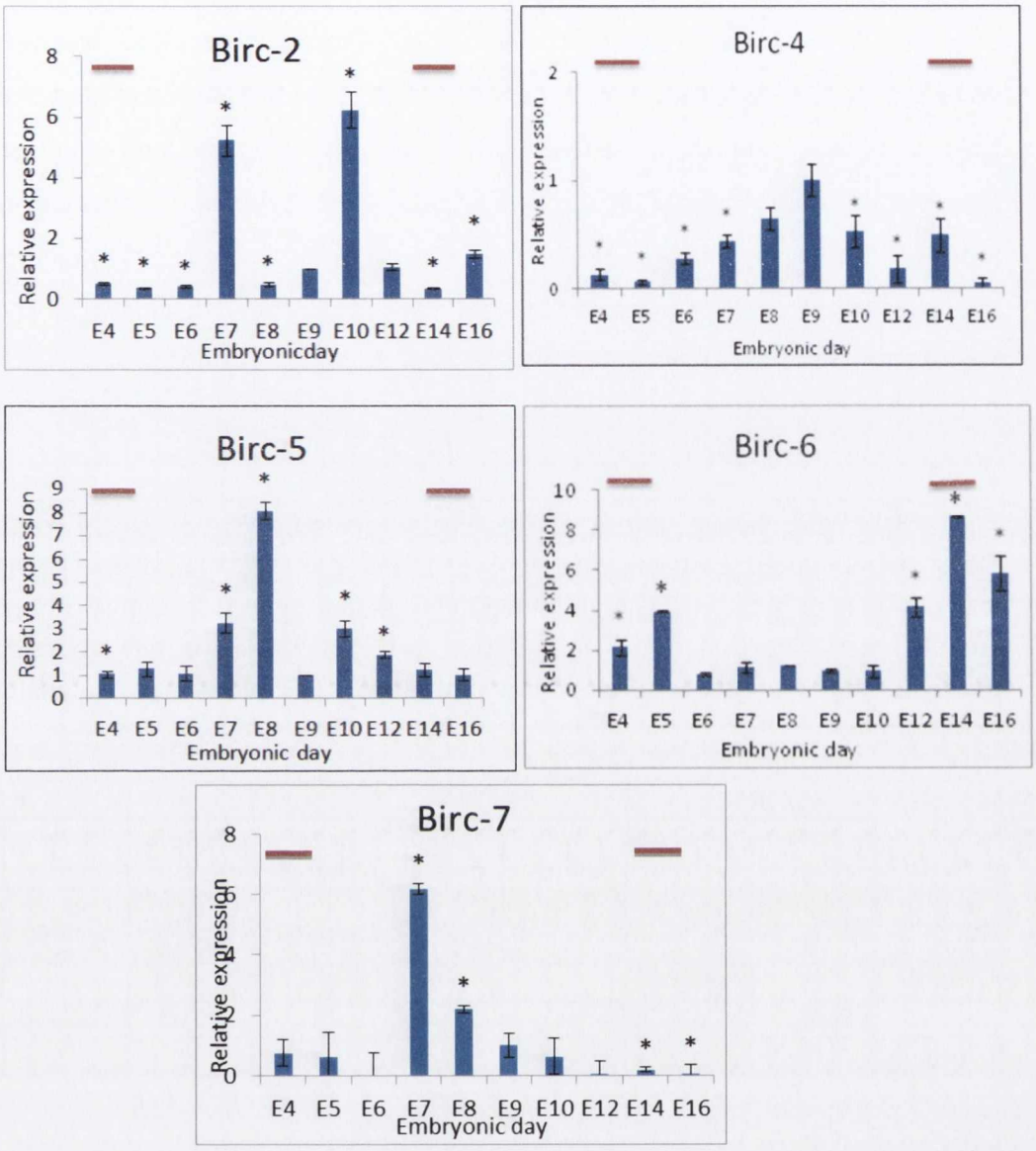

Figure 3.5. RT-qPCR analysis of expression of the five chicken IAPs during embryonic development of the chick retina. Each target gene expression data point was normalised to the corresponding β-actin, then calibrated in relation to the E9 expression value for relative expression of the same gene across the ten embryonic stages. Each data point is a representative of three experimental replicas, and bar value represent the mean ±SEM. Overhead horizontal bars represent the two waves of developmental cell death waves. Statistically significance difference between the expression level of each transcript at all stages compared to E9 (calibrator) is denoted by * (*=p<0.05; n=3).

In correlation with the two waves of developmental cell death in the retina at early (E4 and 5) and late (E12 and 14) stages, Birc-2 expression was generally downregulated, except at E12 where a slightly significant increased value for expression was obtained. Birc-4 (XIAP) and Birc-7 expression was generally downregulated (Table 3.1). Whereas Birc-5 (Survivin) expression was upregulated at both stages, early and late, the increased expression is statistically significant but this was marginal. Birc-6 expression, for exception, showed an overall increased expression, up to 8.6 times at E14.

Table 3.1. Fold change difference for the five IAPs in relation to E9 (calibrator). Early developmental stages (E4 and E5) and late (E12 and E14). Increased expression (upregulation) is highlighted in green, dark green for significant increase, and decreased expression (downregulation) is highlighted in orange where darker is for significant decreased. Difference in expression <1.5 fold change is considered to be marginal.

	E4		E5		E12		E14	
Gene	Fold change	p-value	Fold change	p-value	Fold change	p-value	Fold change	p-value
Birc-2	-2	<0.01	-2.5	0.17	0.9	<0.01	-2.5	0.13
Birc-4	-10	0.2	-14	0.16	-5	<0.01	-2	<0.01
Birc-5	1.1	<0.01	1.3	0.07	1.9	<0.01	1.2	<0.01
Birc-6	2.2	<0.01	4	<0.01	4.1	<0.01	8.6	<0.01
Birc-7	-1.3	0.4	-1.7	0.5	-16	0.5	-5	0.3

3.4.4.2. Caspases gene expression

Figure 3.6 represent bar graphs for the RQ of the ten caspase genes obtained by RT-qPCR and used to interpret the study results.

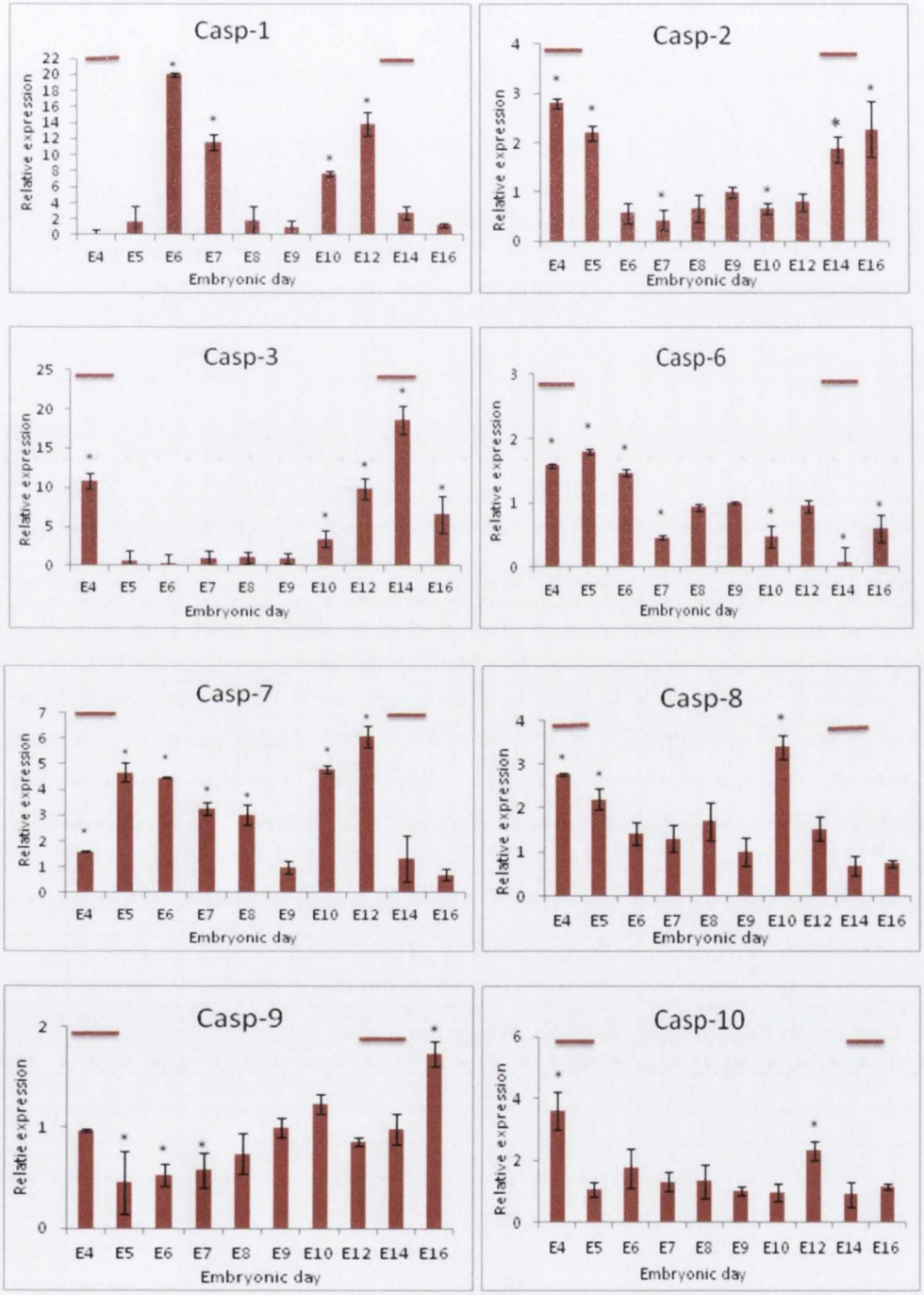

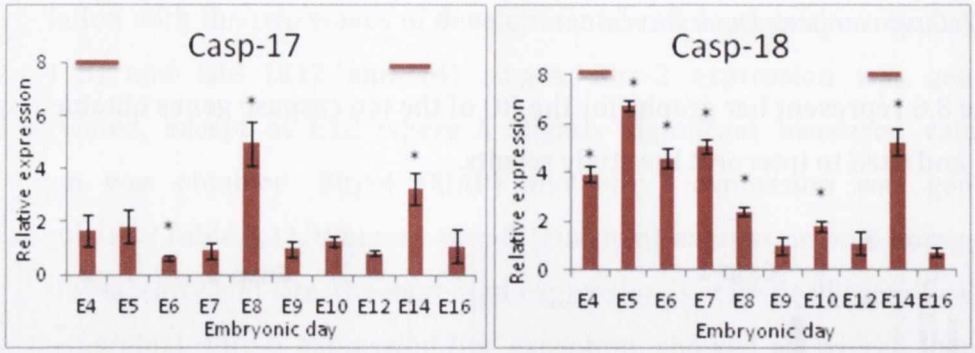

Figure 3.6. RT-qPCR analysis of expression of the ten chicken caspases during embryonic development of the retina. Bar value represent the mean ±SEM of data normalised to β-actin and calibrated to E9. Overhead horizontal bars represent the two waves of developmental cell death waves. Statistically significance difference between the expression level of each transcript at all stages compared to E9 (calibrator) is denoted by * (*=p<0.05; n=3).

The expression profile of the ten chicken caspases exhibited differential patterns of expression (Table 3.2). Only four embryonic stages were analysed for relative expression in relation to the E9 calibrator time point; E4 and 5 for early developmental stage and E12 and 14 for the late stage.

Table 3.2. Fold change difference of the ten chicken caspases in relation to E9. Early developmental stages at E4 and E5 and late (E12 and E14). Increased expression (upregulation) is highlighted in green, dark green for significant increase, and decreased expression (downregulation) is highlighted in orange where darker is for significant decreased. Difference in expression <1.5 fold change is considered to be marginal.

	E4		E5		**E12**		**E14**	
Gene	Fold change	p-value	Fold change	p-value	Fold change	p-value	Fold change	p-value
Casp-1	-10	<0.01	1.7	<0.05	14	0.6	2.7	<0.01
Casp-2	2.8	<0.01	2.2	<0.01	-1.2	0.6	1.9	<0.01
Casp-3	10.8	<0.01	-1.7	<0.01	10	<0.01	18.6	<0.01
Casp-6	1.6	<0.01	1.8	<0.01	-1	<0.01	-12.5	<0.01
Casp-7	1.6	<0.01	4.7	<0.01	6	<0.01	1.3	<0.01
Casp-8	2.7	<0.01	2.2	<0.01	1.5	<0.01	-1.4	<0.05
Casp-9	1	<0.05	-2.2	0.15	-1.1	<0.01	1	<0.01
Casp-10	3.6	<0.01	1.1	<0.01	2.3	<0.01	-1.1	<0.01
Casp-17	1.7	<0.01	1.8	0.19	-1.2	<0.05	3.2	<0.01
Casp-18	4	<0.01	6.7	<0.01	1.1	<0.01	5.2	<0.01

Expression profile of the ten caspases, from RT-qPCR data, can be categorised in four main patterns of expression. A summary of the description and classification of each of the ten caspases is demonstrated below in Table 3.5.

Table 3.3. The five categories of gene expression patterns for ten chicken caspases from RT-qPCR analysis. Fold changes of each gene at early (E4 and 5) and late (E12 and 14) developmental stages (Table 3.2) were used to generate specifications of each category.

Category	Description	Caspases
1	A constant upregulation pattern throughout the early and late stages coinciding with the reported two waves of developmental cell death.	Casp-7 Casp-18
2	Two peaks of upregulation expression at one of/or both early (E4 and 5) and one of/or both late developmental stages (either E12 or 14).	Casp-2 Casp-3 Casp-8 Casp-10 Casp-17
3	Significant decreased expression at early stage, and significant increase later on.	Casp-1
4	A slight increased expression at early stages, and a sharp decreased expression later on.	Casp-6
5	Low differential change throughout both cell death waves periods, with overall low expression level.	Casp-9

3.4.4.3. Correlation of IAPs and caspases temporal gene expression

To illustrate the relationship between IAPs that exhibit an anti-apoptotic temporal expression pattern and pro-apoptotic caspases, the graph below was assembled (Figure 3.7).

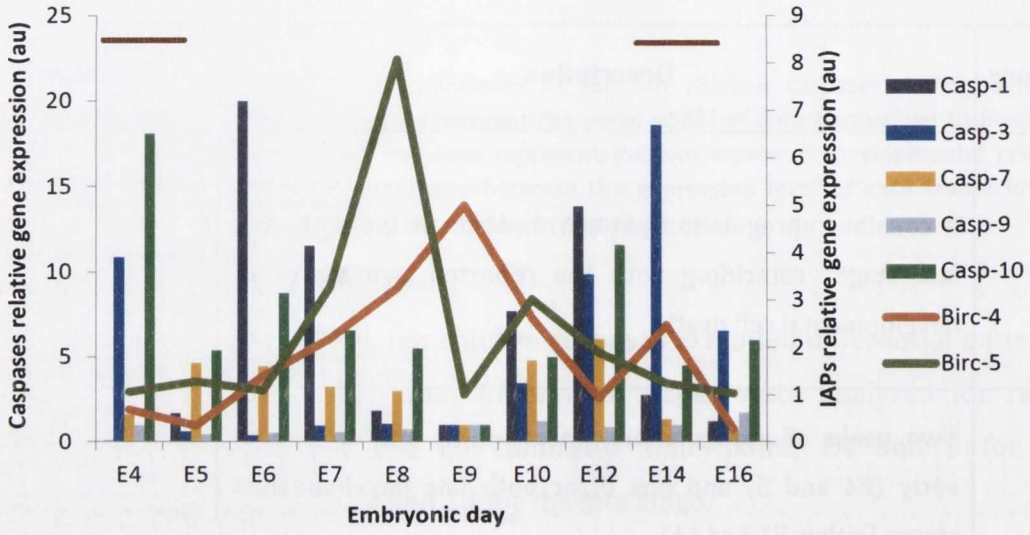

Figure 3.7 Inverse correlation of the temporal expression of Birc-4 (XIAP) and Birc-5 (Survivin) (IAPs) with selected caspases expression throughout the course of normal chick retina embryonic development. The reported two developmental cell death waves are indicated with overhead horizontal bars. (au): arbitrary units.

3.5. Discussion

To study the 15 chicken IAPs and caspases expression during the normal course of early and late development in the chick embryo retinae, two varieties of PCR were used in this study; conventional semi-quantitative and RT-qPCR. Semi-quantitative PCR was utilized for initial gene expression assessment and for reaction conditions optimisation. Faster and more reliable RT-qPCR was run subsequently and results were used for analysis and interpretation. Differential pattern of gene expression was detected for all the 15 genes.

3.5.1 RNA purity and integrity

RNAs are very sensitive to degradation; especially long RNA fragments are less stable (Bustin, 2002). However, RT-qPCR analyses very short regions of RNA and therefore RT-qPCR has been established to be tolerant to partially degraded RNA (Fleige and Pfaffl, 2006). Three main types of RNA nucleases, along with a set of cofactors, found in eukaryotic cells contribute to the regulation of RNA molecules; RNA endonucleases that hydrolyze RNA internally, 5′ exonucleases that cut RNA from the 5′ end, and 3′ exonucleases that cut RNA from the 3′ end yielding a widely different sets of RNA molecule fragments (Houseley and Tollervey, 2009). Several types of RNA molecules are present in eukaryotic cells. The three main types of RNA; messenger (mRNA), ribosomal (rRNA) and transfer (tRNA) in addition to many other small cytoplasmic and nuclear RNAs (scRNA and snRNA; respectively) are present as a part of the cellular genomic materials (Lodish *et al.*, 2000). Protein-coding mRNA; which only comprises less than 5% of the total RNA, is the type of RNA that is utilised in PCR for assessment of transcript expression by means of measuring the number of copies of specific cDNA targets. Numerous studies have shown that gene expression profile obtained from partially degraded RNA where visible ribosomal bands are still visible exhibited meaningful results compared to good quality RNA samples (Schoor *et al.*, 2003, Fleige and Pfaffl, 2006).

Biological replicates were not used so not all sources of possible variation were accounted for. However, each sample analysed was derived from a pool of specimens at that embryonic age which would reduce variation from specimen to specimen.

3.5.2. Semi-quantitative vs. quantitative PCR results

Variation arose in the results using both techniques. These differences in expression patterns can be attributed to many common sources. Despite the care and consistency technical variation factors such as varied protocols for both techniques, sample collection, RNA isolation and processing may have caused these result differences. Animal-to-animal biological variation factors include variability amongst many sample pools most likely to cause such difference in results as well. Although the specific trend of expression for each gene with each technique did not match, however for most of the studied stages, the overall trends were similar.

Tables 3.4 (IAPs) and 3.5 (caspases) summarises expression trend of both PCR techniques for comparison.

Table 3.4. Comparison of gene expression trend for IAPs obtained by conventional semi-quantitative and RT-qPCR techniques. Increased expression is represented in green boxes, decreased expression in orange boxes. Significant change is denoted with an asterisk ($p<0.05$).

		E4	E5	E6	E7	E8	E10	E12	E14	E16
Birc-2	Semi-qPCR	**0.68** ± 0.31	**0.85** ± 0.06	**0.71** ± 0.22	**0.67** ± 0.2	**1.1** ± 0.18	**1.2** ± 0.19	**1.1** ± 0.11	**1.5*** ± 0.1	**1.3** ± 0.1
	RT-qPCR	**0.53** ± 0.05	**0.37** ± 0.04	**0.44** ± 0.04	**5.25** ± 0.51	**0.5** ± 0.05	**6.25** ± 0.6	**1.1** ± 0.1	**0.4** ± 0.03	**1.5** ± 0.14
Birc-4 (XIAP)	Semi-qPCR	**0.88** ± 0.22	**0.47** ± 0.28	**0.72** ± 0.21	**1.1** ± 0.3	**2.6*** ± 0.05	**1.54** ± 0.54	**0.98** ± 0.42	**2.22*** ± 0.45	**2.15*** ± 0.34
	RT-qPCR	**0.13** ± 0.04	**0.06** ± 0.02	**0.28** ± 0.05	**0.43** ± 0.06	**0.65** ± 0.1	**0.52** ± 0.14	**0.18** ± 0.12	**0.49** ± 0.15	**0.05** ± 0.05
Birc-5 (Survivin)	Semi-qPCR	**1.33** ± 0.17	**1.4** ± 0.41	**1.4** ± 0.56	**2.1*** ± 0.57	**2.1*** ± 0.51	**2.0*** ± 0.56	**0.71** ± 0.14	**0.71** ± 0.61	**0.47*** ± 0.11
	RT-qPCR	**1.06** ± 0.15	**1.28** ± 0.32	**1.1** ± 0.31	**3.28** ± 0.42	**8.1** ± 0.38	**3.03** ± 0.35	**1.89** ± 0.15	**1.24** ± 0.3	**1.03** ± 0.26
Birc-6	Semi-qPCR	**0.89** ± 0.23	**0.76** ± 0.33	**0.94** ± 0.13	**1.21*** ± 0.06	**1.36** ± 0.32	**1.75*** ± 0.25	**1.42*** ± 0.11	**2.41*** ± 0.16	**2.27*** ± 0.18
	RT-qPCR	**2.16** ± 0.4	**3.95** ± 0.03	**0.79** ± 0.12	**1.15** ± 0.24	**1.21** ± 0.03	**0.92** ± 0.35	**4.14** ± 0.45	**8.65** ± 0.05	**5.8** ± 0.86
Birc-7	Semi-qPCR	**0.33** ± 0.12	**0.89** ± 0.34	**0.96** ± 0.46	**0.95** ± 0.39	**2.1** ± 0.58	**2.4*** ± 0.43	**0.81** ± 0.42	**0.9** ± 0.23	**0.66** ± 0.21
	RT-qPCR	**0.75** ± 0.45	**0.6** ± 0.82	**0.0** ± 0.75	**6.18** ± 0.16	**2.19** ± 0.12	**0.62** ± 0.6	**0.06** ± 0.4	**0.18** ± 0.08	**0.0** ± 0.35

Table 3.5. Comparison of gene expression trend for caspases obtained by conventional semi-quantitative and RT-qPCR techniques. Upregulation is represented in green boxes, downregulation in orange. Significant change is denoted with an asterisk ($p<0.05$).

		E4	E5	E6	E7	E8	E10	E12	E14	E16
Casp-1	Semi-qPCR	0.93 ± 0.05	1.02 ± 0.06	1.86*± 0.18	1.16 ± 0.16	0.98 ± 0.05	2.48*± 0.13	1.76*± 0.02	1.19 ± 0.16	1.41 ± 0.12
	RT-qPCR	0.08 ± 0.56	1.7 ± 1.9	20.0 ± 3.5	11.54 ± 1.0	1.85 ± 1.68	7.69 ± 0.35	13.8 ± 1.47	2.77 ± 0.76	1.23 ± 2.7
Casp-2	Semi-qPCR	0.65 ± 0.3	0.75 ± 0.12	0.67*± 0.07	0.91 ± 0.13	0.84 ± 0.16	0.45*± 0.21	0.62*± 0.04	0.48*± 0.05	0.61*± 0.03
	RT-qPCR	2.8 ± 0.09	2.2 ± 0.15	0.57 ± 0.21	0.43 ± 0.21	0.67 ± 0.27	0.68 ± 0.1	0.8 ± 0.18	1.87 ± 0.26	2.26 ± 0.73
Casp-3	Semi-qPCR	0.26* ± 0.1	0.1* ± 0.01	0.55*± 0.14	0.9 ± 0.37	1.22 ± 0.24	0.66 ± 0.07	2.23*± 0.21	1.2 ± 0.24	0.36*± 0.11
	RT-qPCR	10.8 ± 0.9	0.62 ± 1.32	0.38 ± 1.1	0.93 ± 0.9	1.1 ± 0.7	3.44 ± 1.0	9.8 ± 1.28	18.6 ± 1.8	6.5 ± 2.3
Casp-6	Semi-qPCR	0.74 ± 0.18	2.51* ± 0.5	0.71 ± 0.16	3.22*± 0.38	2.18* ± 0.4	3.52*± 0.45	1.42*± 0.17	0.72 ± 0.1	2.1* ± 0.56
	RT-qPCR	1.58 ± 0.04	1.8 ± 0.05	1.47 ± 0.05	0.46 ± 0.03	0.93 ± 0.04	0.47 ± 0.17	0.94 ± 0.1	0.08 ± 0.23	0.6 ± 0.21
Casp-7	Semi-qPCR	0.64 ± 0.3	2.45*± 0.84	2.4* ± 0.45	0.7 ± 0.17	6.3* ± 1.2	3.9* ± 0.08	0.82 ± 0.28	0.81 ± 0.27	0.27*± 0.06
	RT-qPCR	1.6 ± 0.03	4.6 ± 0.36	4.4 ± 0.03	3.3 ± 0.23	3.0 ± 0.4	4.8 ± 0.16	6.1 ± 0.43	1.3 ± 0.9	0.71 ± 0.22
Casp-8	Semi-qPCR	2.76*± 0.06	2.17*± 0.17	1.43*± 0.16	1.28 ± 0.18	1.7* ± 0.1	3.37*± 0.13	1.54*± 0.12	0.74*± 0.02	0.68*± 0.02
	RT-qPCR	2.74 ± 0.04	2.2 ± 0.24	1.42 ± 0.25	1.34 ± 0.3	1.7 ± 0.42	3.4 ± 0.27	1.53 ± 0.28	0.68 ± 0.22	0.74 ± 0.07
Casp-9	Semi-qPCR	1.0 ± 0.03	0.4* ± 0.11	0.45*± 0.08	0.83*± 0.04	0.8* ± 0.07	1.48*± 0.19	0.93 ± 0.07	0.78* ± 0.1	0.95 ± 0.04
	RT-qPCR	0.97 ± 0.02	0.46 ± 0.31	0.53 ± 0.11	0.58 ± 0.17	0.74 ± 0.2	1.23 ± 0.1	0.86 ± 0.04	1.0 ± 0.15	1.7 ± 0.12
Casp-10	Semi-qPCR	2.6* ± 0.21	1.32 ± 0.35	1.16 ± 0.02	1.5 ± 0.35	1.46*± 0.01	3.62* ± 0.1	1.32 ± 0.37	0.79 ± 0.42	1.35*± 0.06
	RT-qPCR	3.62 ± 0.63	1.08 ± 0.23	1.74 ± 0.62	1.31 ± 0.3	1.32 ± 0.55	0.96 ± 0.3	2.32 ± 0.3	0.9 ± 0.4	1.17 ± 0.1
Casp-17	Semi-qPCR	1.14 ± 0.55	1.96 ± 0.84	0.77 ± 0.01	0.92 ± 0.14	5.65*± 1.17	4.2* ± 0.37	1.32 ± 0.06	3.7* ± 0.73	1.26 ± 0.63
	RT-qPCR	1.7 ± 0.6	1.83 ± 0.65	0.67 ± 0.1	0.9 ± 0.3	4.96 ± 0.82	1.26 ± 0.2	0.82 ± 0.1	3.25 ± 0.6	1.1 ± 0.6
Casp-18	Semi-qPCR	0.4* ± 0.24	0.9 ± 0.55	1.2 ± 0.73	0.8 ± 0.87	2.9* ± 0.8	1.2 ± 0.61	0.5* ± 0.22	0.4* ± 0.81	0.7 ± 0.51
	RT-qPCR	3.9 ± 0.31	6.75 ± 0.25	4.57 ± 0.4	5.1 ± 0.28	2.4 ± 0.19	1.79 ± 0.25	1.1 ± 0.49	5.2 ± 0.54	0.71 ± 0.17

Only RT-qPCR, but not semi-quantitative PCR, data were analysed here for differential expression analyses. Fold-change differences were relied on RQ values obtained from Applied Biosystems Real-Time PCR system, and significance of the difference was tested with independent two-tailed t-test.

Conventional semi-quantitative PCR has the limitation of being an end-point result assay. Band saturation can arise and cause experiment-to-experiment difference in results. Post-PCR manipulation is another major source of poor precision and low sensitivity. Moreover, resulted gel bands have to be quantified by the researcher, which might compromise consistency as a result of different image resolution and background noise.

On the other hand, RT-qPCR for RNA expression is more reliable, more sensitive and is a consistent gene expression level quantification assay. Less technical and biological variation can arise from using RT-qPCR technique (Mestdagh *et al.*, 2009). All these reasons make RT-qPCR a more reliable technique to use for RNA expression analysis.

3.5.3. IAPs gene expression

A scattered body of research have investigated gene expression for IAPs during embryonic developmental of CNS and/or the retina in specifically. These studies utilized a number of vertebrate species embryo, some of which were the chick embryo or other avian species. Birc-4 (XIAP) and -5 were reported by many investigators to be potent inhibitors of apoptosis in a number of vertebrate species (Vitte-Mony *et al.*, 1997, McKinnon *et al.*, 2002, Oost *et al.*, 2004, Dohi *et al.*, 2004, Jiang *et al.*, 2005). Birc-7 also directly inhibits active forms of apoptotic caspases and attenuates the apoptosis progress (Kasof and Gomes, 2001).

These three IAPs, Birc-4 (XIAP), -5 and -7, were found to be downregulated at the early and late developmental stages covered in this study in relation to the middle stage (around E9) (See Figure 3.5 and Table 3.3). This finding is in line with the previously mentioned role of the three IAPs as chief anti-apoptotic factors in the developing nervous system. It is worth mentioning that Birc-7 is mainly expressed in developing tissues, but not adult tissues except for the placenta (Kasof and Gomes, 2001) and in many forms of tumours (Abd-Elrahman *et al.*, 2009). The fact that increased expression at the middle stages of the studied period was observed is in line with reports of much lower PCD occurring in the neural retina during this period (around E9) (Chavarria *et al.*, 2007).

Only a few studies have looked into gene expression of Birc-2 (cIAP-1) (Kisiswa *et al.*, 2010b) and there were no reports for the role of Birc-6 (Apollon/Bruce) in regulating the apoptotic pathway in embryonic developing neural tissue of any kind. This could be due to the notion that these two IAPs are not direct anti-apoptotic factors. Rather, Birc-2 and -6 mostly regulate apoptosis and other cellular processes by targeting caspases and other related proteins for ubiquitination and modifying their function (Eckelman and Salvesen, 2006). Also Birc-2 was found to modulate

TNF-mediated signalling by interaction with TRAFs (Rothe *et al.*, 1995, Varfolomeev *et al.*, 2007) but not to directly inhibit caspases despite its structural similarity to Birc-4 (XIAP).

Our results for Birc-2 gene expression reflect a downregulation pattern around E4 and E14, while higher expression was observed at E7 and E10 (but not at E8 and E9). While expression of Birc-4 (XIAP) and -5 were observed to be relatively higher throughout all the four middle stages (E7 to E10) (Figure 3.5). This suggests a possible anti-apoptotic role of Birc-2 in the development of the chick neural retina during some of the intermediate stages where less cell death incidences occur.

Birc-6 was reported to play crucial role in embryonic development in the mouse model (Lotz *et al.*, 2004, Ren *et al.*, 2005) by regulating p53 and the mitochondrial apoptotic pathway. This study findings for Birc-6 analysis demonstrated an overall higher expression levels (Figure 3.5). Compared to the rest of the IAPs, Birc-6 gene expression was upregulated during the two cell death periods (early and late) and downregulated at the middle period. This finding is in line with the literature suggesting the crucial role of Birc-6 in embryogenesis.

3.5.4. Caspases gene expression

Different patterns of expression have been obtained from RT-qPCR for the ten caspases in this study. Although belonging to the same enzyme family according to their structural similarity, different caspases have been shown to have different functional roles in apoptosis and/or other cellular processes. Our data reflected this diversity of the physiological roles of caspases.

3.5.4.1. Non-apoptotic caspases gene expression

Casp-1 was reported to be well conserved amongst many species and act to mainly as an anti-inflammatory caspase (Li *et al.*, 1995, Ghayur *et al.*, 1997, Quesada *et al.*, 2010). Apart from its role as a mediator in inflammatory responses, Casp-1 was also reported to participate in immune system maturation (Lamkanfi *et al.*, 2004). Our data demonstrated an upregulation pattern at E6 and E12. At E4 where neural retina cell death peaks, Casp-1 was downregulated. Similarly, at the late cell death wave at E14, Casp-1 expression was slightly upregulated (approx. 2.8 times). These

findings support the idea that Casp-1 is not a direct pro-apoptotic factor. The upregulation pattern of Casp-1 at E6 and E12 might suggest an anti-inflammatory role of Casp-1 at these stages. Following a massive cell death wave during normal embryonic development, clearing of apoptotic cells takes place in the tissue, primarily by autophagy (Qu *et al.*, 2007). Upregulated Casp-1 at E6 might indicate a role of Casp-1 in the immunological clearing up of dying cells by autophagy (Mellen *et al.*, 2008). Strikingly, Mellen *et al.* (2009) found that autophagy is essential for clearing out apoptotic cells in chick developing retina at the early phase corresponding to neurogenesis (at E5) but not at later phase (E9) (Mellen *et al.*, 2009). Casp-1 upregulation was the highest at E6 (figure 3.6 and table 3.5) up to 20± 3.5 times. This is in line with Mellen *et al.* (2009) report that major autophagic (immunological) response is taking place following the earlier phase of developmental cell death. The next surge of expression for Casp-1 at E12 (13.8± 1.5 times increase) could indicate the occurrence of another major inflammatory response taking place at E12.

Casp-17 and -18 were reported to be expressed solely in non-mammalian species (Eckhart *et al.*, 2008, Quesada *et al.*, 2010). The Casp-17 mammalian ortholog Casp-14 was found to be expressed chiefly in human epidermis (Lippens *et al.*, 2000) , RPE, choroid plexus and thymus (Lippens *et al.*, 2003). Until now, no work has investigated tissue-specificity and/or function of chicken Casp-17. Relatively high Casp-17 expression in the neural retina illustrated in this work cannot be explained at this point, especially due to the fact that the RPE was removed in order to study the neural retina exclusively. However, it was proposed by Quesada *et al.* (2010) that mechanisms leading to caspase-dependent apoptosis in avian species depend on more proteases than mammals.

Casp-18, like Casp-17, has not received much attention yet. Many reports have considered Casp-18 to be an initiator caspase due to its structural homology the initiator caspase 8 (Eckhart *et al.*, 2008). Our data showed a relative high expression level of Casp-18; which strongly suggested a role in embryonic development of the neural retina.

3.5.4.2. Apoptotic caspases gene expression

Our data revealed four patterns of expression for apoptotic caspases. Caspases 2, -3, -8 and -10 gene expression showed upregulation at three of the four analysed stages (E4, 5, 12 and 14). Casp-2, -8 and -10 were found to be upregulated at both early stages (E4 and 5) and either one of the later stages. The opposite pattern was obtained for Casp-3 where the only downregulation point was observed at one of the early stages (E5).

Casp-2, -8 and -10 are considered to be initiator caspases (Philchenkov, 2004). However, only Casp-2 was reported to be a versatile multi-functions caspase (Krumschnabel, 2009) where it possibly plays both pro-death as well as pro-survival roles (Bergeron *et al.*, 1998). The pro-apoptotic role of Casp-2 was reported in several works (Li *et al.*, 1997, Harvey *et al.*, 1997, Guo *et al.*, 2002, Olsson *et al.*, 2009, Vigneswara *et al.*, 2013). Interestingly, Casp-2 pro-survival role in DNA repair was well documented (Zhang et al., 2007b, Shi et al., 2009) as well as its anti-tumour role (Ho *et al.*, 2009). This flexibility in Casp-2 functioning led to the belief that Casp-2 is redundant in apoptosis signalling by (Samraj *et al.*, 2007). Our data showed an upregulation pattern of expression for Casp-2 at E4 and E5, and also at E14 and 16. The level of upregulation is slight (maximally up to 2.8 times only), which suggests a probable secondary role of Casp-2 in PCD of developing neural retina. At the late (neurotrophic) stage of retinal development, cell death overlaps with other processes involved in RGC axonal navigation, synaptogenesis and target connection (Linden and Perry, 1982, Linden, 1994).

The Casp-3 relative expression magnitude was much higher at E4 (10.8± 1) and later at E14 (18.6± 1.8). This finding is in line with documented increased expression of Casp-3 as an effector caspase that is needed for bringing about the apoptosis (Kivinen *et al.*, 2005, Hyman and Yuan, 2012). Casp-3 also was found to involve in non-apoptotic processes during neuronal embryonic development; such as dendritic and synaptic physiology (Li *et al.*, 2010, D'Amelio *et al.*, 2012).

Casp-6 was reported to be a major factor in the intrinsic apoptotic pathway by directly interacting with initiator Casp-8 to activate it and promote further cytochrome c release from the mitochondria (Cowling and Downward, 2002).

Another finding (Inoue, 2009) described active Casp-6 as an activator for Casp-10, another initiator caspase by proteolytic processing. Moreover, Casp-6 was shown to simulate Casp-3 action in axonal pruning during neuronal development non-redundantly (Sokolowski *et al.*, 2014). However, our qPCR did neither reflect a high nor a significant increased gene expression level for Casp-6.

Casp-7, an effector caspase in the apoptotic pathway, was found to be expressed highly in the developing brain and retinae of mouse embryo (Zhang *et al.*, 2007a). The expression level was higher than that in adult mouse. This suggests a strong correlation between Casp-7 and developmental cell death/apoptosis in the CNS. Our RT-qPCR data for Casp-7 gene expression revealed a high expression level throughout the studied period. Highest expression levels were detected at E12 (6.1± 0.43 fold increase) and to a lesser extent at both E5 (4.6± 0.36) and E10 (4.8± 0.16 times increase). The relatively lower expression level at E4 may suggest that cell death at this stage may be controlled by other caspases or other enzymes but not Casp-7.

Casp-8, the initiator caspase in the extrinsic apoptotic pathway, was found to proteolytically cleave and activate Casp-3, along with Casp-10 (Stennicke *et al.*, 1998). Our gene expression data revealed a much lesser relative expression level for Casp-8 than Casp-3. However, the Casp-8 expression trend was similar to that of Casp-10 (figure 3.6 and table 3.5) where the highest expression was detected at E4 and either E10 or E12. These findings might indicate the synergistic action of both Casp-8 and -10 in regulating Casp-3 activity. At the later stage (E14) Casp-3 expression was the highest, and this was preceded by the upregulation of Casp-8 and -10. However, it was noted that at the early stage (E4) all three genes were upregulated.

Finally, Casp-9 gene expression analysis data in this study did not reveal any significant expression pattern. The expression was neither high nor significant (Figure 3.6 and table 3.5). Casp-9 has been documented to be an initiator caspase in the intrinsic mitochondrial apoptotic pathway and to be one of the potent activators of downstream effectors Casp-3 (Kuida *et al.*, 1998). It was reported that Casp-9 mRNA was only detected in damaged experimental rat retinae (Kermer *et al.*, 2000,

Grosskreutz *et al.*, 2005). These findings in combination with our data suggest that developmental cell death in the retina occur through the extrinsic apoptotic pathway through caspases other than Casp-9.

3.5.4.3. Correlation between anti-apoptotic IAPs and pro-apoptotic caspases

From the literature, previous work in different species and a wide variety of tissues has illustrated that not all IAPs are anti-apoptotic and neither are all caspases pro-death factors.

Four of the five chicken IAPs were reported to be anti-apoptotic. Birc-2 (cIAP-1), Birc-4 (XIAP), Birc-5 (Survivin), Birc-7 (Livin) were established, in this study, to have been downregulated during the two developmental waves of cell death of the retina. This strongly suggests that these factors are involved in inhibition apoptosis during these stages of development in the chick retina. On the other hand, most of the chicken caspases were shown to be upregulated during the two cell death waves, suggesting their direct pro-apoptotic action.

One of the limitations of this study is the variation in some of the genes expression pattern between the two PCR techniques. Although with some difference, both techniques demonstrated differential patterns of expression for both IAPs and caspases and although there are some specific gene expression differences, the overall trend of expression of the IAPs and caspases investigated here is similar in terms of the correlation to the known (early and late) two cell death waves using both techniques.

In this study, we aimed to screen the relative gene expression behaviour of all chicken (*Gallus gallus*) known IAPs and caspases through a wide range of normal stages of chick neural retina development. The main goal for such analysis was to provide a thorough understanding of the relative level of expression of chicken IAPs and caspases to serve as a complete reference of these genes for interested researchers and to correlate this expression with the known waves of cell death in the chick retina.

We showed that all the IAPs and caspases we investigated were expressed differentially in the developing neural retinae of the developing chicken, which

suggests a diverse function of each of these factors in both inhibition and promoting PCD. Some of the IAPs exhibited a pattern of expression correlated with periods when cell death was not occurring (e.g. Birc-4 (XIAP) and Birc-5 (Survivin)) while others did not. Similarly, while the expression of a number of caspases correlated with the periods of cell death (e.g. Casp-3) not all caspases exhibited such a pro-apoptotic pattern.

Chapter 4

Protein Expression of IAPs and Caspases

4.1. Introduction

Involvement of apoptosis in the elimination of retinal neuronal cells during normal embryonic development, and aging, has been well documented (Young, 1984, Cecconi *et al.* 1998, Neufeld and Gachie, 2003). During mammalian retinal development, successive waves of apoptosis occur over the retina and cause a significant cell loss. Many studies have investigated the onset and time course of apoptosis in the developing retina, with some of these studies focusing on the role of apoptotic IAPs and caspases (Linden *et al.*, 1999, Pequignot *et al.*, 2003, Vecino *et al.*, 2004, Jiang *et al.*, 2005, Wride *et al.*, 2006, Harvey *et al.*, 2009, Valenciano *et al.*, 2009).

The key prosecutors of apoptosis are caspases, a cysteine aspartyl-specific family of proteases (Miura *et al.*, 1993). Caspases have also been shown to involve in non-apoptotic pathways, such as proliferation and differentiation (Schwerk and Schulze-Osthoff, 2003), also within the nervous system in dendritic development (Li and Sheng, 2012).

Inhibitor of apoptosis proteins (IAPs) are a family of enzymes share a structural homology (Prunell and Troy, 2004). Baculovirus Inhibitor of apoptosis protein Repeat (BIR) is a structural motif found in all eight mammalian IAPs (Silke and Vaux, 2001). Birc-4 (XIAP) and -5 (Survivin) were found to be potent players in the apoptotic pathway in the developing nervous system of different mammalian species in the normal course of embryonic development of CNS (Rehen and Linden, 1994, Potts *et al.*, 2003, Jiang *et al.*, 2005, O'Driscoll *et al.*, 2006, Unsain *et al.*, 2013).

Developmental apoptotic cell death has been studied *in vivo* and *in vitro* in a number of species as a naturally occurring physiological process (von Bartheld, 1998, Linden, 1994, Biehlmaier *et al.*, 2001, Vecino *et al.*, 2004). Neurobiologists investigate retinal development to trying to understand how neural circuits assemble and communicate and the role of apoptosis and apoptosis regulators in these processes (Buss *et al.*, 2006, Guerin *et al.*, 2006, Simon *et al.*, 2012, Dekkers *et al.*, 2013).

After acquiring expression profiles for the 15 chicken (*Gallus gallus*) IAP and caspase genes (Chapter 3), an attempt to obtain a correlated protein profile for selected IAPs and caspases was carried out.

Four enzymes, namely: Birc-4 (XIAP), Birc-5 (Survivin), Casp-3 and Casp-7, were selected for more focused analysis of their protein expression using a number a techniques. According to the gene expression profile in this work, these four enzymes show the most relevant patterns of expression in relation with the two cell death waves; the early and late. A significant upregulation for both Casp-3 and Casp-7 at the transcript level was revealed during the two waves of developmental cell death, accompanied by a noticeable plummet of expression during the middle stages where there is no major cell death pattern in the chick embryo developing retina. The exact opposite pattern of expression was seen for the two IAPs; Birc-4 (XIAP) and Birc-5 (Survivin) in this work, which strongly suggests their anti-apoptotic role in the phase between the two cell death periods.

4.2. Aims

To characterise the protein expression pattern for the two IAPs; Birc-4 (XIAP) and Birc-5 (Survivin) and the two apoptotic caspases, Casp-3 and Casp-7. Western blotting (WB) and ELISA was carried out for the four enzymes. Whole neural retina protein lysate was used for protein analyses. The same 10 embryonic stages investigated for gene (transcript) expression analyses were studied here as well. More analysis for transcript and protein expression correlation was carried out as well as time onset correlation between transcription and corresponding protein translation.

4.3. Experimental design

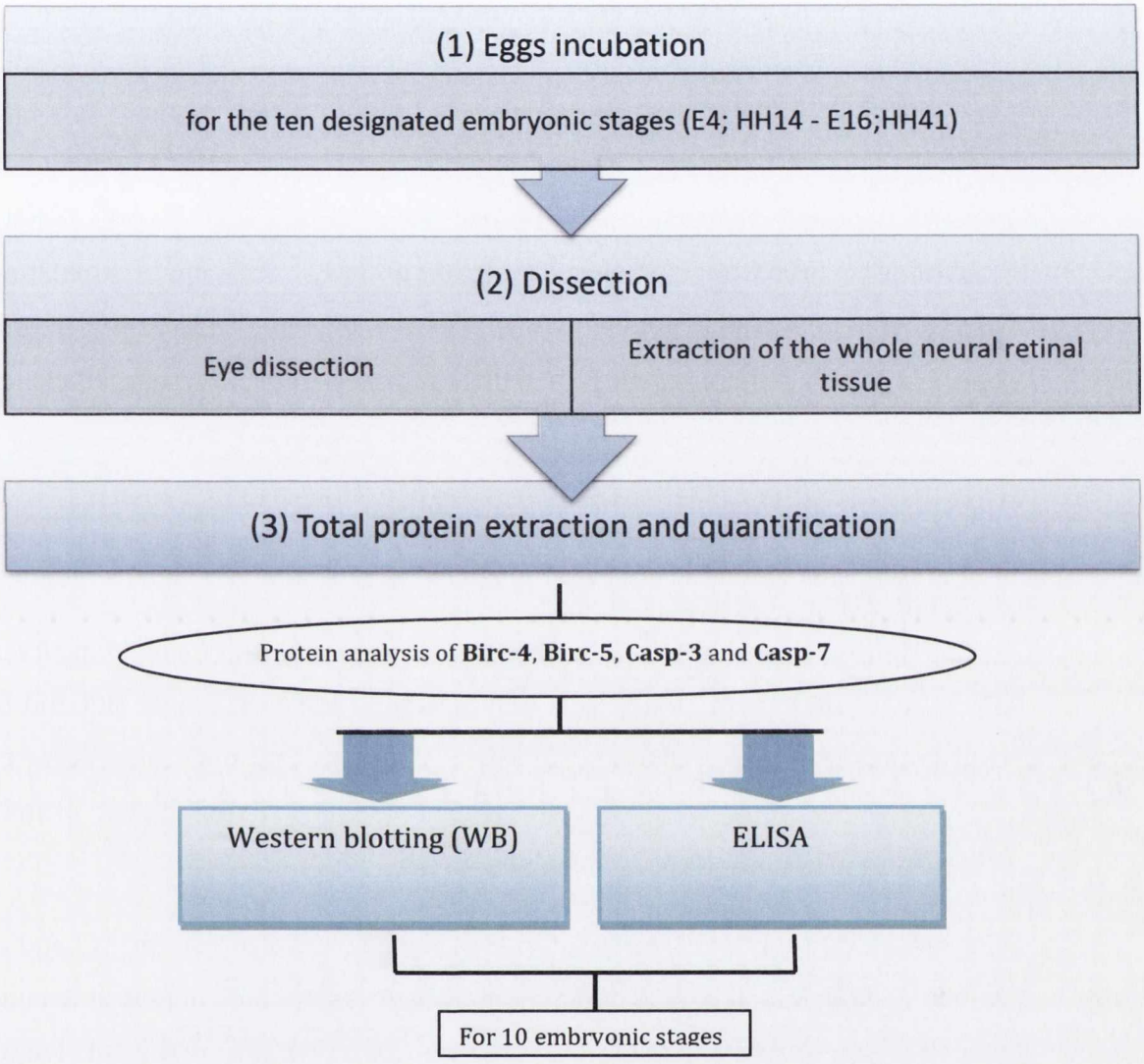

4.4. Results

In this section, the protein expression for selected IAPs and caspases is described. Western blotting (WB) was used for Birc-4 (XIAP), -5 (Survivin) and Casp-3 throughout all the ten designated embryonic stages. Then ELISA validation assay was used for the three proteins along with Casp-7.

4.4.1. WB protein expression profile for Birc-4 (XIAP), Birc-5 (Survivin) and Casp-3

Analyses for two IAPs, Birc-4 (XIAP) and -5 (Survivin) and one caspase, Casp-3 provided results, but not Casp-7, where no bands were obtained. Dot blot analyses was performed for Casp-7 antibody and positive blot was obtained, which suggested reactivity of antibody. Nevertheless, for Casp-7 activity retention by increasing the antibody amount up to two fold and manipulating exposure time did not improve the WB assay for detecting Casp-7 antigen. Dot bolt analysis is a simple testing of antibodies and detection system efficiency (see 2.6.3.3).

Assessment of the three proteins level in the whole neural retina revealed a differential expression throughout the ten embryonic stages (Figure 4.1).

Birc-4 antibody (Anti-XIAP antibody) detected a positive 46 kDa band in all ten stages with remarkably low expression pattern at the early stages (E4 and 5) and with higher expression at E9. Birc-5 (Survivin) antibody also detected positive bands about 16.5 kDa for most of the stages, with higher protein expression in the middle of the profiling series.

Caspase-3 antibody detected two forms of the enzyme. Procaspases-3 band at about 32 kDa was detected, along with cleaved caspases-3 subunit at around 17 kDa. Anti-Caspase 7 antibody was used for detection of the full length procaspase-7, but no bands were obtained using WB analysis.

A single band corresponding to β-actin was observed at all stages (Figure 4.1.A), and densitometry readings for all target protein bands were normalised to β-actin for blotting of expression graph and statistical analyses.

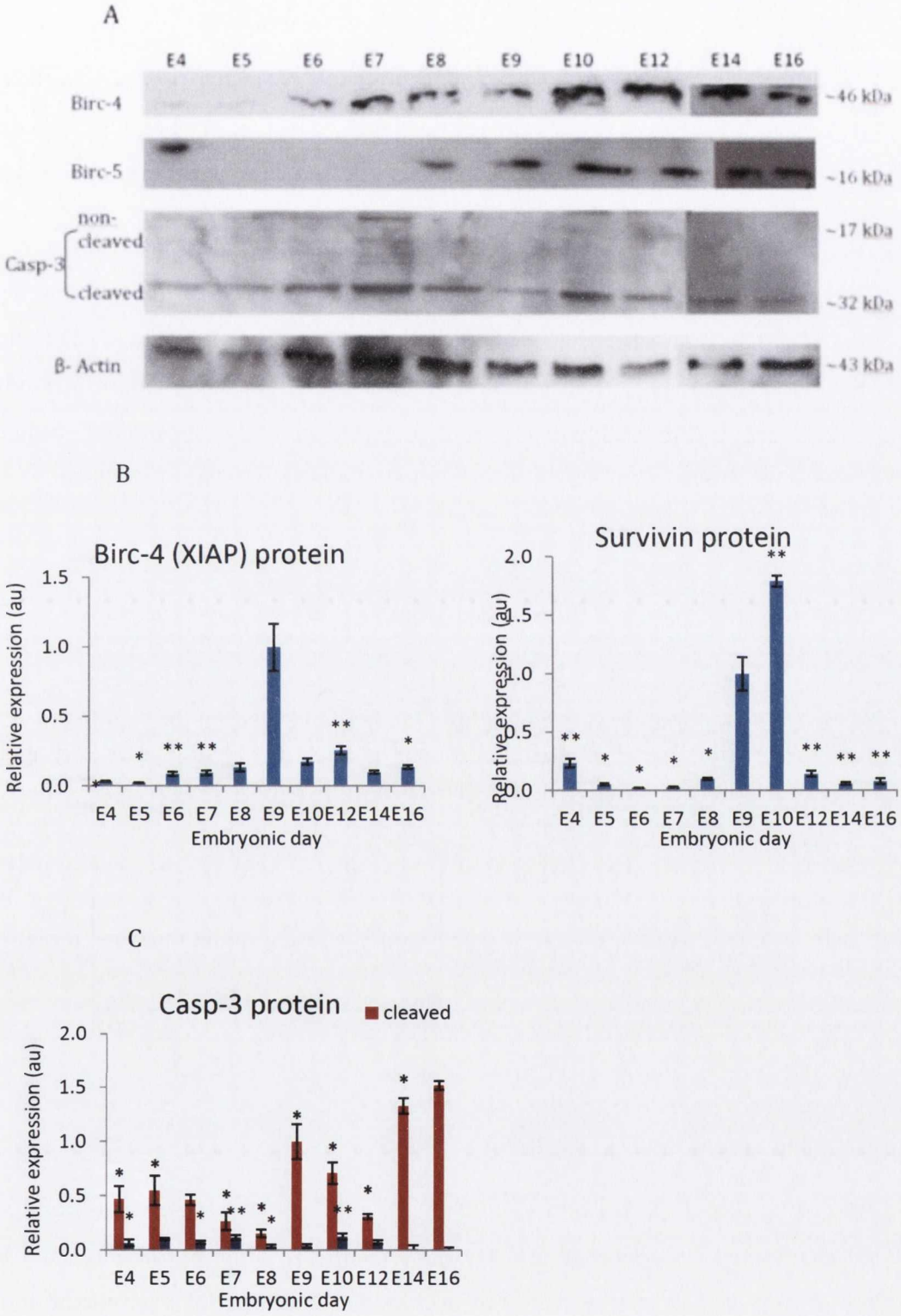

Figure 4.1. Differential expression of Birc-4 (XIAP), -5 (Survivin) and Casp-3 from Western blotting analysis. (A) Bands obtained by WB for the three proteins and β-actin endogenous control and in relation to E9 internal calibrator (=1). (B) Representative graphs of band intensities of target proteins normalised to β-actin. Bars represent the mean ± SEM.

Statistically significance difference between the expression level of each transcript at all stages compared to E9 (calibrator) is denoted by * (*=p<0.05, ** = p<0.05; n=3).

Densitometry analysis confirmed a significant decreased expression pattern for the two IAPs, Birc-4 (XIAP) and 5 (Survivin) at the early (E4 and 5) and late (E14) developmental stages. Table 4.1 lists the fold change difference of each protein in comparison to E9 (calibrator stage).

Casp-3 expression analyses revealed a much higher overall expression pattern for cleaved active Casp-3 that peaked at the late developmental stage (E14 and 16), and changes in expression were significant. Larger pro-caspase 3 bands were detected at much lower levels throughout the early and middle studied time points (from E4 to E12); however, these changes were not significant.

Table 4.1. Fold change of Birc-4 (XIAP), Birc-5 (Survivin) and Casp-3 expression obtained from Western blotting analysis in relation to E9. Early developmental stages at E4 and E5 and late (E12,14 and 16). Increased expression (upregulation) is highlighted in green, dark green for significant increase, and decreased expression (downregulation) is highlighted in orange where darker is for significant decreased. Difference in expression <1.5 fold change is considered to be marginal.

	E4		E5		E12		E14		E16	
	Fold change	p-value	Fold change	p-value	Fold change	p-value	Fold change	p-value	Fold change	p-value
Birc-4	-33.3	< 0.05	-50	< 0.05	-4	< 0.05	-10	< 0.05	-7.1	< 0.05
Birc-5	-4.3	< 0.05	-20	< 0.05	-7.1	< 0.05	-16.7	< 0.05	-12.5	< 0.05
Casp-3	-2.1	< 0.05	-1.8	< 0.05	-3.2	< 0.05	1.33	< 0.05	1.5	< 0.05

4.4.2. Enzyme detection by ELISA

Two IAPs; Birc-4 (XIAP) and -5 (Survivin), and two caspases; Casp-3 and -7 were assessed for presence and quantity using the same antibodies used in WB. Differential protein expression profile was obtained for each of the four enzymes (Figure 4.2).

Table 4.2 summarises the fold change of the four enzymes at early and late stages. The two IAPs were significantly downregulated at both early and late

developmental stages, with the highest expression level detected at the middle of the profiling period (E9 and 10).

Caspases 3 and 7, on the other hand, exhibited different expression patterns. Casp-3 was not strikingly changed at the early developmental stage in relation to E9. However, at the late stage, Casp-3 was significantly downregulated with 3.4 fold times at E14 and up to 63.6 fold decrease at E16. This was statistically significant ($p<0.05$).

A

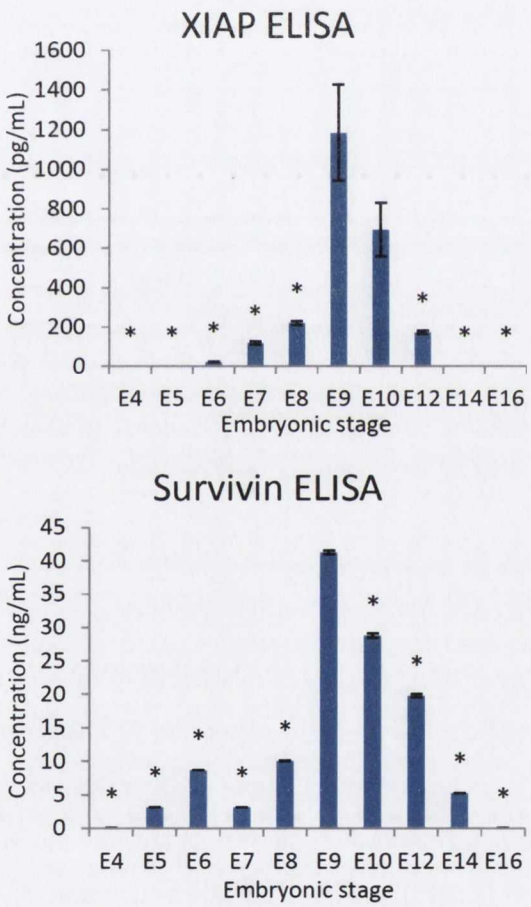

B

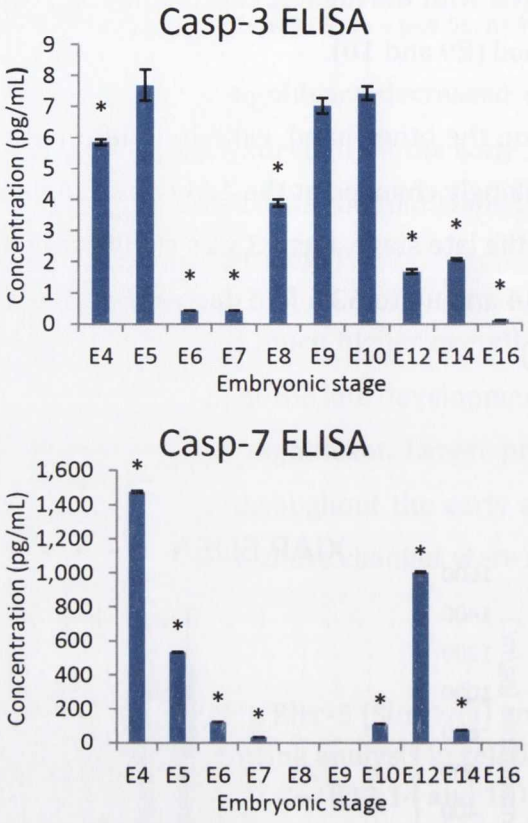

Figure 4.2. ELISA analysis for Birc-4 (XIAP), Birc-5 (Survivin) (A), Casp-3 and Casp-7 (B). Data are representative of same-plate triplicate sample assays, and error bars represents SEM. Statistically significance difference between the expression level of each transcript at all stages compared to E9 (calibrator) is denoted by * (*=p<0.05, ** = p<0.05; n=3).

4.5. Discussion

Following gene expression analysis of the 15 chicken IAPs and caspases, protein analysis with both Western blotting and ELISA were carried in order to investigate the correlation between gene expression and the corresponding protein expression for selected enzymes. WB analysis provided expression profiles for Birc-4 (XIAP), -5 (Survivin) and Casp-3, where differential expression throughout the 10 embryonic stages was obtained. The ELISA assay, on the other hand, revealed a more conclusive differential expression profile for all four enzymes, including Casp-7.

4.5.1. WB vs. ELISA

The trend of protein expression was similar between the two methodologies for Birc-4 (XIAP), -5 (Survivin) but not for Casp-3 (See table 4.2). Although the trend of expression for Birc-4 (XIAP) and -5 (Survivin) was similar, the magnitude of difference varied; *i.e.* fold change value was varied significantly.

Table 4.2. Comparison of WB and ELISA analysis data for IAPs (Birc-4 and Birc-5) and caspases (Casp-3 and Casp-7). Expression trend comparison between the two techniques can be monitored. Significant increased expression is represented in green boxes, significant decreased in orange. Less than 1.5 fold change is considered marginal. WB analyses units are arbitrary for the relative expression where E9 is the internal calibrator and always equals 1, where for ELAIS, actual vlaues for protein quantity is recorded. Increase or decrease in expression is relative to E9, where protein concentration for E9 was as follows; Birc-4 (XIAP)= 1184 pg/mL, Birc-5 (Survivin)=41.3 ng/mL, Casp-3= 7 ng/mL and Casp-7=2.2 pg/mL).

Enzyme	Technique	E4	E5	E6	E7	E8	E10	E12	E14	E16
Birc-4	WB	0.03±0.0	0.02±0.0	0.09±0.01	0.09±0.02	0.13±0.03	0.18±0.02	0.25±0.03	0.1±0.01	0.14±0.01
	ELISA pg/mL	0.32±0.01	0.32±0.0	22.5±0.43	119±7.4	221±9.3	694±136	173±9.3	0.41±0.0	0.36±0.01
Birc-5	WB	0.23±0.04	0.05±0.01	0.02±0.0	0.03±0.01	0.1±0.01	1.79±0.05	0.14±0.03	0.06±0.01	0.08±0.03
	ELISA ng/mL	0.03±0.0	3.1±0.0	8.7±0.02	3.1±0.0	10 ±0.03	28.8±0.31	19.8±0.26	5.2±.01	0.03±0.0
Casp-3 (cleaved)	WB	0.47±0.12	0.55±0.14	0.46±0.05	0.27±0.08	0.15±0.03	0.71±0.1	0.31±0.02	1.33±0.07	1.52±0.04
	ELISA ng/mL	5.8 ±0.1	7.7 ±0.5	0.43±0.0	0.42±0.0	3.9±0.12	7.4±0.22	1.7±0.07	2.1±0.03	0.11±0.0
Casp-7	ELISA pg/mL	1474±6	534±1.6	122±0.02	34.7±0.0	0.22±0.0	111±0.0	1004±4	75.8±0.01	0.22±0.0

4.5.2. Protein expression profile for Birc-4 (XIAP) and Birc-5 (Survivin)

From both WB and ELISA analyses, Birc-4 (XIAP) and -5 (Survivin) were both significantly downregulated at the early and late phases of the studied developmental course (Figure 4.1(B) and Table 4.2). The downregulated expression pattern that was observed coincided with the known early and late cell death waves, while the upregulated expression of Birc-4 (XIAP) and -5 (Survivin) correlated with the period around E9, where cell death is known to be reduced in the developing chick retina (Figure 4.1(B)). This is in line with the report that XIAP is a potent anti-apoptotic enzyme (Vitte-Mony *et al.*, 1997,

McKinnon *et al.*, 2002, Oost *et al.*, 2004) that binds caspases directly to inhibit them (Eckelman *et al.*, 2006).

Like Birc-4 (XIAP), at the middle stages (around E9), increased expression of Birc-5 (Survivin) was observed. Survivin was reported to inhibit apoptosis by reducing Casp-3 and Casp-9 activity and by preventing the formation of the apoptosome (Dohi *et al.*, 2004, Jiang *et al.*, 2005). Survivin is also known for its role in regulating several physiological processes in different eye tissues embryonic development, such as the lens, where Birc-5 (Survivin) was reported to regulate proliferation and differentiation (Jarrin *et al.*, 2012). Moreover, evidence that Birc-5 (Survivin) has a role in regulating cell cycle and apoptosis for neural stem cells was reported (Thiel, 2013).

4.5.3. Protein expression profile for Casp-3 and Casp-7

On the proteomic level, the active form of Casp-3 was demonstrated to be highly expressed around the same period of neuronal apoptosis in mouse CNS (Cheng *et al.*, 2011). Casp-3 was also found to be crucial for apoptosis-independent neuronal differentiation *in vitro* and in synaptic plasticity and neurite pruning (Fernando *et al.*, 2005, D'Amelio *et al.*, 2012). Our WB data of active Casp-3 protein expression showed moderate to high expression levels throughout the ten studied periods. Expression was moderately high during the early stages of PCD, diminishing to E8 with expression, most prominent at E9, E14 and E16 (Figure 4.2). Whereas the ELISA assay for active Casp-3 revealed a different pattern of differential expression, where the enzyme was expressed highly as early as E4 and E5, diminishing to E7 and then increasing again around the middle stage from E8 to E10, diminishing thereafter. This variation in expression is unexplainable. However, Casp-3 is expected to be expressed in the retina for most of the embryonic developmental course due to its proposed role in many physiological processes in the developing neural tissues, *e.g.* apoptosis, differentiation and neuronal synaptogenesis. Our data reflected a general and relatively moderate expression level of Casp-3 for most of the studied embryonic stages, particularly during the first wave of cell death at E4-E5, whereas the high expression of Casp-3 at E12-E14 seen using WB

was not reflected in the data obtained using ELISA. From previous studies, Birc-4 (XIAP) was found to directly bind and inhibit Casp-3. The correlation of expression between the two enzymes from our data reflects a direct or indirect effect of Birc-4 inhibition on Casp-3, where high Birc-4 protein expression around E9 correlated with high Casp-3 expression at the same time. This Birc-4 could be inhibiting Casp-3 apoptotic activity during this period, whereas the lack of Birc-4 expression at E4-E5 would Casp-3 to fulfil its apoptotic function. Some of this variation can be explained in the light of the complexity of the overlapping cellular processes taking place in the developing neural tissue. Differentiation, cell death and synaptogenesis pathways all operate simultaneously, and many factors interact and influence each other's action. Also, some protective agents such as the Bcl-2 anti-apoptotic factors and neurotrophins might exert a neuroprotective action (Gibson *et al.*, 1996, Bonfanti *et al.*, 1996, Nir *et al.*, 2000, Qu *et al.*, 2010).

WB analysis in this study failed to detect any protein bands for Casp-7. This could be explained by insufficient primary antibody, where some antibodies have low affinity to the protein of interest. However increasing the primary antibody concentration (two folds) did not improve the assay result. Although homology between chicken and mouse Casp-7 was reasonable (68% according to BLAST two protein similarity check), antibody affinity could be still very low. Other factors that may affect the WB sensitivity may include insufficient protein sample, poor or incomplete transfer or overtransfer, isoelectric point of protein of interest is lower than 9, sodium azide contamination and insufficient incubation time with the primary antibody.

Casp-7, from the ELISA data, was highly expressed at the two stages of cell death, early at E4 and E5 and then at the later stage at E12. This suggests a direct pro-apoptotic function of Casp-7 in the chick developing retina. (Zhang *et al.*, 2007) confirmed that higher expression of Casp-7 enzyme was detected in the developing mouse brain and retina compared with adult animal tissues, and suggested that apoptosis may be induced by an ER stress mechanism. Moreover both Casp-7and Casp-3 were illustrated to have a role in

reorganisation of cellular microfilament system components that are known to be cleaved during apoptosis (Sgorbissa *et al.*, 1999).

The variation between WB and ELISA results could be attributed to technical variation. WB procedure is cumbersome and more manipulation of sample is involved. However, it is more accurate for detecting proteins as less cross-reactivity of antigens occurs. On the other hand, ELISA is more sensitive and is considered to be a screening assay. Overall, the result of both techniques were used to interpret the protein expression profile. More analyses is needed to assess the protein expression pattern of the rest of chicken IAPs and caspases to provide a complete profile of these two families of enzymes in the chicken (*Gallus gallus*) species.

The protein expression pattern studies here summarises WB and/or ELISA analysis data for two IAPs and two caspases of the chick embryo in the developing neural retina. Birc-4 (XIAP) and Birc-5 Survivin have been found to be upregulated in the middle of the studied period of development, but protein expression plummeted significantly at the beginning (early stage) and end (late) of the studied period. These two stages were reported to coincide with two proposed waves of embryonic developmental cell death in the chick retina. On the contrary, the two caspases studied here showed a different pattern of differential expression, where Casp-3 and Casp-7 were upregulated at the proteomic level during or just proceeding the two cell death waves. At the same time, Casp-7 was significantly downregulated at the middle stage between the two cell death waves, whereas, according to both WB and ELISA, Casp-3 expression remained quite high during the middle stages of development (E8-E10). The latter result could be explained by the concomitant expression of Birc-4 (known to bind to and inhibit Casp-3) during this time period. From these expression data, it can be tentatively proposed that Casp-3 has a role mainly at early stages of PCR (E4-E5) whereas Casp-7 has a role during the later wave of cell death (around E12).

4.5.4. Correlation between gene and protein expression

The Central Dogma of molecular biology declares that DNA makes RNA and mRNA makes proteins. However, there is always a significant indecision regarding the common genome-wide correlation between levels of mRNA and equivalent proteins. mRNA abundance and protein synthesis level in different cell types and different species exhibit a wide range of correlation patterns for different genes. Other aspects that can influence how transcript abundance reflects protein expression level include protein turnover rate, *i.e.* protein stability and half-life extent and the choice of analytical technique (Maier *et al.*, 2009, Taniguchi *et al.*, 2010, Gedeon and Bokes, 2012, Vogel and Marcotte, 2012).

From observing the graphs of RT-qPCR data of mRNA expression and those of protein expression obtained by WB, different patterns of correlation can be observed for the four proteins (Birc-4, Birc-5, Casp-3 and Casp-7). Upregulated genes at certain developmental stages measured by RT-qPCR did not always reflect a subsequent high protein expression. This inconsistency could be attributed to all or some of the factors mentioned above. Figure 4.3 summarises the relationship between each of the four enzymes regarding relative transcript expression and corresponding protein expression.

A

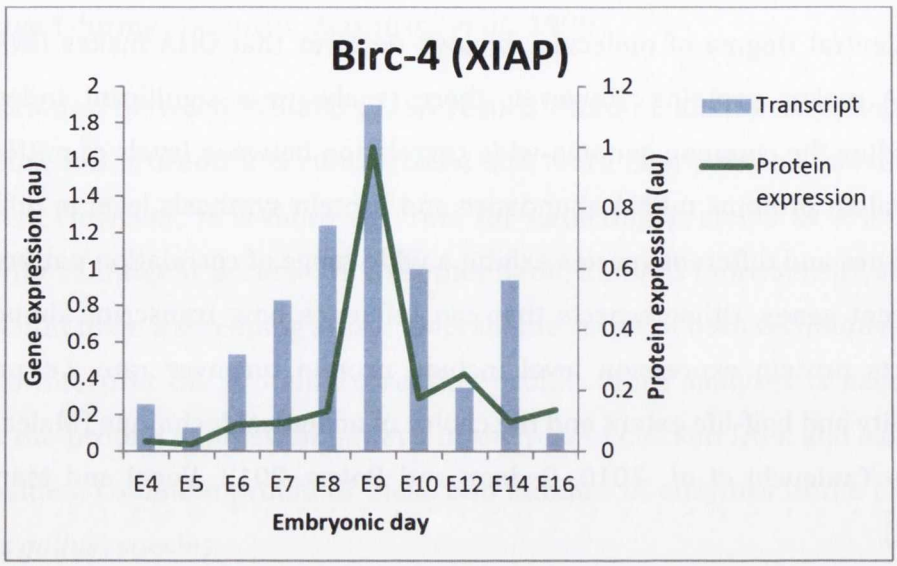
Birc-4 (XIAP)
Gene expression (au)
Protein expression (au)
Transcript
Protein expression
2
1.8
1.6
1.4
1.2
1
0.8
0.6
0.4
0.2
0
1.2
1
0.8
0.6
0.4
0.2
0
E4 E5 E6 E7 E8 E9 E10 E12 E14 E16
Embryonic day

B

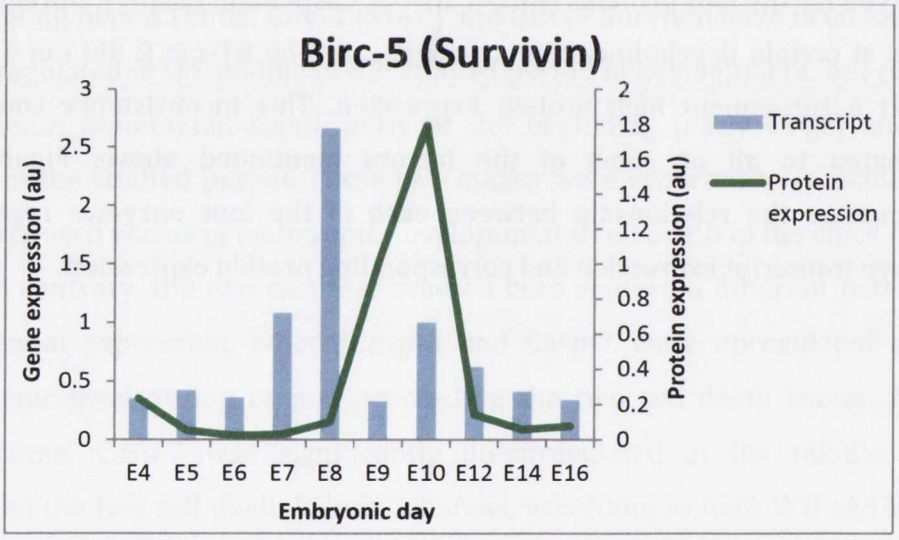
Birc-5 (Survivin)
Gene expression (au)
Protein expression (au)
Transcript
Protein expression
3
2.5
2
1.5
1
0.5
0
2
1.8
1.6
1.4
1.2
1
0.8
0.6
0.4
0.2
0
E4 E5 E6 E7 E8 E9 E10 E12 E14 E16
Embryonic day

C

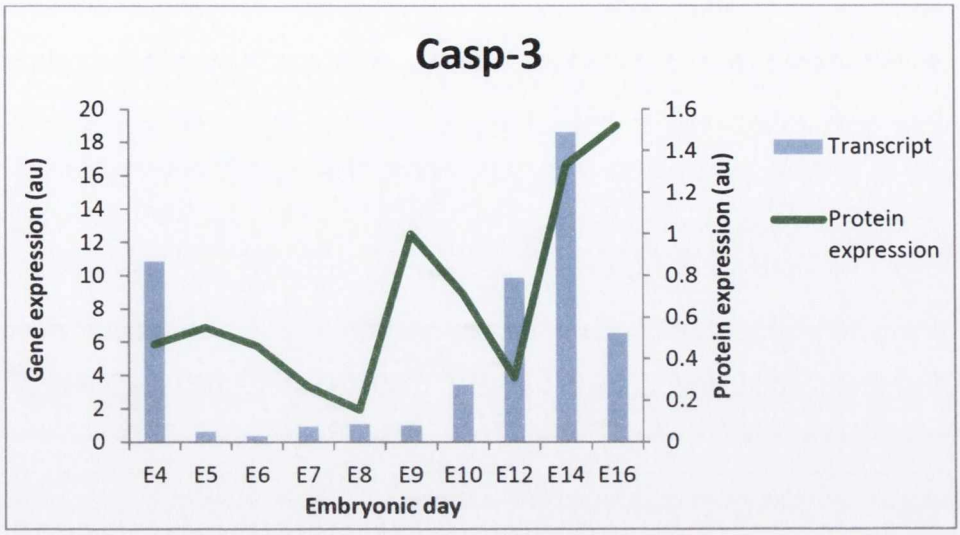

D

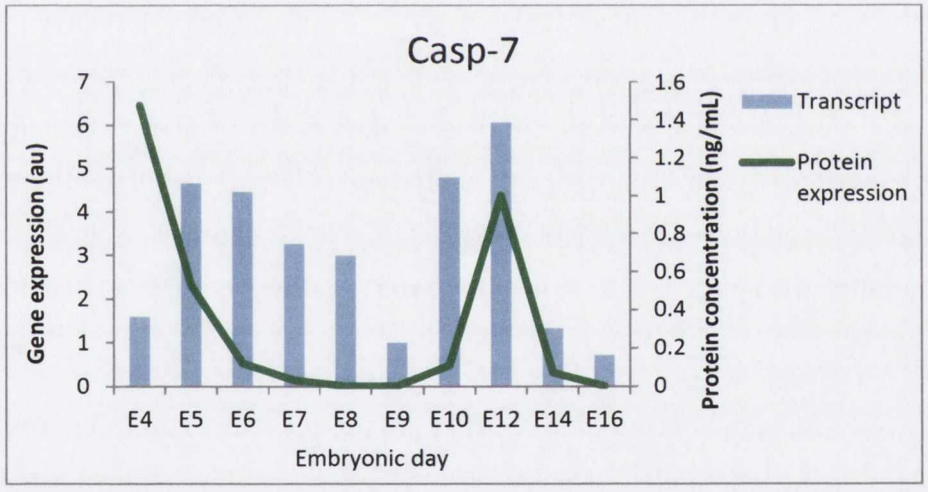

Figure 4.3. Correlation of mRNA (transcript) and protein expression for Birc-4 (XIAP), Birc-5 (Survivin), Casp-3 and Casp-7. RT-qPCR relative gene expression are represented by blue bars and WB protein relative expression for Birc-4, Birc-5 and Casp-3 in green line. Data values represent mean value for triplicate sample analysis.

It was noticed that Birc-4 transcript and protein expression were directly correlated especially at the middle of the studied range of embryonic stages where the highest level of expression for both was observed. It is also noticed that both upregulation pattern coincided particularly at E9. This suggests a fairly instantaneous translation of the protein at the same embryonic stage where the gene was upregulated. Overall correlation for all the ten embryonic stages was determined (Figure 4.4) by blotting a scattered correlation coefficient graph and a strongly positive linear relationship between Birc-4 transcript and protein expression was found (correlation coefficient (r) =0.74) (Figure 4.4 A).

Whereas Birc-5 exhibited a similar trend of transcript and protein expression as Birc-4 (Figure 4.3 A), it was noted that protein expression for Birc-5 was delayed (Figure 4.3 B). While RT-qPCR analysis for Birc-5 revealed maximum upregulation of the gene at E8, Survivin protein highest expression level was shown to occur two days later at E10. This suggests a delayed protein synthesis. When measuring the correlation between transcript and protein expression, delayed protein synthesis significantly reduces the correlation value (Gedeon and Bokes, 2012), where r=0.0 (Figure 4.4 B). Another factor that has to be considered when assessing protein expression level is protein stability and turnover rate and mRNA degradation rate (Vogel and Marcotte, 2012).

Casp-3 transcript expression correlation to protein expression revealed a slight direct relationship where r =0.44 (Figure 4.4 C). Whereas Casp-3 mRNA expression peaked at E4 and E14 (early and late), protein highest levels were detected at E9 (middle development stage) and later at E14 and E16 (Figure 4.3 C). High transcript expression was observed at E4, and simultaneous subsequent protein increased level was observed. Likewise, high protein level of Casp-3 was detected at E9. Later, high transcript expression level of Casp-3 was accompanied simultaneously with high protein levels at E14 and E16.

Similarly, Casp-7 revealed a weak correlation between transcript and protein expression (r =0.21) (Figure 4.4 D). An overall high transcript relative

expression for Casp-7 was measured, especially at E5 and -6 and then later at E10 and -12, whereas highest protein level was detected at E4 (Figure 4.3 D) and later at E12. The increased level of Casp-7 protein at E4 could be a result of upregulation of the Casp-7 gene earlier before E4, which was not covered in this study. However, high Casp-7 protein expression at E12 is following the E10 upregulation and coinciding simultaneously with E12 transcript expression. These data strongly suggest a vital physiological role of Casp-7 around E12 in the chick developing retina either in apoptosis or other developmental pathways. Similarly, these data are in line with reports of Casp-7 abundance in the embryonic brain and retina more than adult mouse tissues (Zhang et al., 2007).

A

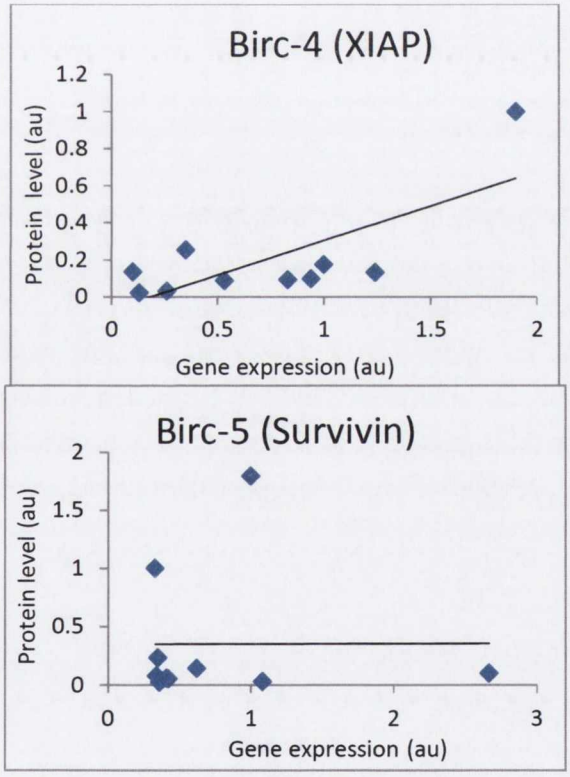

C

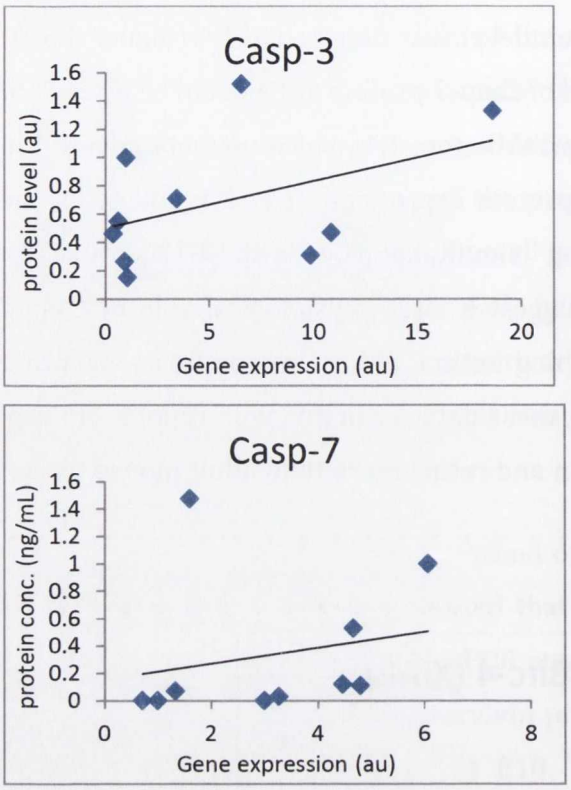

Figure 4.4. Correlation coefficient plot for the relationship between transcript (mRNA) and protein expression Birc-4, Birc-5, Casp-3 and Casp-7. Gene expression was assessed by RT-qPCR analyses and values represented are relative expression level to E9 (calibrator). Protein expression levels were analysed by WB for Birc-4, Birc-5 and Casp-3 and by ELISA for Casp-7. (A) Moderate direct correlation between Birc-4 (XIAP) gene and protein expression (correlation coefficient (r)=0.74). (B) No significant correlation for Birc-5 (Survivin) (r=0.0). (C) Moderate direct correlation for Casp-3 (r=0.44). (D) Low direct correlation for Casp-7 gene and protein expression (r=0.21).

Chapter 5

Immunohistochemistry (IHC) Analysis for IAPs and Caspases

5.1. Introduction

Pro-apoptotic caspases and anti-apoptotic IAP enzymes were demonstrated to have a role in the regulation of apoptotic cell deletion in vertebrate retinae during normal embryonic development, tissue homeostasis and in retinal neurodegenerative diseases (Rosenbaum *et al.*, 1997, Nickells, 1999, Tezel and Wax, 1999, Doonan and Cotter, 2004, Kim and Park, 2005, Kisiswa *et al.*, 2010a, Varfolomeev *et al.*, 2012, Roy *et al.*, 2013).

The neural retina is a highly specialised structure separated from the outer layer of the whole retina by the intraretinal space and consists of a neuroepithelial layer (or photoreceptors), a bipolar ganglion layer, a multipolar ganglion layer and their axons (Figure 1.2) (Perry, 1981, Prada *et al.*, 1991). During early embryogenesis, the retinal tissue is subjected to a differentiation process that starts with the specification of a neural retinal domain within the neuroepithelium of the optic vesicle. Undifferentiated retinal progenitor cells undergo a sequential overlapping differentiation into the distinct cell types organised into retinal cell layers (Adler and Canto-Soler, 2007, Vergara and Canto-Soler, 2012).

In chick embryos, the retinal development process lasts about three weeks and is complete at the time of hatching. At the early stages (E4 and E5) the retinal tissue is composed of two main areas: retinal pigmented epithelium (RPE) precursor and the neural epithelium (NE). The ventricular neural epithelium comprises a multipotential neuroepithelium (Mey and Thanos, 2000). At the middle embryonic stage (E8), retinal progenitor cells are still in cell division phase. However, at this middle stage, the self-renewal of progenitor cells falls below 50% and most postmitotic cells start to differentiate into different neurons and glia, with RGCs being the first to differentiate, followed by photoreceptors and then the rest of the retinal cell types (Dutting *et al.*, 1983). By E16, the pseudostratified NE is transformed into the multi-layered specialised retinal tissue (Mey and Thanos, 2000).

Retinal ganglion cells (RGCs) are a type of interneuron located near the inner cavity of the eye globe in contact with the vitreous humour and they receive

visual input from photoreceptors via bipolar cells and amacrine interneurons. RGCs are responsible for transmitting image-forming and non-image forming information by means of action potentials through the optic nerve, which is formed from long RGC axons, to several target regions in the brain, including the hypothalamus, lateral geniculate nucleus, pretectal nuclei, superior colliculus and the primary visual cortex (Margalit and Sadda, 2003, Selhorst and Chen, 2009, Masland, 2012, Coubard *et al.*, 2014).

Based on analyses of both transcript and protein expression of caspases and IAPs of interest (as presented in Chapters 3 and 4), it is necessary to analyse the correlation between these expression patterns and *in situ* localisation of proteins within the neural retina. This would assist in understanding of the role of each of these enzymes in the apoptotic cell death mechanism. Such assessment becomes possible when localisation of proteins is carried out simultaneously with apoptosis assay simultaneously. Neural retina sections were used for IHC localisation of two IAPs, Birc-4 (XIAP) and Birc-5 (Survivin), and the two effector caspases, Casp-3 and Casp-7.

According to the protein expression profiling carried out in Chapter 4, these four enzymes showed the most relevant pattern of expression in terms of correlation with the early and late cell death waves. Immunostaining of retina sections with target protein antibodies was performed by IHC at three developmental stages (early, intermediate and late) and fluorescent microscopy was utilised for detection (immunofluorescence or IF).

Immunofluorescence (IF) allows qualitative detection of proteins within a tissue section by exploiting the principle of antibody-specific binding to a target protein. Secondary (indirect) immunofluorescence uses two antibodies, an unlabelled primary antibody that binds specifically to the target protein, and a species-specific secondary antibody that binds the primary antibody. Visualisation of antigen-antibody interaction can then be achieved by a fluorophore-tagged antibody and detected by fluorescent microscopy, which allows visualisation of the exact location of the target protein *in situ*. The different fluorescent filters allowed a distinction to be made between the

nucleic acid stained with Cytox Green images and fluorophore stained secondary antibody Alexa Fluor images.

5.2. Aims

The aim of this chapter is to better understand the relationship between temporal and spatial expression of four enzymes, Birc-4 (XIAP), Birc-5 (Survivin), Casp-3 and Casp-7, by performing IHC for selected embryonic stages (early: E4 and E5; intermediate: E8.8; and late: E14 and E16). At the early and late embryonic stages, apoptotic cell death was proposed to occur naturally. The intermediate stage was used to compare enzyme activity where developmental cell death was less prominent and to assess the four protein enzymes throughout the whole studied period of embryonic retinal development. Correlation between temporal and spatial expression would assist in identifying each protein expression location within retinal layers/cell type. Utilisation of neuronal cell marker counterstaining helps identifying target protein spatial expression within specific cell type.

5.3. Experimental design

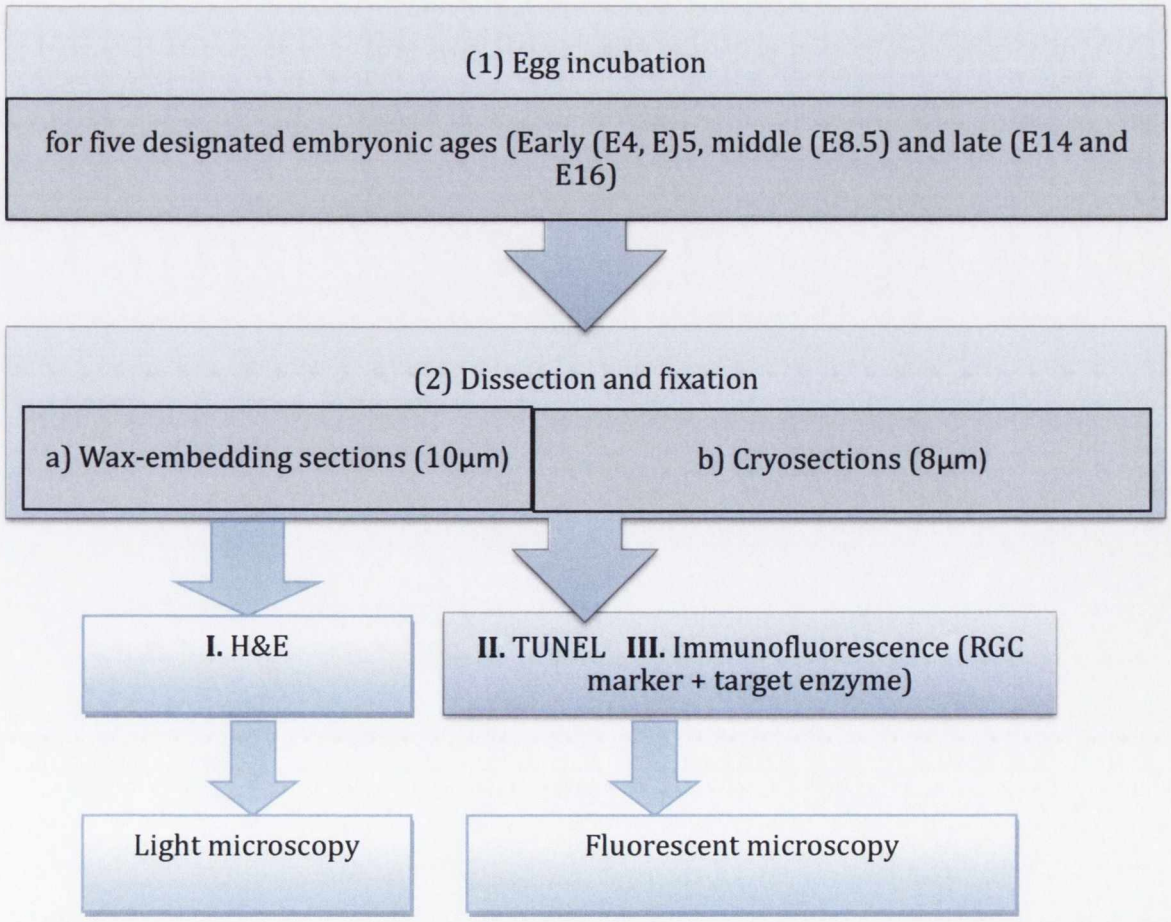

5.4. Results

5.4.1. Retina morphology analysis by Hematoxylin and Eosin staining (H&E) and Cytox Green nuclei staining

Standard H&E staining was carried out to show the laminar and cellular structure of the retina during the different developmental stages (Figure 5.1). The progressive normal morphological changes of the retina during embryogenesis between E4 and E16 can be tracked from early to late embryonic stages. At E4, which is considered an early stage of development, the whole neural retina is pre-laminated and coinciding with cell-fate determination (Edqvist *et al.*, 2006). At this very early age, the retinal tissue is referred to as the neuroretina and its orientation can be identified by the neighbouring retinal pigmented epithelium (RPE) that border the outer side of the retina which corresponds to the photoreceptors layer side. By E8.5 age, the retina is larger in size but laminae are still not well defined visually. However, immunostaining studies with cell-specific markers at this middle age have successfully identified different neuron types (Doh *et al.*, 2010). At later ages (E14 and E16), more defined laminar structure can be identified where cells are arranged into defined layers within the neuroretina.

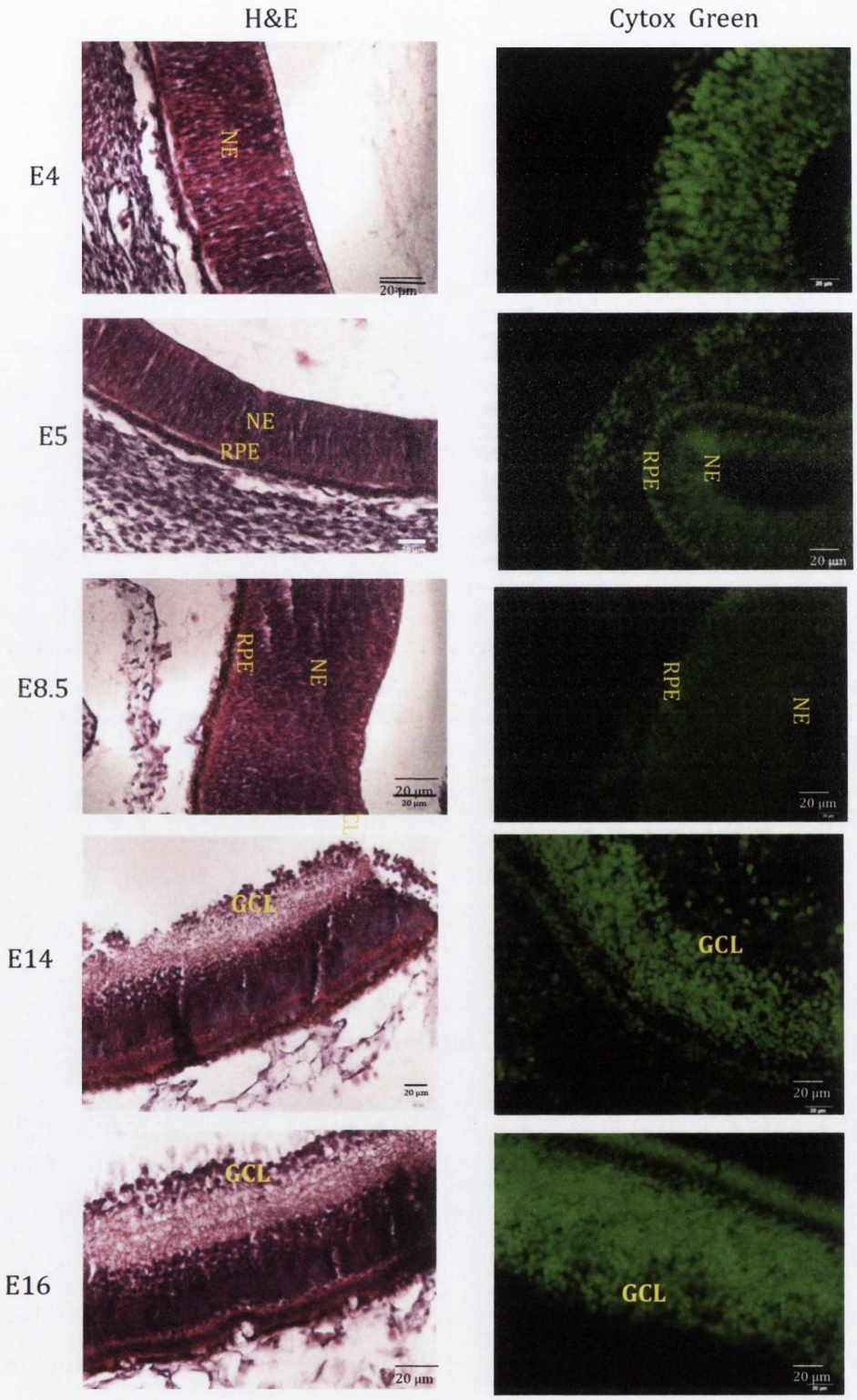

Figure 5.1. H&E and Cytox Green staining of chick embryo developing retinae at early (E4, E5), intermediate (E8.5) and late (E14, E16). Abbreviations: NE, neural epithelium; GCL, ganglion cell layer; RPE, retinal pigmented epithelium.

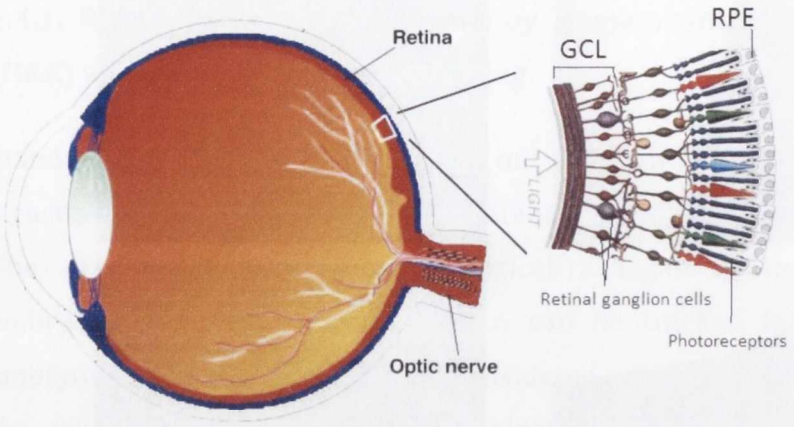

Figure 5.2. A diagram of the eye showing the location of the neural retina and the orientation of retinal layers. Ganglion cell layer (GCL) is lining the inside of the eye globe attaching directly to the vitreous humour filling the eye ball. Retinal Ganglion cells (RGCs) are the first set of retinal cells to receive the light rays entering the eye from the pupil. The outermost layer of the neural retina is the photoreceptors that is lined by the retinal pigmented epithelium (RPE).

5.4.2. Immunohistochemistry (IHC) and Immunofluorescence (IF)

Five developmental stages, E4 and E5 (early), E8.5 (intermediate) and E14 and E16 (late) were studied for antigen localisation in fixed tissue by using four antibodies. Anti-XIAP (anti-Birc-4), anti-Survivin (anti-Birc-5), anti-caspase 3 and anti-caspase 7 were utilised as primary antibodies for estimating the presence and abundance of these four enzymes in the chick developing retinae (Figures 5.4, 5.5, 5.6 and 5.7). A two-step IF procedure was run with double staining of each embryonic stage with both Islet-1, a marker for RGCs, and one of the primary antibodies for the four enzymes.

5.4.2.1. TUNEL apoptosis assay

TUNEL assay coupled with PI nuclei stai ning showed the apoptosis pattern for E4 (early), E8.5 (intermediate) and E14 (late embryonic stage) (Figure 5.3). At both E4 and E14, where apoptotic cell death occurs according to many reports, a high level of TUNEL staining is shown throughout the whole neural retinal tissue, whereas at E8.5, what appears to be only single cell staining was detected at the photoreceptors layer.

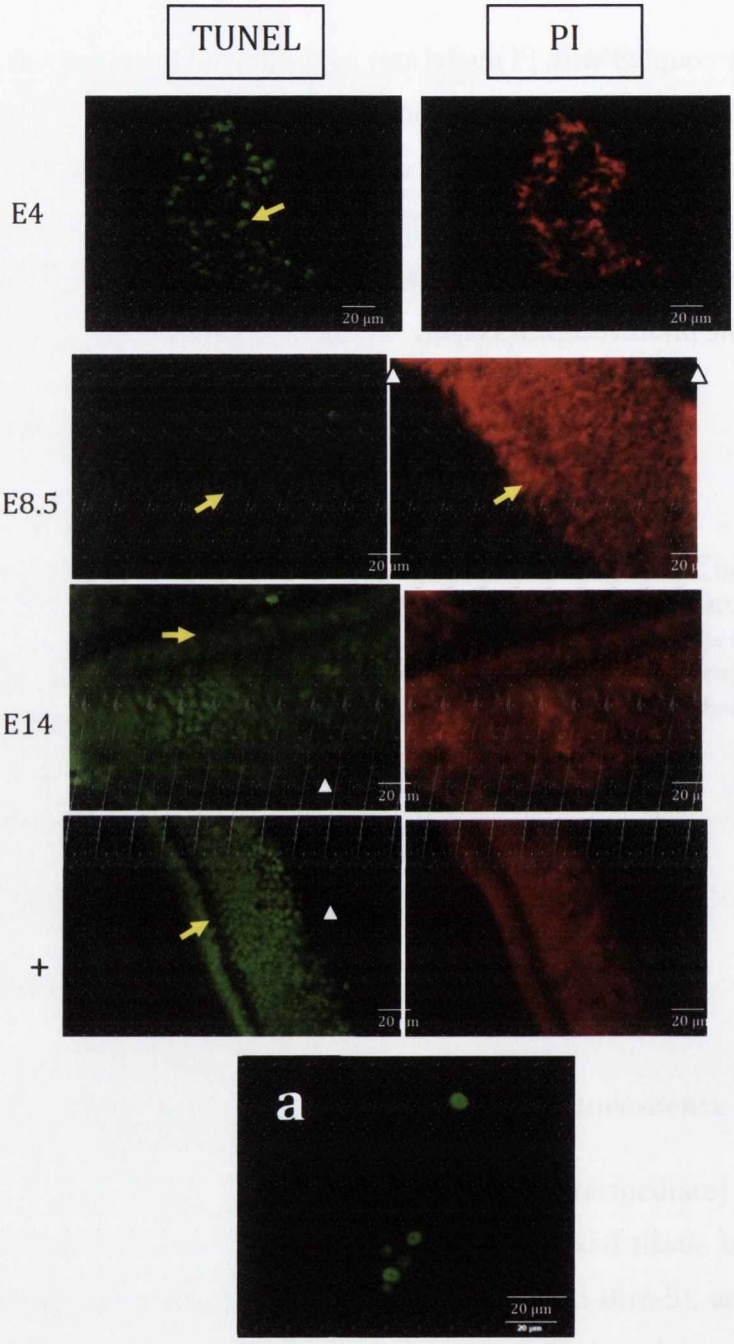

Figure 5.3. TUNEL assay for E4 (early), E8.5 (intermediate) and E14 (late developmental stage) coupled with propidium iodide (PI) nuclei staining. A positive control (+) for DNase-digested E14 section following proteinase K incubation shows a massive DNA fragmentation. (a) A magnification of TUNEL-positive cells from the E14 sample showing the distinctive apoptotic nuclei appearance where chromatin is fragmented and condensed in the form of bright green dots. Early and late stages (E4 and E14) retina sections are strongly TUNEL-positive, indicating a prominent DNA fragmentation pattern. In contrast, at E8.5 apoptotic nuclei were very scarce. Yellow arrows indicate the RPE (and photoreceptor) layer and white arrow heads indicate GCL.

5.4.2.2. Spatiotemporal analysis of IAPs and Islet1 with double-staining IHC

Two-step IF for both IAPs (Birc-4 (XIAP) and Birc-5 (Survivin)) showed a downregulation pattern of protein expression in the neural retina at both early (E4 and E5) and late (E14 and E16) developmental stages (Figures 5.4 and 5.5), whereas at intermediate stage (E8.5) the protein expression for both IAPs was upregulated indicated by a higher intensity of primary antibody fluorescence detection in the whole neural retina layers, i.e. all retinal cell types.

At E5, although overall downregulation of Birc-4 (XIAP) but few clusters of expressed Birc-4 can be detected at the GCL (Figure 5.4), which suggests a possible anti-apoptotic activity of Birc-4 (XIAP) enzyme in a small population of retinal ganglion cells during E5. Whereas at E8.5 where a major Birc-4 (XIAP) activity is proposed, the whole neural retina, i. e. all neural cell types are undergoing a proteolytic activity of anti-apoptotic Birc-4 (XIAP).

Similarly, Birc-5 (Survivin) antibody is predominantly expressed at E8.5 in all retinal neural cells equally (Figure 5.5). This is especially clear when examining the merge mage of both Islet-1 and Birc-5 (Survivin) expression images where it is clear that all cells marked with Islet1 are also immunostained with Birc-5 as expected. At the middle stages a massive cellular protective (anti-apoptotic) activity is expected in the retinal tissue and it is proposed that antiapoptotic agents such as Birc-4 (XIAP) and Birc-5 (Survivin) play a major role in this protective mechanism. These remarks are supported by our data presented here in Figure 5.4 and 5.5.

Islet1 antibody (a neuronal marker) fluorescence was obviously taken up by the whole retinal tissue and not specifically by limited number of cell types, this suggests equal distribution of neural cells throughout the neural retina and that Islet1 antibody is universal for different retinal neurons. Adjacent non-neuronal tissues such as RPE and connective tissues were not immunostained with Islet1 marker and all fluorescence was confined to the neural retina in all analysed sections (Figures 5.4 to 5.7).

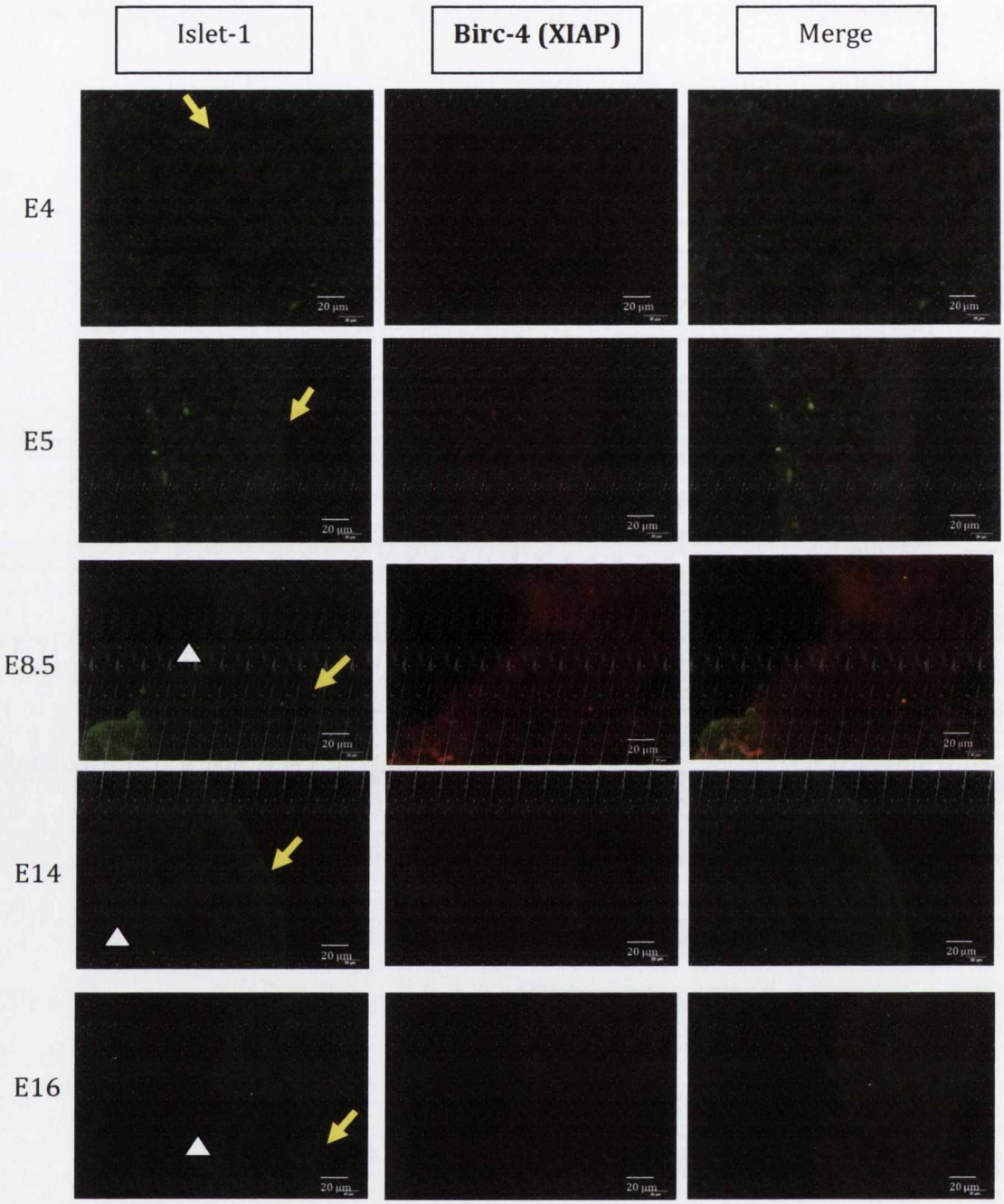

Figure 5.4. Spatiotemporal expression pattern for Islet-1 and Birc-4 (XIAP). Double-immunostaining against Islet-1, a marker of neuronal cells at early (E4 and E5), intermediate (E8.5) and late (E14 and E16) embryonic stages with Birc-4 (XIAP) enzyme. Yellow arrows indicate RPE (and photoreceptor) layer and white arrow heads indicate GCL. Note that At early ages (E4 and E5) no defined GCL layers are present yet.

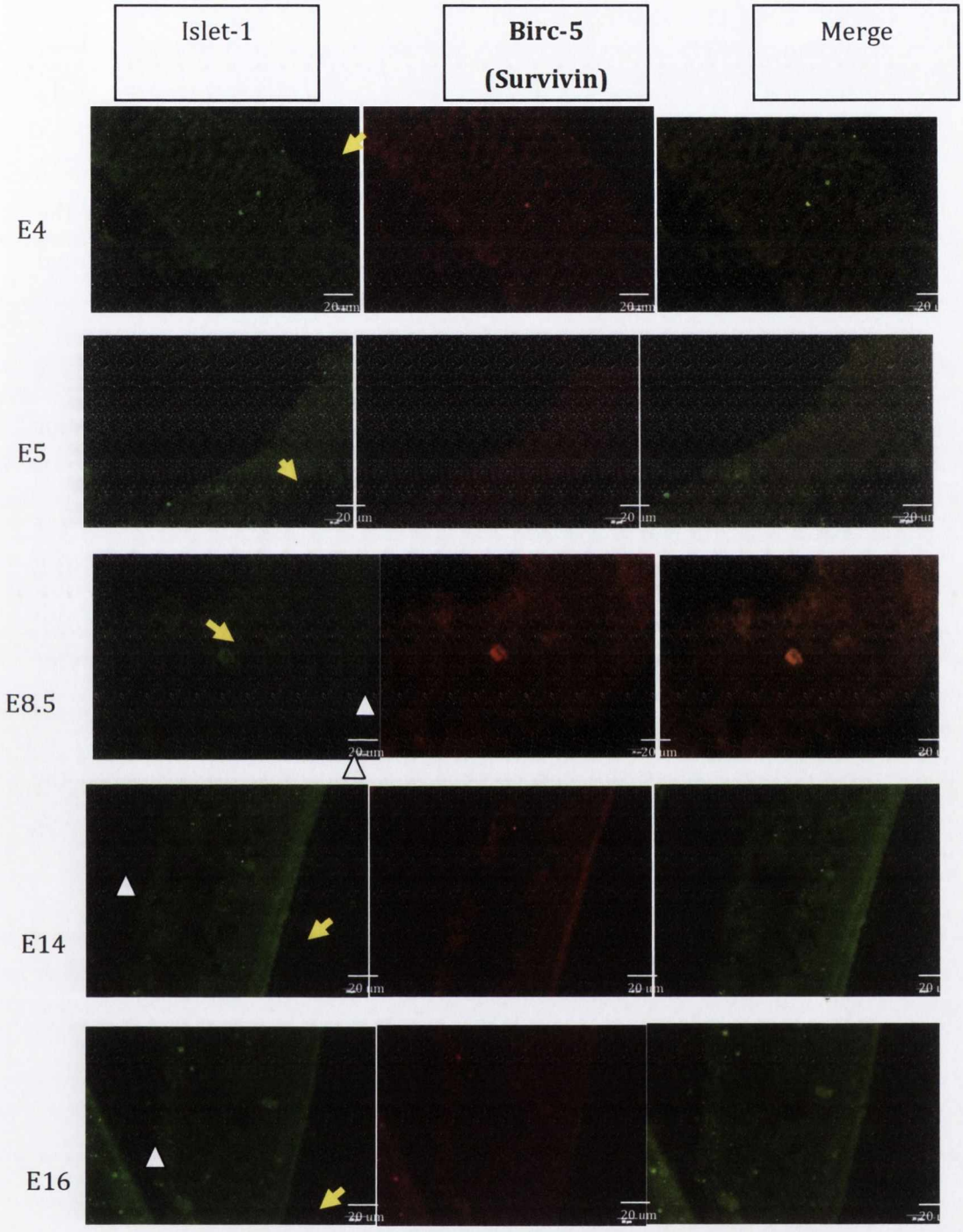

Figure 5.5. Birc-5 (Survivin) spatiotemporal expression pattern along with Islet-1 neuronal marker at early (E4 and E5), intermediate (E8.5) and late (E14 and E16) embryonic stages. Yellow arrows indicate RPE (and photoreceptor) layer and white arrow heads indicate GCL.

5.4.2.3. Spatiotemporal analysis of caspases and Islet-1 with double-staining IHC

The expression pattern of the two caspases, 3 and 7, was the direct opposite of that of the two IAPs (Figure 5.6 and 5.7). Much lower fluorescence intensity was detected for E8.5 than E4, E5, E14 and E16.

Islet1 neuronal marker was seemingly taken up by all retinal layers for all the studied ages. An equal distribution was detected for Islet1 by the entire retinal tissue (Figure 5.6 and 5.7).

Casp-3 was expressed mainly at the early (E4 and E5) and late (E14 and E16) ages, but not for the middle age (E8.5). This notion is expected as a major apoptotic activity is proposed at the early and late developmental stages, but much less apoptotic activity was reported for the middle stages. It was observed that especially at E5 Casp-3 was expressed highly at the RPE corresponding to the photoreceptors layer (Figure 5.6). Whereas at E16, both Islet1 and Casp-3 antibodies detection showed a higher expression pattern for both markers at the RGL that mainly includes retinal ganglion cells.

Casp-7, like Casp-3, illustrated an overall expression distribution in all the retinal tissue. At E16 especially, more prominent expression pattern was detected at both RGL and RPE layers (Figure 5.7).

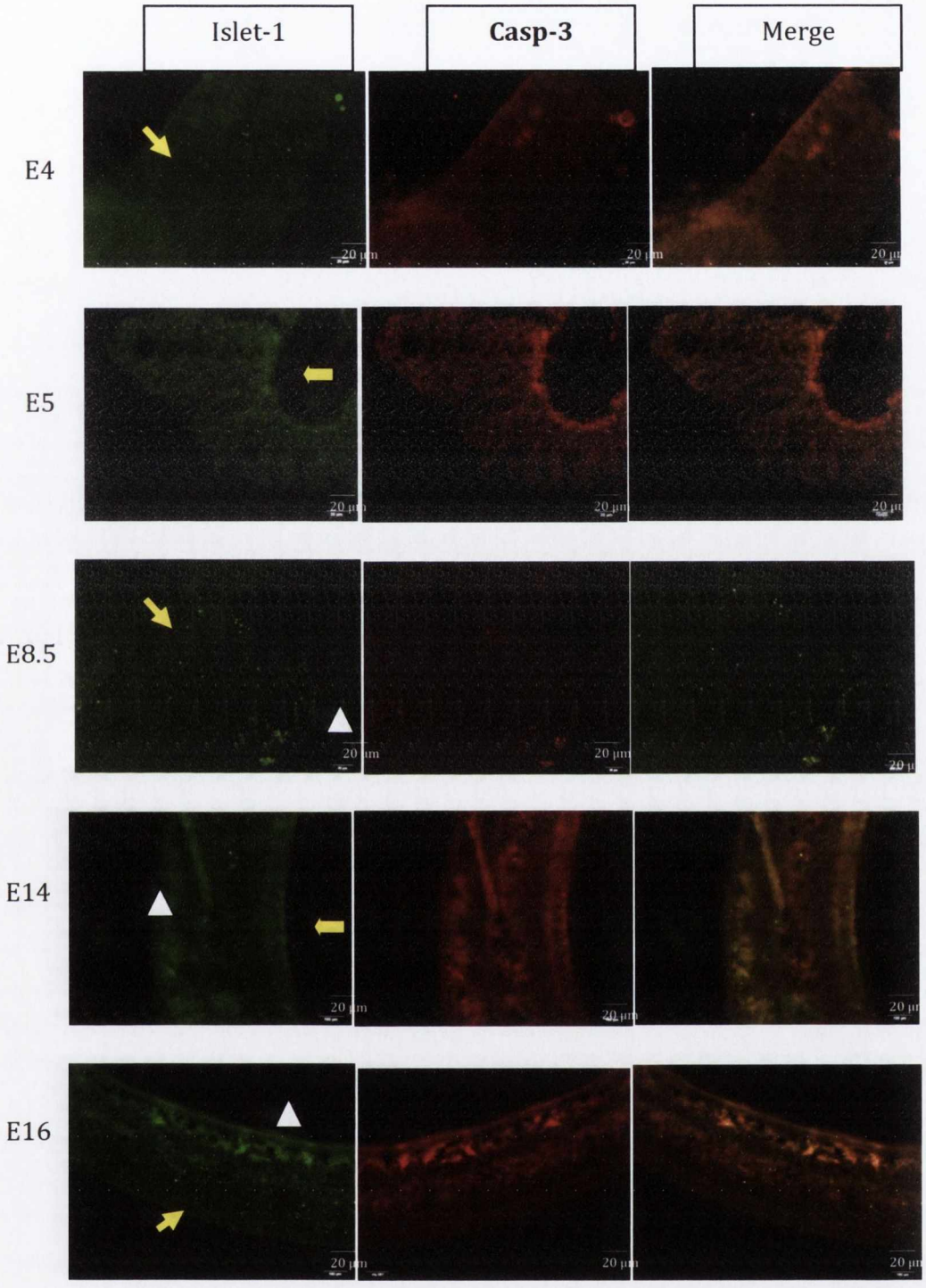

Figure 5.6. Casp-3 spatiotemporal expression pattern along with Islet-1 neuronal marker at early (E4 and E5), intermediate (E8.5) and late (E14 and E16) embryonic stages. Yellow arrows indicate RPE (and photoreceptor) layer and white arrow heads indicate GCL. Note that At early ages (E4 and E5) no defined GCL layers are present yet.

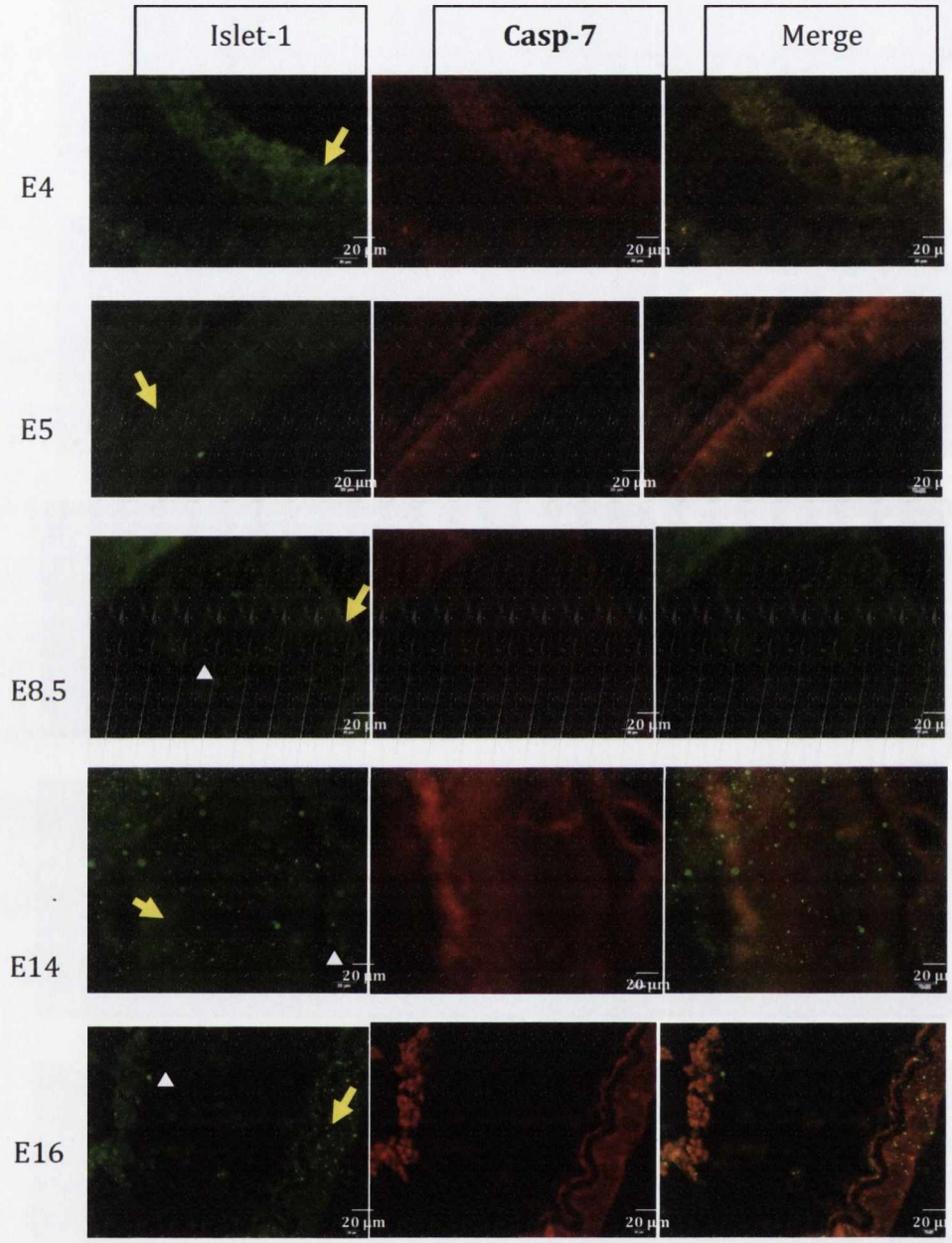

Figure 5.7. Casp-7 spatiotemporal expression pattern along with Islet-1 neuronal marker at early (E4 and E5), intermediate (E8.5) and late (E14 and E16) embryonic stages. Yellow arrows indicate RPE (and photoreceptor) layer and white arrow heads indicate GCL.

5.5. Discussion

The chicken embryo developing eye model is widely used in the study of the mechanism and pathophysiology of apoptotic cell deletion during embryogenesis. Advances in IHC and IF made it possible to trace protein localisation and abundance *in situ* for many proteins of interest.

Temporal gene and protein expression was attempted earlier in this work. In this chapter, spatio-temporal protein distribution of selected IAPs and caspases (the same proteins studied in Chapter 4) were determined using IHC and IF techniques.

Previously, many investigators have reported apoptosis, expressed caspases and IAPs in developing retinae in many vertebrate species (de la Rosa and de Pablo, 2000, Cole and Ross, 2001, Vecino *et al.*, 2004, Harvey *et al.*, 2009, Steinle, 2012, Lee *et al.*, 2013). In current research, both IAPs, Birc-4 (XIAP) and Birc-5 (Survivin) have demonstrated a major anti-apoptotic role by means of overexpression during the middle period where no apoptotic cell death is reported to occur. Conversely, Casp-3 and Casp-7 exhibited a potent apoptotic action during embryogenesis where expression was upregulated significantly during both early and late apoptotic waves in the developing retina. These four enzymes were a natural choice for in-depth protein analysis based on both previous studies and the findings of this work.

5.5.1. Morphological retinal structure staining

Both H&E and Cytox Green staining helped in visualising the laminar and cellular organisation of the different retinal cell types. RGCs are naturally located facing the inner space of the eye globe, directly attached to the vitreous humour that has been lost during tissue dissection, whereas the photoreceptors are on the opposite side of the retinal tissue bordering the RPE.

5.5.2. Assessment of apoptosis by TUNEL assay

Figure 5.3 shows bright green TUNEL staining for the detection of apoptotic activity at different embryonic stages (early (E4), intermediate (E8.5) and late (E14)). Nucleic acid-specific staining with propidium iodide (PI) red fluorochrome was employed to visualize the nuclear morphology of the various retinal cell types. Pre-treatment of sections with RNase ensures that only DNA is stained with PI.

In situ labelling with the TUNEL assay allowed for visualisation of apoptotic cells by detecting the bright green fluorescence of retinal cells (see Figure 5.3). At both E4 (early) and E14 (late stage/cell death period) a high level of apoptotic activity can be observed and this is in line with the numerous previous reports of apoptotic cell death occurrence during these two embryonic stages for the embryo developing retina (Martin-Partido *et al.*, 1988, Cook *et al.*, 1998, Diaz *et al.*, 1999, de la Rosa and de Pablo, 2000, Mayordomo *et al.*, 2003, Valenciano *et al.*, 2009, Chavarria *et al.*, 2013). In contrast, at the middle stage (E8.5), much less apoptotic activity was observed and this observation is in line with the same reports above.

Figure 5.3a shows a magnified image of a few apoptotic cells that have been stained with TUNEL. Classic apoptotic morphology can be observed where nuclear chromatin is defragmented and condensed in the form of granules.

5.5.3. Apoptotic enzymes expression assessment

Two-step IF was employed for the detection of each of the four enzymes: Birc-4 (XIAP), Birc-5 (Survivin), Casp-3 and Casp-7 along with Islet1, an antibody against the neuronal marker Islet1 antigen.

From IHC images, it was observed that the two IAPs (Birc-4 and Birc-5), and two caspases (Casp-3 and Casp-7), were all expressed in the whole neural retina to different extents in different embryonic stages (Figures 5.4 to 5.7)

compared with the negative control sample (not provided).

A broad sample of immunostained sections was analysed to assure that the staining is specific to the retinal tissue. The Islet1 neuronal marker aided in specifying the neural tissue of the retina and it was possible to define the four target enzymes reactivity specifically in the neural retina and not the surrounding areas.

5.5.3.1. Birc-4 (XIAP) and Birc-5 (Survivin) downregulation during cell death waves in the developing retina

As anticipated, both IAPs (Birc-4 (XIAB) and Birc-5 (Survivin)) were observed to be highly expressed in the middle stage of development (E8.5) where it is proposed that cell death levels are at their lowest (Figures 5.4 and 5.5). Meanwhile, at the early stages (E4 and E5) and late stages (E14 and E16), fluorescent intensity was lower where apoptotic cell death is higher (Frade *et al.*, 1997, Diaz *et al.*, 2000). As discussed in Chapter 4, both Birc-4 and Birc-5 were proven to participate in antiapoptotic activity by directly binding caspases and therefore inhibiting their apoptotic activity or by preventing the formation of the apoptosome (Vitte-Mony *et al.*, 1997, McKinnon *et al.*, 2002, Potts *et al.*, 2003, Dohi *et al.*, 2004, Oost *et al.*, 2004, Jiang *et al.*, 2005, Eckelman *et al.*, 2006, Unsain *et al.*, 2013). These findings for Birc-4 and -5 are in line with our protein expression data from WB and ELISA analyses (Chapter 4) where both IAPs exhibited very low levels of protein expression at early and late developmental stages and a very high relative expression pattern at the middle stages (E9 and E10) (see Figure 4.1 and 4.2 and Tables 4.1 and 4.2.).

5.5.3.2. Casp-3 and Casp-7 upregulation coincides with cell death waves in the developing retina

The two caspases (Casp-3 and Casp-7) exhibited the exact opposite pattern of expression, where higher fluorescent intensity was observed at the early and late stages than at E8.5 (Figures 5.6 and 5.7). These findings are in line with previous reports revealing the potent apoptotic action of both Casp-3 and

Casp-7. Active caspases 3 and 7 are widely used as an assessment tool for apoptosis in many systems (Bressenot *et al.*, 2009). Casp-3 is the main executer of the apoptosis pathway in both embryogenesis and in adult tissues (Kuida *et al.*, 1996, Philchenkov, 2004, Kivinen *et al.*, 2005, Hyman and Yuan, 2012). Additionally, Casp-7 also executes apoptosis potently and independently of mitochondrial pathways and it has been proposed that Casp-7 partially substitutes for Casp-3 in Casp-3-deficient cells (Mooney *et al.*, 2002, Davidson *et al.*, 2005, Lakhani *et al.*, 2006, Pyrko *et al.*, 2007, Zhang *et al.*, 2007a). Data shown in the current chapter are also consistent with our findings in the previous chapter for protein expression analyses. In Chapter 4, Casp-3 expression (from WB and ELISA) demonstrated a high expression pattern at early and late stages (Figures 4.1 and 4.2). Casp-7 (from ELISA data) also demonstrated a high expression pattern at the two stages of cell death waves. Moreover, both Casp-7and Casp-3 have been illustrated to be expressed highly during embryogenesis and to have a role in the reorganisation of cellular microfilament system components that are known to be cleaved during apoptosis (Sgorbissa *et al.*, 1999), and our findings here support this notion.

5.5.4. Conclusion

IHC presented here show clearly the direct correlation between caspases expression pattern and the spatiotemporal pattern of cell death in the chick retina during development. Conversely, IAPs exhibited an inverse correlation between protein expression and retinal cell death. These findings generally supports the concept that both IAPs; Birc-4 (XIAP) and Birc-5 (Survivin), are anti-apoptotic factors, whereas Casp-3 and Casp-7 are considered to be a potent pro-apoptotic factors.

From previous studies, Birc-4 (XIAP) was found to directly bind and inhibits Casp-3. Birc-5 (Survivin) was also reported to inhibit apoptosis by regulating a number of factors in the apoptotic cascade (McKinnon *et al.*, 2002, Potts *et al.*,

2003, Oost *et al.*, 2004, Jiang *et al.*, 2005, Unsain *et al.*, 2013). Our data supports these notions, where higher protein expression patterns for IAPs were inversely correlated temporally with caspase expression.

Chapter 6

Final Discussion and Conclusion

6.1. General discussion and conclusion

Each of the IAP and caspase family of enzymes were categorised based on their structural similarities. The baculovirus IAP repeat (BIR) motif domain and the RING finger domain are the two prominent structural features of all IAPs (Miller, 1999, Hinds *et al.*, 1999). On the other hand, all procaspases share large and small subunits, a prodomain, that upon proteolytic cleavage and/or undergoing allosteric conformational changes form the active form of the enzyme (Nicholson, 1999, Hyman and Yuan, 2012).

IAPs and caspases were shown to have a wide range of functions in embryonic development as well as homeostasis that include, but are not limited to, PCD regulation (O'Riordan *et al.*, 2008, Hyman and Yuan, 2012). In the developing nervous system, PCD is essential for proper neuronal development and connectivity and later, in adult life, also contributes to the origin and progression of neurodegenerative diseases (Varela-Nieto *et al.*, 2003).

From the literature, it has been elucidated that most of, but not all, IAPs and caspases have a chief role in the apoptotic pathway of metazoan cells. However, some IAPs and caspases play a modulatory role in PCD as well as in other physiological processes in neuronal cells during embryonic development in particular. These processes include inflammatory and immune responses and synaptogenesis (Wilson *et al.*, 1994, Eckhart *et al.*, 2000, Kuida *et al.*, 1996, Kasof and Gomes, 2001, Pohl and Jentsch, 2008, Delvaeye *et al.*, 2009, Shi *et al.*, 2009, Quesada *et al.*, 2010, Al-Shabrawey *et al.*, 2012). Moreover, some IAPs and caspases and the Bcl-2-mediated apoptotic pathway have been reported to be implicated in pathological conditions such as neurodegenerative diseases, including Alzheimer's (Cotman *et al.*, 2005, Ayala-Grosso *et al.*, 2006) and glaucoma (Nickells *et al.*, 2008), and in a vast variety of cancers (Cotter, 2009, Abd-Elrahman *et al.*, 2009, Ho *et al.*, 2009, Olsson and Zhivotovsky, 2011). These findings elucidating the role of apoptosis and the role of its regulators in the initiation and progression of many diseases provide an insight into novel approaches for prevention of these pathological conditions. In modern medicine, manipulating apoptosis regulators, including IAPs and caspases, is being introduced as a therapeutic strategy to prevent

the progression and/or to treat the symptoms of a number of genetic and malignant diseases (Hiss and Gabriels, 2009, Doonan *et al.*, 2012, Hensley *et al.*, 2013, Hassan *et al.*, 2014).

This study aimed to characterise the temporal gene and protein expression of all five chicken (*Gallus gallus*) IAPs and ten caspases known so far in the chick embryonic developing retinae. By utilising conventional semi-quantitative PCR and RT-qPCR, we investigated the relative expression level of all the 15 mRNA transcripts. Subsequently, WB, ELISA and IHC assays were used to assess the corresponding protein quantity levels and patterns of expression for correlation across ten embryonic developmental stages ranging from early (E4) to late (E16). We hypothesized that PCD/apoptosis pro-death agents would be expressed in the developing chick retina and that they would be upregulated during the time of the reported two cell death waves in the chick developing retina (Table 1.3) (Rager and Rager, 1979, Frade *et al.*, 1997, Cook *et al.*, 1998, Diaz *et al.*, 2000, Mayordomo *et al.*, 2003). The chick embryo proved to be an excellent model for studying the molecular biology of retinal cell death. Its relatively large eye, rapid development, availability of resources such as Hamburger and Hamilton (HH) staging and completed genome database made it possible to study cell death in the chick embryo eye at the molecular level.

Whereas the developmental role of neuronal cell death has been widely studied, the significance of cell death during early neurogenesis, the specific cell types affected and the regulatory factors involved remain fairly un-characterized.

6.1.1. Gene (Transcript) expression analyses for IAPs and caspases

From genetic expression analyses in this study, differential expression patterns were observed for all the 15 genes normalised to β-actin endogenous control gene and calibrated to E9 middle stage. Two-step quantitative PCR was used starting with extraction of total RNA from chick embryo retinae, then selectively synthesising cDNA from mRNA sample pools. Optimised conditions and preliminary gene expression relative levels were assessed initially via conventional gel-electrophoresis PCR, and then RT-qPCR was run for validation and for more reliable gene expression analysis. Overall, gene expression analyses revealed a differential

expression pattern for all five IAPs and ten caspases in the developing chick embryo neural retina. From RT-qPCR analyses data, it was observed that all IAPs were downregulated at both early (E4 and E5) and late developmental stages (E12 and E14) compared to the middle stage (E9) except for Birc-6 where a complete opposite pattern of expression was observed.

In summary, Birc-4 (XIAP) and -5 (Survivin) were reported by many investigators to be potent inhibitors of apoptosis in a number of vertebrate species, and Birc-7 directly attenuate apoptosis progress by inhibiting active forms of apoptotic caspases (Kasof and Gomes, 2001, McKinnon *et al.*, 2002, Oost *et al.*, 2004, Jiang *et al.*, 2005). Our findings for the three IAPs; Birc-4 (XIAP) and -5 (Survivin) and Birc-7, confirmed the downregulation pattern at the early and late developmental stages covered in this study in relation to the middle stage, around E9 (Figure 3.6 and Table 3.6). Moreover, the increased expression of Birc-4, -5 and -7 at the middle stages of the studied period is in line with reports of much lower PCD occurring in the neural retina during this period (Chavarria *et al.*, 2007).

The other two IAPs, Birc-2 and -6 were reported to regulate apoptosis and other physiological processes by targeting caspases and other related proteins for ubiquitination and by TNF-mediated signalling modulation, but not to directly inhibit caspases (Rothe *et al.*, 1995, Eckelman and Salvesen, 2006, Varfolomeev *et al.*, 2007). The results for Birc-2 reflect a similar gene expression pattern to that of both Birc-4 and -5 (Figure 3.6), which suggests a direct role of Birc-2 in the apoptotic pathway during chick embryo retinal development. Finally, our findings for Birc-6 also reflect the literature in that this enzyme is crucial for embryonic development (Ren *et al.*, 2005) - our data showed overall high expression levels (Figure 3.6). However, and to the contrary to the rest of IAPs, Birc-6 gene expression was upregulated during the two cell death periods (early and late) and downregulated at the middle period.

Our findings for Birc-2, -4, -5 and -7 strongly support the literature identifying the role of these enzymes as anti-apoptotic factors and the role of Birc-6 in embryogenesis in general.

The expression profile of the ten chicken caspases, also exhibited differential patterns of expression, and these patterns were summarised in five expression categories (Table 3.5). Some caspases showed an overall upregulation pattern at both early and late developmental stages, but not at the middle stage. This pattern was represented by Casp-7 and -18. Most of the studied caspases represented the second pattern of expression where an upregulation was observed coinciding with at least one of the stages of early (E4 and/or E5) or late (E12 and/or E14) stages. Casp-2, -3, -8, -10 and -17 exhibited this pattern. Only Casp-1 showed a downregulation pattern at the early stages, and then was significantly upregulated at the late stage. Casp-6 was slightly downregulated at the early stages, and then its expression level plummeted sharply at the late stage (E14). Finally, only Casp-9 was observed to be expressed at low levels throughout the whole period of development studied with no significant down- or upregulation pattern.

The known apoptotic caspases analysed in this study revealed four patterns of expression for apoptotic caspases. Caspases 2, -3, -8 and -10 gene expression showed upregulation at three of the four analysed stages (E4, 5, 12 and 14). Casp-2, -8 and -10 were found to be upregulated at both early stages (E4 and 5) and either one of the later stages. The opposite pattern was obtained for Casp-3, where the only downregulation point was observed at one of the early stages (E5). Amongst the apoptotic caspases, only Casp-2 appeared to have both pro-death and pro-survival actions (Bergeron *et al.*, 1998, Guo *et al.*, 2002, Krumschnabel, 2009, Vigneswara *et al.*, 2013). Our gene expression data for Casp-2 showed a moderate upregulation pattern of expression for Casp-2 at E4 and E5, and also at E14 and 16 (up to 2.8 times only) (Table 3.7), which suggests a probable secondary role of Casp-2 in PCD of developing neural retina. In fact, redundancy of the role of Casp-2 in apoptosis was proposed by Samraj *et al.* (2007).

Casp-3 was confirmed to be involved in apoptosis as an effector caspase as well as its role in other non-apoptotic processes during neuronal embryonic development; such as dendritic and synaptic physiology (Kivinen *et al.*, 2005, Li *et al.*, 2010, D'Amelio *et al.*, 2012). RT-qPCR data revealed a significantly high expression level of Casp-3 at both early at late developmental stages (Table 3.7), which strongly suggests the crucial role of Casp-3 as an apoptotic role in the developing neural

retina. Moreover, it has been illustrated that at the late stage of retinal development, cell death overlaps with retinal neuronal axonal navigation, synaptogenesis and target connection (Linden, 1994), and our findings for Casp-3 gene expression also support the concept that Casp-3 plays a role in neuronal maturation of the retina.

Casp-6 was reported to have a role in activation of Casp-8 and Casp-10 initiator apoptotic enzymes (Cowling and Downward, 2002, Inoue, 2009). Another non-apoptotic role for Casp-6 is the simulation of Casp-3 in axonal pruning during neuronal development (Sokolowski *et al.*, 2014). Although our findings for Casp-6 gene expression did not reveal a high overall expression level, the increased relative expression of Casp-6 around E4, E5 and E8-E12 might reflect the notion that Casp-6 has a regulatory role with respect to Casp-3, Casp-8 and Casp-10 where their gene expression was relatively higher as well (Figure 3.7 and Table 3.7).

Casp-7, an effector caspase, was found to be expressed highly in the developing brain and retinae of mouse embryos (Zhang *et al.*, 2007). Our data is in line with this notion where Casp-7 expression level was significantly high throughout the studied period, especially at E5 and later at E12, but at E14. The high expression level suggests a strong correlation between Casp-7 and the development of the retina. The relatively lower expression level at E4 and E14 may suggest that cell death at these stages may be controlled by other caspases or other enzymes but not chiefly by Casp-7.

Casp-8 and Casp-10 were found to proteolytically activate Casp-3 through the extrinsic apoptotic pathway (Stennicke *et al.*, 1998). Our gene expression data revealed a much lesser relative expression level for Casp-8 than Casp-3, and Casp-8 expression trend was similar to that of Casp-10 (Figure 3.7 and Table 3.7) where the highest expression was detected at E4 and either E10 or E12. These findings might indicate the synergistic action of both Casp-8 and -10 in the regulation of Casp-3 activity. At the later stage (E14) Casp-3 expression was at its highest, and this was preceded by the upregulation of Casp-8 and -10. At the same time, it was noted also that at E4 all three genes were upregulated.

Finally, Casp-9 gene expression data in this study did not reveal any significant high expression level for Casp-9 (Figure 3.7 and Table 3.7). Although Casp-9 is known for

its action as a potent initiator in the mitochondrial apoptotic pathway (Hakem *et al.*, 1998, Kuida *et al.*, 1998), our findings suggest that developmental cell death in the chick neural retina occur through the extrinsic, but not the intrinsic, apoptotic pathway and activation of Casp-3 possibly occur independent of Casp-9 through other caspases, for instance Casp-8.

The known non-apoptotic caspases, Casp-1, -17 and -18, analysed here for gene expression revealed different patterns of expression during the two waves of cell death of interest. Casp-1, the pro-inflammatory caspase (Li *et al.*, 1995), was shown to be significantly and sharply downregulated at E4, where apoptotic cell death occurs, and upregulated during the late stage. Casp-1 was also reported to have a potent role in immune system maturation (Lamkanfi *et al.*, 2004). An upregulation pattern for Casp-1 was observed at E6, E7 and E12, which might suggest an anti-inflammatory role of Casp-1 at the early stage following a massive cell death wave at E4 and E5. It was reported that clearing of apoptotic cells takes place in the tissue following apoptotic cell death in RGCs, primarily by autophagy (Qu *et al.*, 2010, Mellen *et al.*, 2009). The next surge of expression for Casp-1 at E12 indicates an occurrence of another major inflammatory response taking place at this stage.

The non-mammalian Casp-17 and Casp-18 also showed an overall upregulation pattern at the two cell death waves periods (Figure 3.7 and Table 3.4). Whereas, no reports for these two caspases in development has been published, some studies have shown that Casp-14, a Casp-17 mammalian ortholog, is mainly expressed in the RPE (Lippens *et al.*, 2003). Moreover, Quesada *et al.* (2010) have suggested that mechanisms leading to caspase-dependent apoptosis in avian species depend on more proteases than mammals. Likewise, Casp-18 did not receive much attention in the past. However, our data for both Casp-17 and -18 suggest a role of both factors in the development of the chick neural retina as their expression was significantly upregulated (Figure 3.7 and Table 3.4).

Correlation of relative gene expression between the two PCR methods, conventional semi-quantitative and RT-qPCR, was made where some variation in expression pattern was detected (Table 3.6 and 3.7), and only RT-qPCR were relied on for

analysis and interpretation of this study results. Discussion of the source of variation between the two techniques was reviewed in Chapter 3.

An overall correlation between the proposed anti-apoptotic IAPs and pro-apoptotic caspases was drawn (Figure 3.7) where a clear inverse relationship can be observed between some IAPs of this study vs. some of the caspases. These apoptotic related IAPs and caspases were suggested by a large volume of literature to be chiefly involved in apoptotic cell death. Our data for Birc-4, Birc-5, and to a lesser extent Casp-7, supported the previous findings that these factors are directly and potently involved in cell death by apoptosis. Similarly, Casp-2, -3 and -10 were shown to exhibit classic pro-apoptotic behaviour where expression was significantly upregulated during the two proposed cell death waves in the chick developing retina. The other caspases showed a lesser degree of correlation at these two cell death waves, suggesting a secondary role in apoptotic cell death in the developing retina It is also possible that other non-caspase cell death pathways occur in the developing retina independently of some apoptotic caspases, such as Casp-8 and -9. Autophagy is another mechanism by which cell can be cleared during embryonic development independent of, or following, apoptotic cell death (Bursch, 2001, Qu *et al.*, 2007, Petrovski *et al.*, 2007), and it has been observed in the developing retina in particular (Mellen *et al.*, 2009).

6.1.2. Protein expression analyses for Birc-4 (XIAP), Birc-5 (Survivin), Casp-3 and Casp-7

Following gene expression analysis, protein analyses were carried out by Western blotting, ELISA and Immunohistochemistry (IHC). Correlation between gene and protein relative expression levels was attempted in order to compare the temporal pattern of expression between mRNA transcript and protein level in tissue lysate. The same ten stages of development were used as for the gene expression analysis to prepare tissue homogenate samples containing total protein of the neural retina. Only selected IAPs and caspases, based on the gene expression analysis findings, were analysed for protein expression levels; namely, Birc-4 (XIAP), Birc-5 (Survivin), Casp-3 and Casp-7.

WB results revealed a differential protein expression pattern for Birc-4, -5 and Casp-3. Both IAPs exhibited a classical anti-apoptotic expression pattern where reduction in protein levels was detected at the early and late developmental stages where it has been demonstrated that cell death occurs. Similarly, upregulation in protein expression for cleaved (active) Casp-3 at the two cell death waves was detected, which strongly suggests the direct effect of Casp-3 as a pro-death agent in retinal development. WB analyses for Casp-7 protein did not result in bands despite attempting to increase the antibody concentration. The reasons for such result were discussed in Chapter 4.

However, validation of the protein expression assay performed with ELISA resulted in a profile for protein presence and quantity for all the four enzymes under investigation, including Casp-7 (Figure 4.3). Similar to WB results, the ELISA data revealed similar protein expression pattern for both Birc-4 and Birc-5 where very low amounts of enzyme were detected at early and late stages, and the highest protein concentrations were at the middle stage (E9 and E10). This is consistence with previous reports of the potency of Birc-4 (XIAP) and Birc-5 (Survivin) as anti-apoptotic factors and the results are also in line with our gene expression analysis data where a similar pattern of upregulation was observed for these two enzymes. On the other hand, active Casp-3 ELISA analysis revealed a different protein expression pattern than WB. In both WB and ELISA, Casp-3 showed a trend towards increased protein expression at the middle stages of development (E9 and E10), which made the increased expression level at the early and late stages insignificant. However, from WB, Casp-3 protein level was higher at the late stage (E14 and E16) but lower at the early stage (E4 and E5), whereas ELISA data revealed the highest Casp-3 level at the early, but not the late, stage. This variance in results can be attributed to the different sensitivity of the techniques and to technical variance. Lastly, Casp-7 ELISA assay revealed a different expression pattern than Casp-3 where two peaks of expression were observed at the early developmental stage and later at E12, but not at E14 or E16. At the middle stage of development (around E9) Casp-7 was at its lowest level of expression. This protein expression pattern for Casp-7 is in line with the enzyme's important role as an effector caspases in the

apoptotic cascade. Also, our gene expression analysis revealed an overall high expression level of Casp-7 throughout the whole studied developmental stages.

Taken together, WB and ELISA analyses also revealed a differential expression pattern for Birc-4, Birc-5, Casp-3 and Casp-7, and ELISA data were more reliable and were relied on primarily for interpretation of the results.

An overall correlation between gene and protein expression for the four enzymes: Birc-4, Birc-5, Casp-3 and Casp-7 was analysed (Figure 4.6) for comparison between the two expression phenomena. Analyses for mRNA abundance and corresponding protein synthesis level have been studied in many species under different contexts and have exhibited a wide range of correlations patterns for different genes due to many influential factors (Maier *et al.*, 2009, Vogel and Marcotte, 2012). This study was no exception, gene and corresponding protein expression revealed different extents of variation (Figure 4.5 and 4.6). The Birc-4 gene and protein expression overall trend across the ten developmental days were observed to be directly correlated especially at the middle stage (E8 to E10). Birc-5, on the other hand, revealed a delayed protein expression pattern (Figure 4.6B), where the peak for gene upregulation was at E8, while protein level peaked at E10. At the same time, Birc-5 gene and protein expression trend were similar, and significantly low, at the early and late stages. Overall, both IAPs exhibited a classical model of anti-apoptotic agents on both levels, genetic and proteomic.

Casp-3 gene expression correlation to protein expression revealed a slight direct relationship (Figure 4.6C). High gene expression was observed at early stage, and direct subsequent protein increased level was observed. Likewise, high protein level of Casp-3 was detected at the middle stage, and then later, high gene expression level of Casp-3 was accompanied simultaneously with high protein levels at the late stages. Overall, Casp-3 gene and protein expression patterns are in line with the documented role of Casp-3 as a pro-apoptotic agent.

Casp-7 revealed a weak correlation between gene and protein expression (Figure 4.6D). Whereas Casp-7 gene expression revealed an overall relative high expression throughout the whole studied period of development, however, high Casp-7 protein expression was detected at E12 following the E10 upregulation and also coinciding

simultaneously with E12 gene expression. These findings strongly suggest the vital physiological role of Casp-7, especially at the late developmental stage in the chick retina in apoptosis and/or other developmental pathways.

In summary, protein and associated mRNA expression analyses revealed different extents of individual correlation levels, which were mostly a direct relationship, except for Birc-5 (Survivin) where r=0 (Figure 4.6).

6.1.3. IHC analysis for Birc-4 (XIAP), Birc-5 (Survivin), Casp-3 and Casp-7

Finally, IHC analysis carried out in this study attempted to detect and localise proteins of interest at the whole neural retina during the three developmental stages, early (E4) intermediate (E8.5) and late (E14) using species-specific primary antibodies. TUNEL apoptosis assay also was carried as well as nuclei and whole tissue histological staining. This attempt aimed to compare protein expression of the two IAPs; Birc-4 and -5, and two caspases 3 and 7. Fluorescent microscope images were obtained using commercially available species-homologous Alexa Fluor secondary antibodies.

In situ TUNEL assay for apoptosis revealed the high apoptotic cell death activity of the neural retinal tissue during the two cell death wave periods, the early (E4) and late (E14) (Figure 5.2) but not during the intermediate stage (E8.5) where much less apoptosis level is reported.

In summary for IHC results, higher fluorescent intensity for the two IAPs, Birc-4 (XIAP) and Birc-5 (Survivin) was observed at the middle stage (E8.5) than that of early (E4) and late stage (E14) and to the negative control. At the middle developmental stage (E8.5) minimal cell death level is reported to occur, IAPs are expected to inhibit the action of apoptotic factors at this stage, especially apoptotic caspases. Conversely, Birc-4 (XIAP) and Birc-5 (Survivin) IHC results at early and late (E4 and E14) stages reveals the exact opposite expression pattern where fluorescence intensity is much less than at E8.5. At these stages that cell death is relatively high in the retina as revealed by our TUNEL data. These findings for IHC are reflection of our findings for the two IAPs from WB and ELISA in Chapter 4.

As for the two caspases Casp-3 and Casp-7, the exact opposite pattern of expression was observed from IHC. High expression pattern was detected for both caspases was observed at E4 and E14 but much less expression level at E8.5. This is expected because both caspases are considered to be effector caspases that are involved in the execution of the apoptotic cell death pathway during development of tissues.

These IHC findings initially suggest the relevant role (pro- or anti-apoptotic) of each of these enzymes in the apoptotic pathway as proposed by previous literature and these findings are in line with the corresponding findings in Chapters 3 and 4.

6.2. Future directions

This study profiled the temporal gene relative expression of all chicken (*Gallus gallus*) IAPs and caspases, and temporal protein expression for two IAPs and two caspases. Further protein analysis is indeed still needed to characterise the pattern of expression for the rest of these enzymes by WB and IHC.

The significance of developmental cell death has been studied widely. However, more is still to be unravelled regarding the exact mechanism of apoptotic pathway and apoptotic modulator action.

Spatial expression of IAPs and caspases, in combination with the temporal expression will be helpful in the advance of the knowledge of the role of each of these factors, more specifically when combined with functional analyses of IAPs and caspases in the neural retina.

To study regulators of apoptosis in relation to apoptosis, TUNEL labelling used in combination with other assays such as IF provides a great functional analysis tool for assessment of certain factors role in different physiological pathways. Thus, it will be of high interest to determine the relationship between chicken IAPs and caspases expression and apoptosis by co-localisation of IAPs and caspases within the developing neural retina and apoptotic cells by TUNEL.

The advances in gene modification experiment techniques such as gene knockout and gene silencing models made it possible to investigate the role of specific genes

or mRNAs (Summerton, 2007). Use of gene silencing or small interfering RNA (siRNA) would be fruitful in further functional studies. siRNA is commonly used to prevent mRNA translation into protein (Agrawal *et al.*, 2003) and can be used in the future to knockdown expression of chicken IAPs and caspases to elucidate the exact role of them in relation to the apoptotic activity in the developing neural retina. Commercially available drug inhibitors of IAPs and caspases can be used as well for damping the action of IAPs and caspase enzymes *in vivo* and/or *in vitro*. *In ovo* microinjection of chick embryos eyes (Sanders *et al.*, 2005) or use of electroporation (Dezawa *et al.*, 2002) at appropriate stages of development can be used to deliver siRNA expression vectors, IAP inhibitors and a wide range of caspase inhibitors in order to manipulate IAP and caspase expression. Effects on morphology and apoptosis (TUNEL and caspase activity) can be assayed as well.

As the neural retina is a multi-layered, multi-cellular specialised tissue, investigating the role of IAPs and caspases during development in a particular cell type can be made possible by a number of approaches; specific cell type extraction, cell culture and the use of cell-specific available immunochemical markers. For example, extraction of RGCs by immunopanning technique (Sanders *et al.*, 2005), RGC culture (Bähr, 1993) and/or histiotypic retinal spheres (Rothermel *et al.*, 1997) where a three-dimensional *in vitro* model of the embryonic chicken retina is cultured from dissociated chicken retina under permanent rotation allowing for the genetic manipulation and study of retinogenesis in culture can be used. Other techniques that can be used to isolate specific layers of the retina include laser-captured microdissection (Hackler *et al.*, 2012) preferably to be used for downstream RT-qPCR analysis and retinal shaving technique (Sokolov, 2002, Donovan *et al.*, 2006) for protein analyses. Moreover, available retina cell-specific markers such as Neurofilament 68 kDa, Thy-1 and gamma synuclein (Syncg) for RGCs, and other markers (Cheng *et al.*, 2013) can be utilised to identify specific cell population in combination with functional assays of protein of interest. The use of other animal models such as mouse and zebrafish (Bahr, 2000, de la Rosa and de Pablo, 2000, Donovan *et al.*, 2006, Gramage *et al.*, 2014) have proven beneficial in the study of retinal development molecular physiology. Finally, the use of knock out models also

is a powerful tool to examine the function of certain gene factors (Qiao *et al.*, 2004, May *et al.*, 2007, Schafer *et al.*, 2009) can utilised for investigated the role of caspases and IAPs in chick embryos and other animal models.

References

ABD-ELRAHMAN, I., HERSHKO, K., NEUMAN, T., NACHMIAS, B., PERLMAN, R. & BEN-YEHUDA, D. 2009. The inhibitor of apoptosis protein Livin (ML-IAP) plays a dual role in tumorigenicity. *Cancer Res,* 69, 5475-80.

ADAMS, J. M. 2003. Ways of dying: multiple pathways to apoptosis. *Genes Dev,* 17, 2481-95.

ADLER, R. 2000. A model of retinal cell differentiation in the chick embryo. *Prog Retin Eye Res,* 19, 529-57.

ADLER, R. & CANTO-SOLER, M. V. 2007. Molecular mechanisms of optic vesicle development: complexities, ambiguities and controversies. *Dev Biol,* 305, 1-13.

ADLER, R. & HATLEE, M. 1989. Plasticity and differentiation of embryonic retinal cells after terminal mitosis. *Science,* 243, 391-3.

AGARWAL, N., AGARWAL, R., KUMAR, D. M., ONDRICEK, A., CLARK, A. F., WORDINGER, R. J. & PANG, I. H. 2007. Comparison of expression profile of neurotrophins and their receptors in primary and transformed rat retinal ganglion cells. *Mol Vis,* 13, 1311-8.

AHMED, Y., HAYASHI, S., LEVINE, A. & WIESCHAUS, E. 1998. Regulation of armadillo by a Drosophila APC inhibits neuronal apoptosis during retinal development. *Cell,* 93, 1171-82.

AL-SHABRAWEY, M., AHMAD, S., MEGYERDI, S., OTHMAN, A., BABAN, B., PALENSKI, T. L., SHIN, E. S., GUREL, Z., HSU, S. & SHEIBANI, N. 2012. Caspase-14: a novel caspase in the retina with a potential role in diabetic retinopathy. *Mol Vis,* 18, 1895-906.

ALTIERI, D. C. 2010. Survivin and IAP proteins in cell-death mechanisms. *Biochem J,* 430, 199-205.

AMBROSINI, G., ADIDA, C. & ALTIERI, D. C. 1997. A novel anti-apoptosis gene, survivin, expressed in cancer and lymphoma. *Nat Med,* 3, 917-21.

AUSTIN, C. P., FELDMAN, D. E., IDA, J. A., JR. & CEPKO, C. L. 1995. Vertebrate retinal ganglion cells are selected from competent progenitors by the action of Notch. *Development,* 121, 3637-50.

BAI, L., SMITH, D. C. & WANG, S. 2014. Small-molecule SMAC mimetics as new cancer therapeutics. *Pharmacol Ther,* 144, 82-95.

BALLIOS, B. G., CLARKE, L., COLES, B. L. K., SHOICHET, M. S. AND KOOY, D. V. 2012. The adult retinal stem cell is a rare cell in the ciliary epithelium whose progeny can differentiate into photoreceptors *Biology Open,* 1, 237-246.

BAUDET, M. L., SANDERS, E. J. & HARVEY, S. 2003. Retinal growth hormone in the chick embryo. *Endocrinology,* 144, 5459-68.

BELECKY-ADAMS, T., COOK, B. & ADLER, R. 1996. Correlations between terminal mitosis and differentiated fate of retinal precursor cells in vivo and in vitro: analysis with the "window-labeling" technique. *Dev Biol,* 178, 304-15.

BELECKY-ADAMS, T. L., HAYNES, T., WILSON, J. M. AND DEL RIO-TSONIS, K. 2008. The Chick as a Model for retina Development and Regeneration. *In:* TSONIS, P. A. (ed.) *Animal Models in Eye Research.* 1 ed.: Elsevier.

BERGERON, L., PEREZ, G. I., MACDONALD, G., SHI, L., SUN, Y., JURISICOVA, A., VARMUZA, S., LATHAM, K. E., FLAWS, J. A., SALTER, J. C., HARA, H., MOSKOWITZ, M. A., LI, E., GREENBERG, A., TILLY, J. L. & YUAN, J. 1998. Defects in regulation of apoptosis in caspase-2-deficient mice. *Genes Dev,* 12, 1304-14.

BIEHLMAIER, O., NEUHAUSS, S. C. & KOHLER, K. 2001. Onset and time course of apoptosis in the developing zebrafish retina. *Cell Tissue Res,* 306, 199-207.

BLASCHKE, A. J., WEINER, J. A. & CHUN, J. 1998. Programmed cell death is a universal feature of embryonic and postnatal neuroproliferative regions throughout the central nervous system. *J Comp Neurol,* 396, 39-50.

BONFANTI, L., STRETTOI, E., CHIERZI, S., CENNI, M. C., LIU, X. H., MARTINOU, J. C., MAFFEI, L. & RABACCHI, S. A. 1996. Protection of retinal ganglion cells from natural and axotomy-induced cell death in neonatal transgenic mice overexpressing bcl-2. *J Neurosci,* 16, 4186-94.

BOVOLENTA, P., FRADE, J. M., MARTI, E., RODRIGUEZ-PENA, M. A., BARDE, Y. A. & RODRIGUEZ-TEBAR, A. 1996. Neurotrophin-3 antibodies disrupt the normal development of the chick retina. *J Neurosci,* 16, 4402-10.

BOVOLENTA, P., MALLAMACI, A., BRIATA, P., CORTE, G. & BONCINELLI, E. 1997. Implication of OTX2 in pigment epithelium determination and neural retina differentiation. *J Neurosci,* 17, 4243-52.

BOYA, P. & DE LA ROSA, E. J. 2005. Cell death in early neural life. *Birth Defects Res C Embryo Today,* 75, 281-93.

BOYA, P., MELLEN, M. A. & DE LA ROSA, E. J. 2008. How autophagy is related to programmed cell death during the development of the nervous system. *Biochem Soc Trans,* 36, 813-7.

BRAUNGER, B. M., DEMMER, C. & TAMM, E. R. 2014. Programmed cell death during retinal development of the mouse eye. *Adv Exp Med Biol,* 801, 9-13.

BRESSENOT, A., MARCHAL, S., BEZDETNAYA, L., GARRIER, J., GUILLEMIN, F. & PLENAT, F. 2009. Assessment of apoptosis by immunohistochemistry to active caspase-3, active caspase-7, or cleaved PARP in monolayer cells and spheroid and subcutaneous xenografts of human carcinoma. *J Histochem Cytochem,* 57, 289-300.

BROCCO, M. A. & PANZETTA, P. 1997. Survival and differentiation of purified embryonic chick retinal ganglion cells cultured at low density in a chemically defined medium. *J Neurosci Methods,* 75, 15-20.

BRUHN, S. L. & CEPKO, C. L. 1996. Development of the pattern of photoreceptors in the chick retina. *J Neurosci,* 16, 1430-9.

BUNT, S. M. & LUND, R. D. 1981. Development of a transient retino-retinal pathway in hooded and albino rats. *Brain Res,* 211, 399-404.

BUSS, R. R., SUN, W. & OPPENHEIM, R. W. 2006. Adaptive roles of programmed cell death during nervous system development. *Annu Rev Neurosci,* 29, 1-35.

BUSTIN, S. A. 2002. Quantification of mRNA using real-time reverse transcription PCR (RT-PCR): trends and problems. *J Mol Endocrinol,* 29, 23-39.

CAMPENOT, R. B. 1977. Local control of neurite development by nerve growth factor. *Proc Natl Acad Sci U S A,* 74, 4516-9.

CARTER, B. D., KALTSCHMIDT, C., KALTSCHMIDT, B., OFFENHAUSER, N., BOHM-MATTHAEI, R., BAEUERLE, P. A. & BARDE, Y. A. 1996. Selective activation of NF-kappa B by nerve growth factor through the neurotrophin receptor p75. *Science,* 272, 542-5.

CECCONI, F., ALVAREZ-BOLADO, G., MEYER, B. I., ROTH, K. A. & GRUSS, P. 1998. Apaf1 (CED-4 homolog) regulates programmed cell death in mammalian development. *Cell,* 94, 727-37.

CEPKO, C. L. 1999. The roles of intrinsic and extrinsic cues and bHLH genes in the determination of retinal cell fates. *Curr Opin Neurobiol,* 9, 37-46.

CHAKRABORTI, S., ALAM, M. N., PAIK, D., SHAIKH, S. & CHAKRABORTI, T. 2012. Implications of calpains in health and diseases. *Indian J Biochem Biophys,* 49, 316-28.

CHAN, S. L. & MATTSON, M. P. 1999. Caspase and calpain substrates: roles in synaptic plasticity and cell death. *J Neurosci Res,* 58, 167-90.

CHAO, M. V. 2003. Neurotrophins and their receptors: a convergence point for many signalling pathways. *Nat Rev Neurosci,* 4, 299-309.

CHAVARRIA, T., BALERIOLA, J., MAYORDOMO, R., DE PABLO, F. & DE LA ROSA, E. J. 2013. Early neural cell death is an extensive, dynamic process in the embryonic chick and mouse retina. *ScientificWorldJournal,* 2013, 627240.

CHAVARRIA, T., VALENCIANO, A. I., MAYORDOMO, R., EGEA, J., COMELLA, J. X., HALLBOOK, F., DE PABLO, F. & DE LA ROSA, E. J. 2007. Differential, age-dependent MEK-ERK and PI3K-Akt activation by insulin acting as a survival factor during embryonic retinal development. *Dev Neurobiol,* 67, 1777-88.

CHEN, M., CHEN, Q., SUN, X., SHEN, W., LIU, B., ZHONG, X., LENG, Y., LI, C., ZHANG, W., CHAI, F., HUANG, B., GAO, Q., XIANG, A. P., ZHUO, Y. & GE, J. 2010. Generation of retinal ganglion-like cells from reprogrammed mouse fibroblasts. *Invest Ophthalmol Vis Sci,* 51, 5970-8.

CHENG, C. L., DJAJADI, H. & MOLDAY, R. S. 2013. Cell-specific markers for the identification of retinal cells by immunofluorescence microscopy. *Methods Mol Biol,* 935, 185-99.

CHINNAIYAN, A. M., O'ROURKE, K., TEWARI, M. & DIXIT, V. M. 1995. FADD, a novel death domain-containing protein, interacts with the death domain of Fas and initiates apoptosis. *Cell,* 81, 505-12.

CHINSKEY, N. D., BESIRLI, C. G. & ZACKS, D. N. 2014. Retinal cell death and current strategies in retinal neuroprotection. *Curr Opin Ophthalmol,* 25, 228-33.

CLARKE, P. G., POSADA, A., PRIMI, M. P. & CASTAGNE, V. 1998. Neuronal death in the central nervous system during development. *Biomed Pharmacother,* 52, 356-62.

COLE, L. K. & ROSS, L. S. 2001. Apoptosis in the developing zebrafish embryo. *Dev Biol,* 240, 123-42.

COOK, B., PORTERA-CAILLIAU, C. & ADLER, R. 1998. Developmental neuronal death is not a universal phenomenon among cell types in the chick embryo retina. *J Comp Neurol,* 396, 12-9.

COUBARD, O. A., URBANSKI, M., BOURLON, C. & GAUMET, M. 2014. Educating the blind brain: a panorama of neural bases of vision and of training programs in organic neurovisual deficits. *Front Integr Neurosci,* 8, 89.

COWLING, V. & DOWNWARD, J. 2002. Caspase-6 is the direct activator of caspase-8 in the cytochrome c-induced apoptosis pathway: absolute requirement for removal of caspase-6 prodomain. *Cell Death Differ,* 9, 1046-56.

CRNKOVIC-MERTENS, I., HOPPE-SEYLER, F. & BUTZ, K. 2003. Induction of apoptosis in tumor cells by siRNA-mediated silencing of the livin/ML-IAP/KIAP gene. *Oncogene,* 22, 8330-6.

CUADROS, M. A. & RIOS, A. 1988. Spatial and temporal correlation between early nerve fiber growth and neuroepithelial cell death in the chick embryo retina. *Anat Embryol (Berl),* 178, 543-51.

CULLEN, S. P. & MARTIN, S. J. 2009. Caspase activation pathways: some recent progress. *Cell Death Differ,* 16, 935-8.

D'AMELIO, M., SHENG, M. & CECCONI, F. 2012. Caspase-3 in the central nervous system: beyond apoptosis. *Trends Neurosci,* 35, 700-9.

DAI, Y., LAWRENCE, T. S. & XU, L. 2009. Overcoming cancer therapy resistance by targeting inhibitors of apoptosis proteins and nuclear factor-kappa B. *Am J Transl Res,* 1, 1-15.

DAVIDSON, D. J., HASKELL, C., MAJEST, S., KHERZAI, A., EGAN, D. A., WALTER, K. A., SCHNEIDER, A., GUBBINS, E. F., SOLOMON, L., CHEN, Z., LESNIEWSKI, R. & HENKIN, J. 2005. Kringle 5 of human plasminogen induces apoptosis of endothelial and tumor cells through surface-expressed glucose-regulated protein 78. *Cancer Res,* 65, 4663-72.

DE LA ROSA, E. J. & DE PABLO, F. 2000. Cell death in early neuronal development: beyond the neurotrophic theory. *Trends Neurosci.,* 23, 454-8.

DEGTEREV, A., BOYCE, M. & YUAN, J. 2003. A decade of caspases. *Oncogene,* 22, 8543-67.

DEITCHER, D. L., FEKETE, D. M. & CEPKO, C. L. 1994. Asymmetric expression of a novel homeobox gene in vertebrate sensory organs. *J Neurosci,* 14, 486-98.

DEKKERS, M. P., NIKOLETOPOULOU, V. & BARDE, Y. A. 2013. Cell biology in neuroscience: Death of developing neurons: new insights and implications for connectivity. *J Cell Biol,* 203, 385-93.

DELVAEYE, M., DE VRIESE, A., ZWERTS, F., BETZ, I., MOONS, M., AUTIERO, M. & CONWAY, E. M. 2009. Role of the 2 zebrafish survivin genes in vasculo-angiogenesis, neurogenesis, cardiogenesis and hematopoiesis. *BMC Dev Biol,* 9, 25.

DEVERAUX, Q. L., TAKAHASHI, R., SALVESEN, G. S. & REED, J. C. 1997. X-linked IAP is a direct inhibitor of cell-death proteases. *Nature,* 388, 300-4.

DEZAWA, M., TAKANO, M., NEGISHI, H., MO, X., OSHITARI, T. & SAWADA, H. 2002. Gene transfer into retinal ganglion cells by in vivo electroporation: a new approach. *Micron,* 33, 1-6.

DIAZ, B., SERNA, J., DE PABLO, F. & DE LA ROSA, E. J. 2000. In vivo regulation of cell death by embryonic (pro)insulin and the insulin receptor during early retinal neurogenesis. *Development,* 127, 1641-9.

DOH, S. T., HAO, H., LOH, S. C., PATEL, T., TAWIL, H. Y., CHEN, D. K., PASHKOVA, A., SHEN, A., WANG, H. & CAI, L. 2010. Analysis of retinal cell development in chick embryo by immunohistochemistry and in ovo electroporation techniques. *BMC Dev Biol,* 10, 8.

DOHI, T., BELTRAMI, E., WALL, N. R., PLESCIA, J. & ALTIERI, D. C. 2004. Mitochondrial survivin inhibits apoptosis and promotes tumorigenesis. *J Clin Invest,* 114, 1117-27.

DONOVAN, M. & COTTER, T. G. 2002. Caspase-independent photoreceptor apoptosis in vivo and differential expression of apoptotic protease activating factor-1 and caspase-3 during retinal development. *Cell Death Differ,* 9, 1220-31.

DONOVAN, M., DOONAN, F. & COTTER, T. G. 2006. Decreased expression of pro-apoptotic Bcl-2 family members during retinal development and differential sensitivity to cell death. *Dev Biol,* 291, 154-69.

DOONAN, F. & COTTER, T. G. 2004. Apoptosis: a potential therapeutic target for retinal degenerations. *Curr Neurovasc Res,* 1, 41-53.

DOONAN, F., GROEGER, G. & COTTER, T. G. 2012. Preventing retinal apoptosis--is there a common therapeutic theme? *Exp Cell Res,* 318, 1278-84.

DUBREZ, L., BERTHELET, J. & GLORIAN, V. 2013. IAP proteins as targets for drug development in oncology. *Onco Targets Ther,* 9, 1285-304.

DUTTING, D., GIERER, A. & HANSMANN, G. 1983. Self-renewal of stem cells and differentiation of nerve cells in the developing chick retina. *Brain Res,* 312, 21-32.

EARNSHAW, W. C., MARTINS, L. M. & KAUFMANN, S. H. 1999. Mammalian caspases: structure, activation, substrates, and functions during apoptosis. *Annu Rev Biochem,* 68, 383-424.

ECKELMAN, B. P. & SALVESEN, G. S. 2006. The human anti-apoptotic proteins cIAP1 and cIAP2 bind but do not inhibit caspases. *J Biol Chem,* 281, 3254-60.

ECKELMAN, B. P., SALVESEN, G. S. & SCOTT, F. L. 2006. Human inhibitor of apoptosis proteins: why XIAP is the black sheep of the family. *EMBO Rep,* 7, 988-94.

ECKHART, L., BALLAUN, C., HERMANN, M., VANDEBERG, J. L., SIPOS, W., UTHMAN, A., FISCHER, H. & TSCHACHLER, E. 2008. Identification of novel mammalian caspases reveals an important role of gene loss in shaping the human caspase repertoire. *Mol Biol Evol,* 25, 831-41.

ECKHART, L., BAN, J., FISCHER, H. & TSCHACHLER, E. 2000. Caspase-14: analysis of gene structure and mRNA expression during keratinocyte differentiation. *Biochem Biophys Res Commun,* 277, 655-9.

EDGAR, D. 1985. Nerve growth factors and molecules of the extracellular matrix in neuronal development. *J Cell Sci Suppl,* 3, 107-13.

FERNANDO, P., BRUNETTE, S. & MEGENEY, L. A. 2005. Neural stem cell differentiation is dependent upon endogenous caspase 3 activity. *FASEB J,* 19, 1671-3.

FLEIGE, S. & PFAFFL, M. W. 2006. RNA integrity and the effect on the real-time qRT-PCR performance. *Mol Aspects Med,* 27, 126-39.

FRADE, J. M., BOVOLENTA, P., MARTINEZ-MORALES, J. R., ARRIBAS, A., BARBAS, J. A. & RODRIGUEZ-TEBAR, A. 1997. Control of early cell death by BDNF in the chick retina. *Development,* 124, 3313-20.

FRADE, J. M., RODRIGUEZ-TEBAR, A. & BARDE, Y. A. 1996. Induction of cell death by endogenous nerve growth factor through its p75 receptor. *Nature,* 383, 166-8.

FREEMAN, W. M., WALKER, S. J. & VRANA, K. E. 1999. Quantitative RT-PCR: pitfalls and potential. *Biotechniques,* 26, 112-22, 124-5.

FULDA, S. & VUCIC, D. 2012. Targeting IAP proteins for therapeutic intervention in cancer. *Nat Rev Drug Discov,* 11, 109-24.

GALLI-RESTA, L. & ENSINI, M. 1996. An intrinsic time limit between genesis and death of individual neurons in the developing retinal ganglion cell layer. *J Neurosci,* 16, 2318-24.

GEDEON, T. & BOKES, P. 2012. Delayed protein synthesis reduces the correlation between mRNA and protein fluctuations. *Biophys J,* 103, 377-85.

GHAYUR, T., BANERJEE, S., HUGUNIN, M., BUTLER, D., HERZOG, L., CARTER, A., QUINTAL, L., SEKUT, L., TALANIAN, R., PASKIND, M., WONG, W., KAMEN, R., TRACEY, D. & ALLEN, H. 1997. Caspase-1 processes IFN-gamma-inducing factor and regulates LPS-induced IFN-gamma production. *Nature,* 386, 619-23.

GIBSON, L., HOLMGREEN, S. P., HUANG, D. C., BERNARD, O., COPELAND, N. G., JENKINS, N. A., SUTHERLAND, G. R., BAKER, E., ADAMS, J. M. & CORY, S. 1996. bcl-w, a novel member of the bcl-2 family, promotes cell survival. *Oncogene,* 13, 665-75.

GLUCKSMANN, A. 1965. Cell death in normal development. *Arch Biol (Liege),* 76, 419-37.

GOTTWALD, E., MULLER, O. & POLTEN, A. 2001. Semiquantitative reverse transcription-polymerase chain reaction with the Agilent 2100 Bioanalyzer. *Electrophoresis,* 22, 4016-22.

GRAMAGE, E., LI, J. & HITCHCOCK, P. 2014. The expression and function of midkine in the vertebrate retina. *Br J Pharmacol,* 171, 913-23.

GRAY, C. W., WARD, R. V., KARRAN, E., TURCONI, S., ROWLES, A., VIGLIENGHI, D., SOUTHAN, C., BARTON, A., FANTOM, K. G., WEST, A., SAVOPOULOS, J., HASSAN, N. J., CLINKENBEARD, H., HANNING, C., AMEGADZIE, B., DAVIS, J. B., DINGWALL, C., LIVI, G. P. & CREASY, C. L. 2000. Characterization of human HtrA2, a novel serine protease involved in the mammalian cellular stress response. *Eur J Biochem,* 267, 5699-710.

GREEN, D. R. & REED, J. C. 1998. Mitochondria and apoptosis. *Science,* 281, 1309-12.

GROSS, A., MCDONNELL, J. M. & KORSMEYER, S. J. 1999. BCL-2 family members and the mitochondria in apoptosis. *Genes Dev,* 13, 1899-911.

GROSSKREUTZ, C. L., HANNINEN, V. A., PANTCHEVA, M. B., HUANG, W., POULIN, N. R. & DOBBERFUHL, A. P. 2005. FK506 blocks activation of the intrinsic caspase cascade after optic nerve crush. *Exp Eye Res,* 80, 681-6.

GUERIN, M. B., MCKERNAN, D. P., O'BRIEN, C. J. & COTTER, T. G. 2006. Retinal ganglion cells: dying to survive. *Int J Dev Biol,* 50, 665-74.

GUO, Y., SRINIVASULA, S. M., DRUILHE, A., FERNANDES-ALNEMRI, T. & ALNEMRI, E. S. 2002. Caspase-2 induces apoptosis by releasing proapoptotic proteins from mitochondria. *J Biol Chem,* 277, 13430-7.

HAHN, P., LINDSTEN, T., YING, G. S., BENNETT, J., MILAM, A. H., THOMPSON, C. B. & DUNAIEF, J. L. 2003. Proapoptotic bcl-2 family members, Bax and Bak, are essential for developmental photoreceptor apoptosis. *Invest Ophthalmol Vis Sci,* 44, 3598-605.

HAKEM, R., HAKEM, A., DUNCAN, G. S., HENDERSON, J. T., WOO, M., SOENGAS, M. S., ELIA, A., DE LA POMPA, J. L., KAGI, D., KHOO, W., POTTER, J., YOSHIDA, R., KAUFMAN, S. A., LOWE, S. W., PENNINGER, J. M. & MAK, T. W. 1998. Differential requirement for caspase 9 in apoptotic pathways in vivo. *Cell,* 94, 339-52.

HAMBURGER, V. & HAMILTON, H. L. 1992. A series of normal stages in the development of the chick embryo. 1951. *Dev Dyn,* 195, 231-72.

HARADA, H. & GRANT, S. 2003. Apoptosis regulators. *Rev Clin Exp Hematol,* 7, 117-38.

HARRIS, W. A. 1997. Cellular diversification in the vertebrate retina. *Curr Opin Genet Dev,* 7, 651-8.

HARVEY, N. L., BUTT, A. J. & KUMAR, S. 1997. Functional activation of Nedd2/ICH-1 (caspase-2) is an early process in apoptosis. *J Biol Chem,* 272**,** 13134-9.

HARVEY, S., BAUDET, M. L. & SANDERS, E. J. 2009. Growth hormone-induced neuroprotection in the neural retina during chick embryogenesis. *Ann N Y Acad Sci,* 1163**,** 414-6.

HARVEY, S., KAKEBEEKE, M., MURPHY, A. E. & SANDERS, E. J. 2003. Growth hormone in the nervous system: autocrine or paracrine roles in retinal function? *Can J Physiol Pharmacol,* 81**,** 371-84.

HASSAN, M., WATARI, H., ABUALMAATY, A., OHBA, Y. & SAKURAGI, N. 2014. Apoptosis and molecular targeting therapy in cancer. *Biomed Res Int,* 2014**,** 150845.

HENNESSY, E. J., ADAM, A., AQUILA, B. M., CASTRIOTTA, L. M., COOK, D., HATTERSLEY, M., HIRD, A. W., HUNTINGTON, C., KAMHI, V. M., LAING, N. M., LI, D., MACINTYRE, T., OMER, C. A., OZA, V., PATTERSON, T., REPIK, G., ROONEY, M. T., SAEH, J. C., SHA, L., VASBINDER, M. M., WANG, H. & WHITSTON, D. 2013. Discovery of a novel class of dimeric Smac mimetics as potent IAP antagonists resulting in a clinical candidate for the treatment of cancer (AZD5582). *J Med Chem,* 56**,** 9897-919.

HENSLEY, P., MISHRA, M. & KYPRIANOU, N. 2013. Targeting caspases in cancer therapeutics. *Biol Chem,* 394**,** 831-43.

HERNANDEZ-SANCHEZ, C., LOPEZ-CARRANZA, A., ALARCON, C., DE LA ROSA, E. J. & DE PABLO, F. 1995. Autocrine/paracrine role of insulin-related growth factors in neurogenesis: local expression and effects on cell proliferation and differentiation in retina. *Proc Natl Acad Sci U S A,* 92**,** 9834-8.

HICKS, D. 1998. Putative functions of fibroblast growth factors in retinal development, maturation and survival. *Semin Cell Dev Biol,* 9**,** 263-9.

HINDS, M. G., NORTON, R. S., VAUX, D. L. & DAY, C. L. 1999. Solution structure of a baculoviral inhibitor of apoptosis (IAP) repeat. *Nat Struct Biol,* 6**,** 648-51.

HISS, D. C. & GABRIELS, G. A. 2009. Implications of endoplasmic reticulum stress, the unfolded protein response and apoptosis for molecular cancer therapy. Part II: targeting cell cycle events, caspases, NF-kappaB and the proteasome. *Expert Opin Drug Discov,* 4**,** 907-21.

HO, L. H., TAYLOR, R., DORSTYN, L., CAKOUROS, D., BOUILLET, P. & KUMAR, S. 2009. A tumor suppressor function for caspase-2. *Proc Natl Acad Sci U S A,* 106**,** 5336-41.

HOFER, M., PAGLIUSI, S. R., HOHN, A., LEIBROCK, J. & BARDE, Y. A. 1990. Regional distribution of brain-derived neurotrophic factor mRNA in the adult mouse brain. *EMBO J,* 9**,** 2459-64.

HOFMANN, K., BUCHER, P. & TSCHOPP, J. 1997. The CARD domain: a new apoptotic signalling motif. *Trends Biochem Sci,* 22**,** 155-6.

HOUSELEY, J. & TOLLERVEY, D. 2009. The many pathways of RNA degradation. *Cell,* 136**,** 763-76.

HTTP://WWW.GENENAMES.ORG/. 2014. *Caspases* [Online]. Available: http://www.genenames.org/genefamilies/CASP [Accessed 14/09/2014.

HUANG, W., FILETA, J. B., DOBBERFUHL, A., FILIPPOPOLOUS, T., GUO, Y., KWON, G. & GROSSKREUTZ, C. L. 2005. Calcineurin cleavage is triggered by elevated intraocular pressure, and calcineurin inhibition blocks retinal ganglion cell death in experimental glaucoma. *Proc Natl Acad Sci U S A,* 102**,** 12242-7.

HUGGETT, J., DHEDA, K., BUSTIN, S. & ZUMLA, A. 2005. Real-time RT-PCR normalisation; strategies and considerations. *Genes Immun,* 6, 279-84.

HYMAN, B. T. & YUAN, J. 2012. Apoptotic and non-apoptotic roles of caspases in neuronal physiology and pathophysiology. *Nat Rev Neurosci,* 13, 395-406.

INOUE, S., BROWNE, G., MELINO, G., COHEN, G. M. 2009. Ordering of caspases in cells undergoing apoptosis by the intrinsic pathway. *Cell Death Differ.* , 16, 1053-61.

JARRIN, M., MANSERGH, F. C., BOULTON, M. E., GUNHAGA, L. & WRIDE, M. A. 2012. Survivin expression is associated with lens epithelial cell proliferation and fiber cell differentiation. *Mol Vis,* 18, 2758-69.

JIANG, Y., DE BRUIN, A., CALDAS, H., FANGUSARO, J., HAYES, J., CONWAY, E. M., ROBINSON, M. L. & ALTURA, R. A. 2005. Essential role for survivin in early brain development. *J Neurosci,* 25, 6962-70.

JOAZEIRO, C. A. & WEISSMAN, A. M. 2000. RING finger proteins: mediators of ubiquitin ligase activity. *Cell,* 102, 549-52.

KAPLAN, D. R. & MILLER, F. D. 2000. Neurotrophin signal transduction in the nervous system. *Curr Opin Neurobiol,* 10, 381-91.

KASOF, G. M. & GOMES, B. C. 2001. Livin, a novel inhibitor of apoptosis protein family member. *J Biol Chem,* 276, 3238-46.

KATAOKA, T., SCHROTER, M., HAHNE, M., SCHNEIDER, P., IRMLER, M., THOME, M., FROELICH, C. J. & TSCHOPP, J. 1998. FLIP prevents apoptosis induced by death receptors but not by perforin/granzyme B, chemotherapeutic drugs, and gamma irradiation. *J Immunol,* 161, 3936-42.

KERMER, P., ANKERHOLD, R., KLOCKER, N., KRAJEWSKI, S., REED, J. C. & BAHR, M. 2000. Caspase-9: involvement in secondary death of axotomized rat retinal ganglion cells in vivo. *Brain Res Mol Brain Res,* 85, 144-50.

KIM, H. S. & PARK, C. K. 2005. Retinal ganglion cell death is delayed by activation of retinal intrinsic cell survival program. *Brain Res,* 1057, 17-28.

KISCHKEL, F. C., LAWRENCE, D. A., TINEL, A., LEBLANC, H., VIRMANI, A., SCHOW, P., GAZDAR, A., BLENIS, J., ARNOTT, D. & ASHKENAZI, A. 2001. Death receptor recruitment of endogenous caspase-10 and apoptosis initiation in the absence of caspase-8. *J Biol Chem,* 276, 46639-46.

KISISWA, L., ALBON, J., MORGAN, J. E. & WRIDE, M. A. 2010a. Cellular inhibitor of apoptosis (cIAP1) is down-regulated during retinal ganglion cell (RGC) maturation. *Exp Eye Res,* 91, 739-47.

KISISWA, L., DERVAN, A. G., ALBON, J., MORGAN, J. E. & WRIDE, M. A. 2010b. Retinal ganglion cell death postponed: giving apoptosis a break? *Ophthalmic Res,* 43, 61-78.

KIVINEN, K., KALLAJOKI, M. & TAIMEN, P. 2005. Caspase-3 is required in the apoptotic disintegration of the nuclear matrix. *Exp Cell Res,* 311, 62-73.

KRAMMER, P. H., DHEIN, J., WALCZAK, H., BEHRMANN, I., MARIANI, S., MATIBA, B., FATH, M., DANIEL, P. T., KNIPPING, E., WESTENDORP, M. O. & ET AL. 1994. The role of APO-1-mediated apoptosis in the immune system. *Immunol Rev,* 142, 175-91.

KROEMER, G., EL-DEIRY, W. S., GOLSTEIN, P., PETER, M. E., VAUX, D., VANDENABEELE, P., ZHIVOTOVSKY, B., BLAGOSKLONNY, M. V., MALORNI, W., KNIGHT, R. A., PIACENTINI, M., NAGATA, S., MELINO, G. & NOMENCLATURE COMMITTEE ON CELL, D. 2005. Classification of cell death: recommendations of the Nomenclature Committee on Cell Death. *Cell Death Differ,* 12 Suppl 2, 1463-7.

KROEMER, G., GALLUZZI, L. & BRENNER, C. 2007. Mitochondrial membrane permeabilization in cell death. *Physiol Rev,* 87, 99-163.

KRUMSCHNABEL, G., SOHM, B., BOCK, F., MANZL,C., VILLUNGER, A. 2009. The enigma of caspase-2: the laymen's view *Cell Death and Differentiation,* 16, 195–207.

KUIDA, K., HAYDAR, T. F., KUAN, C. Y., GU, Y., TAYA, C., KARASUYAMA, H., SU, M. S., RAKIC, P. & FLAVELL, R. A. 1998. Reduced apoptosis and cytochrome c-mediated caspase activation in mice lacking caspase 9. *Cell,* 94, 325-37.

KUIDA, K., ZHENG, T. S., NA, S., KUAN, C., YANG, D., KARASUYAMA, H., RAKIC, P. & FLAVELL, R. A. 1996. Decreased apoptosis in the brain and premature lethality in CPP32-deficient mice. *Nature,* 384, 368-72.

LAKHANI, S. A., MASUD, A., KUIDA, K., PORTER, G. A., JR., BOOTH, C. J., MEHAL, W. Z., INAYAT, I. & FLAVELL, R. A. 2006. Caspases 3 and 7: key mediators of mitochondrial events of apoptosis. *Science,* 311, 847-51.

LAMKANFI, M., KALAI, M., SAELENS, X., DECLERCQ, W. & VANDENABEELE, P. 2004. Caspase-1 activates nuclear factor of the kappa-enhancer in B cells independently of its enzymatic activity. *J Biol Chem,* 279, 24785-93.

LEE, J., CHOI, J. H. & JOO, C. K. 2013. TGF-beta1 regulates cell fate during epithelial-mesenchymal transition by upregulating survivin. *Cell Death Dis,* 4, e714.

LEMMON, V. & GOTTLIEB, D. I. 1982. Monoclonal antibodies selective for the inner portion of the chick retina. *J Neurosci,* 2, 531-5.

LEWIN, G. R. & BARDE, Y. A. 1996. Physiology of the neurotrophins. *Annu Rev Neurosci,* 19, 289-317.

LI, H., BERGERON, L., CRYNS, V., PASTERNACK, M. S., ZHU, H., SHI, L., GREENBERG, A. & YUAN, J. 1997. Activation of caspase-2 in apoptosis. *J Biol Chem,* 272, 21010-7.

LI, P., ALLEN, H., BANERJEE, S., FRANKLIN, S., HERZOG, L., JOHNSTON, C., MCDOWELL, J., PASKIND, M., RODMAN, L., SALFELD, J. & ET AL. 1995. Mice deficient in IL-1 beta-converting enzyme are defective in production of mature IL-1 beta and resistant to endotoxic shock. *Cell,* 80, 401-11.

LI, Z., JO, J., JIA, J. M., LO, S. C., WHITCOMB, D. J., JIAO, S., CHO, K. & SHENG, M. 2010. Caspase-3 activation via mitochondria is required for long-term depression and AMPA receptor internalization. *Cell,* 141, 859-71.

LI, Z. & SHENG, M. 2012. Caspases in synaptic plasticity. *Mol Brain,* 5, 15.

LIN, N. Y., BEYER, C., GIESSL, A., KIREVA, T., SCHOLTYSEK, C., UDERHARDT, S., MUNOZ, L. E., DEES, C., DISTLER, A., WIRTZ, S., KRONKE, G., SPENCER, B., DISTLER, O., SCHETT, G. & DISTLER, J. H. 2013. Autophagy regulates TNFalpha-mediated joint destruction in experimental arthritis. *Ann Rheum Dis,* 72, 761-8.

LINDEN, R. 1994. The survival of developing neurons: a review of afferent control. *Neuroscience,* 58, 671-82.

LINDEN, R., AND REESE, B. E., 2006. Programmed cell death. *In:* AL, S. E. (ed.) *Retinal Development.*

LINDEN, R. & PERRY, V. H. 1982. Ganglion cell death within the developing retina: a regulatory role for retinal dendrites? *Neuroscience,* 7, 2813-27.

LINDEN, R., REHEN, S. K. & CHIARINI, L. B. 1999. Apoptosis in developing retinal tissue. *Prog Retin Eye Res,* 18, 133-65.

LIPPENS, S., KOCKX, M., KNAAPEN, M., MORTIER, L., POLAKOWSKA, R., VERHEYEN, A., GARMYN, M., ZWIJSEN, A., FORMSTECHER, P., HUYLEBROECK, D., VANDENABEELE, P. & DECLERCQ, W. 2000. Epidermal differentiation does not involve the pro-apoptotic executioner caspases, but is associated with caspase-14 induction and processing. *Cell Death Differ,* 7, 1218-24.

LIPPENS, S., VANDENBROECKE, C., VAN DAMME, E., TSCHACHLER, E., VANDENABEELE, P. & DECLERCQ, W. 2003. Caspase-14 is expressed in the epidermis, the choroid plexus, the retinal pigment epithelium and thymic Hassall's bodies. *Cell Death Differ,* 10, 257-9.

LISTON, P., FONG, W. G., KELLY, N. L., TOJI, S., MIYAZAKI, T., CONTE, D., TAMAI, K., CRAIG, C. G., MCBURNEY, M. W. & KORNELUK, R. G. 2001. Identification of XAF1 as an antagonist of XIAP anti-Caspase activity. *Nat Cell Biol,* 3, 128-33.

LIU, W., KHARE, S. L., LIANG, X., PETERS, M. A., LIU, X., CEPKO, C. L. & XIANG, M. 2000. All Brn3 genes can promote retinal ganglion cell differentiation in the chick. *Development,* 127, 3237-47.

LIUZZO, J. P., PETANCESKA, S. S. & DEVI, L. A. 1999. Neurotrophic factors regulate cathepsin S in macrophages and microglia: A role in the degradation of myelin basic protein and amyloid beta peptide. *Mol Med,* 5, 334-43.

LIVAK, K. J. & SCHMITTGEN, T. D. 2001. Analysis of relative gene expression data using real-time quantitative PCR and the 2(-Delta Delta C(T)) Method. *Methods,* 25, 402-8.

LODISH, H., BERK, A. & ZIPURSKY, S. L., ET AL. 2000. Processing of rRNA and tRNA. *In:* FREEMAN, W. H. (ed.) *Molecular Cell Biology.* 4th ed. New York.

LOPATNIUK, P. & WITKOWSKI, J. M. 2011. Conventional calpains and programmed cell death. *Acta Biochim Pol,* 58, 287-96.

LOTZ, K., PYROWOLAKIS, G. & JENTSCH, S. 2004. BRUCE, a giant E2/E3 ubiquitin ligase and inhibitor of apoptosis protein of the trans-Golgi network, is required for normal placenta development and mouse survival. *Mol Cell Biol,* 24, 9339-50.

MACE, P. D., SHIRLEY, S. & DAY, C. L. 2010. Assembling the building blocks: structure and function of inhibitor of apoptosis proteins. *Cell Death Differ,* 17, 46-53.

MAIER, T., GUELL, M. & SERRANO, L. 2009. Correlation of mRNA and protein in complex biological samples. *FEBS Lett,* 583, 3966-73.

MANEV, H., FAVARON, M., GUIDOTTI, A. & COSTA, E. 1989. Delayed increase of Ca2+ influx elicited by glutamate: role in neuronal death. *Mol Pharmacol,* 36, 106-12.

MARGALIT, E. & SADDA, S. R. 2003. Retinal and optic nerve diseases. *Artif Organs,* 27, 963-74.

MARTIN-PARTIDO, G., RODRIGUEZ-GALLARDO, L., ALVAREZ, I. S. & NAVASCUES, J. 1988. Cell death in the ventral region of the neural retina during the early development of the chick embryo eye. *Anat Rec,* 222, 272-81.

MASLAND, R. H. 2001. Neuronal diversity in the retina. *Curr Opin Neurobiol,* 11, 431-6.

MAYORDOMO, R., VALENCIANO, A. I., DE LA ROSA, E. J. & HALLBOOK, F. 2003. Generation of retinal ganglion cells is modulated by caspase-dependent programmed cell death. *Eur J Neurosci,* 18, 1744-50.

MAZUMDER, S., PLESCA, D. & ALMASAN, A. 2008. Caspase-3 activation is a critical determinant of genotoxic stress-induced apoptosis. *Methods Mol Biol,* 414, 13-21.

MCKERNAN, D. P. & COTTER, T. G. 2007. A Critical role for Bim in retinal ganglion cell death. *J Neurochem,* 102, 922-30.

MCKINNON, S. J., LEHMAN, D. M., TAHZIB, N. G., RANSOM, N. L., REITSAMER, H. A., LISTON, P., LACASSE, E., LI, Q., KORNELUK, R. G. & HAUSWIRTH, W. W. 2002. Baculoviral IAP repeat-containing-4 protects optic nerve axons in a rat glaucoma model. *Mol Ther,* 5, 780-7.

MELLEN, M. A., DE LA ROSA, E. J. & BOYA, P. 2008. The autophagic machinery is necessary for removal of cell corpses from the developing retinal neuroepithelium. *Cell Death Differ,* 15, 1279-90.

MELLEN, M. A., DE LA ROSA, E. J. & BOYA, P. 2009. Autophagy is not universally required for phosphatidyl-serine exposure and apoptotic cell engulfment during neural development. *Autophagy,* 5, 964-72.

MERRY, D. E. & KORSMEYER, S. J. 1997. Bcl-2 gene family in the nervous system. *Annu Rev Neurosci,* 20, 245-67.

MESTDAGH, P., VAN VLIERBERGHE, P., DE WEER, A., MUTH, D., WESTERMANN, F., SPELEMAN, F. & VANDESOMPELE, J. 2009. A novel and universal method for microRNA RT-qPCR data normalization. *Genome Biol,* 10, R64.

MEY, J. & THANOS, S. 2000. Development of the visual system of the chick. I. Cell differentiation and histogenesis. *Brain Res Brain Res Rev,* 32, 343-79.

MILLER, L. K. 1999. An exegesis of IAPs: salvation and surprises from BIR motifs. *Trends Cell Biol,* 9, 323-8.

MISHIMA, N. & TOMAREV, S. 1998. Chicken Eyes absent 2 gene: isolation and expression pattern during development. *Int J Dev Biol,* 42, 1109-15.

MIURA, M., ZHU, H., ROTELLO, R., HARTWIEG, E. A. & YUAN, J. 1993. Induction of apoptosis in fibroblasts by IL-1 beta-converting enzyme, a mammalian homolog of the C. elegans cell death gene ced-3. *Cell,* 75, 653-60.

MOONEY, L. M., AL-SAKKAF, K. A., BROWN, B. L. & DOBSON, P. R. 2002. Apoptotic mechanisms in T47D and MCF-7 human breast cancer cells. *Br J Cancer,* 87, 909-17.

MU, X., FU, X., SUN, H., BEREMAND, P. D., THOMAS, T. L. & KLEIN, W. H. 2005. A gene network downstream of transcription factor Math5 regulates retinal progenitor cell competence and ganglion cell fate. *Dev Biol,* 280, 467-81.

MUTKA, A. L., HAAPANEN, A., KAKELA, R., LINDFORS, M., WRIGHT, A. K., INKINEN, T., HERMANSSON, M., ROKKA, A., CORTHALS, G., JAUHIAINEN, M., GILLINGWATER, T. H., IKONEN, E. & TYYNELA, J. 2010. Murine cathepsin D deficiency is associated with dysmyelination/myelin disruption and accumulation of cholesteryl esters in the brain. *J Neurochem,* 112, 193-203.

NAKANISHI, H. 2003. Microglial functions and proteases. *Mol Neurobiol,* 27, 163-76.

NEUFELD, A. H. & GACHIE, E. N. 2003. The inherent, age-dependent loss of retinal ganglion cells is related to the lifespan of the species. *Neurobiol Aging,* 24, 167-72.

NICKELLS, R. W. 1999. Apoptosis of retinal ganglion cells in glaucoma: an update of the molecular pathways involved in cell death. *Surv Ophthalmol,* 43 Suppl 1, S151-61.

NIR, I., KEDZIERSKI, W., CHEN, J. & TRAVIS, G. H. 2000. Expression of Bcl-2 protects against photoreceptor degeneration in retinal degeneration slow (rds) mice. *J Neurosci,* 20, 2150-4.

NUCCI, C., OSBORNE, N. N., CERULLI, L. . 2008. *Glaucoma An Open Window to Neurodegeneration and Neuroprotection,* Elsevier Science Publishing.

O'DRISCOLL, C., DONOVAN, M. & COTTER, T. G. 2006. Analysis of apoptotic and survival mediators in the early post-natal and mature retina. *Exp Eye Res,* 83, 1482-92.

O'RIORDAN, M. X., BAULER, L. D., SCOTT, F. L. & DUCKETT, C. S. 2008. Inhibitor of apoptosis proteins in eukaryotic evolution and development: a model of thematic conservation. *Dev Cell,* 15, 497-508.

OLSSON, M., VAKIFAHMETOGLU, H., ABRUZZO, P. M., HOGSTRAND, K., GRANDIEN, A. & ZHIVOTOVSKY, B. 2009. DISC-mediated activation of caspase-2 in DNA damage-induced apoptosis. *Oncogene,* 28, 1949-59.

OOST, T. K., SUN, C., ARMSTRONG, R. C., AL-ASSAAD, A. S., BETZ, S. F., DECKWERTH, T. L., DING, H., ELMORE, S. W., MEADOWS, R. P., OLEJNICZAK, E. T., OLEKSIJEW, A., OLTERSDORF, T., ROSENBERG, S. H., SHOEMAKER, A. R., TOMASELLI, K. J., ZOU, H. & FESIK, S. W. 2004. Discovery of potent antagonists of the antiapoptotic protein XIAP for the treatment of cancer. *J Med Chem,* 47, 4417-26.

OPPENHEIM, R. W. 1991. Cell death during development of the nervous system. *Annu Rev Neurosci,* 14, 453-501.

PAPERMASTER, D. S. 1997. Apoptosis of the mammalian retina and lens. *Cell Death Differ,* 4, 21-8.

PARK, H. H. 2012. Structural features of caspase-activating complexes. *Int J Mol Sci,* 13, 4807-18.

PEQUIGNOT, M. O., PROVOST, A. C., SALLE, S., MENASCHE, M., SAULE, S., JAIS, J. P. & ABITBOL, M. 2011. The retinal pigment epithelium undergoes massive apoptosis during early differentiation and pigmentation of the optic cup. *Mol Vis,* 17, 989-96.

PEQUIGNOT, M. O., PROVOST, A. C., SALLE, S., TAUPIN, P., SAINTON, K. M., MARCHANT, D., MARTINOU, J. C., AMEISEN, J. C., JAIS, J. P. & ABITBOL, M. 2003. Major role of BAX in apoptosis during retinal development and in establishment of a functional postnatal retina. *Dev Dyn,* 228, 231-8.

PEREZ, H. L., CHAUDHRY, C., EMANUEL, S. L., FANSLAU, C., FARGNOLI, J., GAN, J., KIM, K. S., LEI, M., NAGLICH, J. G., TRAEGER, S. C., VUPPUGALLA, R., WEI, D. D., VITE, G. D., TALBOTT, R. L. & BORZILLERI, R. M. 2015. Discovery of potent heterodimeric antagonists of inhibitor of apoptosis proteins (IAPs) with sustained antitumor activity. *J Med Chem,* 58, 1556-62.

PERRY, V. H. 1981. Evidence for an amacrine cell system in the ganglion cell layer of the rat retina. *Neuroscience,* 6, 931-44.

PFAFFL, M. W. 2001. A new mathematical model for relative quantification in real-time RT-PCR. *Nucleic Acids Res,* 29, e45.

PHILCHENKOV, A. 2004. Caspases: potential targets for regulating cell death. *J Cell Mol Med,* 8, 432-44.

PITTACK, C., JONES, M. & REH, T. A. 1991. Basic fibroblast growth factor induces retinal pigment epithelium to generate neural retina in vitro. *Development,* 113, 577-88.

POHL, C. & JENTSCH, S. 2008. Final stages of cytokinesis and midbody ring formation are controlled by BRUCE. *Cell,* 132, 832-45.

POTTS, P. R., SINGH, S., KNEZEK, M., THOMPSON, C. B. & DESHMUKH, M. 2003. Critical function of endogenous XIAP in regulating caspase activation during sympathetic neuronal apoptosis. *J Cell Biol,* 163, 789-99.

PRADA, C., PUGA, J., PEREZ-MENDEZ, L., LOPEZ, R. & RAMIREZ, G. 1991. Spatial and Temporal Patterns of Neurogenesis in the Chick Retina. *Eur J Neurosci,* 3, 559-569.

PROSKURYAKOV, S. Y., KONOPLYANNIKOV, A. G. & GABAI, V. L. 2003. Necrosis: a specific form of programmed cell death? *Exp Cell Res,* 283, 1-16.

PRUNELL, G. F. & TROY, C. M. 2004. Balancing neuronal death. *J Neurosci Res,* 78, 1-6.

PYRKO, P., SCHONTHAL, A. H., HOFMAN, F. M., CHEN, T. C. & LEE, A. S. 2007. The unfolded protein response regulator GRP78/BiP as a novel target for increasing chemosensitivity in malignant gliomas. *Cancer Res,* 67, 9809-16.

QU, J., WANG, D. & GROSSKREUTZ, C. L. 2010. Mechanisms of retinal ganglion cell injury and defense in glaucoma. *Exp Eye Res,* 91, 48-53.

QU, X., ZOU, Z., SUN, Q., LUBY-PHELPS, K., CHENG, P., HOGAN, R. N., GILPIN, C. & LEVINE, B. 2007. Autophagy gene-dependent clearance of apoptotic cells during embryonic development. *Cell,* 128, 931-46.

QUESADA, V., VELASCO, G., PUENTE, X. S., WARREN, W. C. & LOPEZ-OTIN, C. 2010. Comparative genomic analysis of the zebra finch degradome provides new insights into evolution of proteases in birds and mammals. *BMC Genomics,* 11, 220.

QUIGLEY, H. A., NICKELLS, R. W., KERRIGAN, L. A., PEASE, M. E., THIBAULT, D. J. & ZACK, D. J. 1995. Retinal ganglion cell death in experimental glaucoma and after axotomy occurs by apoptosis. *Invest Ophthalmol Vis Sci,* 36, 774-86.

RAFF, M. C., BARRES, B. A., BURNE, J. F., COLES, H. S., ISHIZAKI, Y. & JACOBSON, M. D. 1993. Programmed cell death and the control of cell survival: lessons from the nervous system. *Science,* 262, 695-700.

RAGER, G. & RAGER, U. 1978. Systems-matching by degeneration. I. A quantitative electron microscopic study of the generation and degeneration of retinal ganglion cells in the chicken. *Exp Brain Res,* 33, 65-78.

RAGER, G. & RAGER, U. 1979. Systems-matching by degeneration in the developing retino-tectal projection of the chicken. *Prog Brain Res,* 51, 439-43.

RAGER, G. H. 1980. Development of the retinotectal projection in the chicken. *Adv Anat Embryol Cell Biol,* 63, I-VIII, 1-90.

RAPAPORT, D. H. 2006. Retinal neurogenesis. *In:* AL., S. E. (ed.) *Retinal Development.*

RAPAPORT, D. H., WONG, L. L., WOOD, E. D., YASUMURA, D. & LAVAIL, M. M. 2004. Timing and topography of cell genesis in the rat retina. *J Comp Neurol,* 474, 304-24.

REH, T. A., JONES, M. & PITTACK, C. 1991. Common mechanisms of retinal regeneration in the larval frog and embryonic chick. *Ciba Found Symp,* 160, 192-204; discussion 204-8.

REH, T. A. & LEVINE, E. M. 1998. Multipotential stem cells and progenitors in the vertebrate retina. *J Neurobiol,* 36, 206-20.

REHEN, S. K. & LINDEN, R. 1994. Apoptosis in the developing retina: paradoxical effects of protein synthesis inhibition. *Braz J Med Biol Res,* 27, 1647-51.

REN, J., SHI, M., LIU, R., YANG, Q. H., JOHNSON, T., SKARNES, W. C. & DU, C. 2005. The Birc6 (Bruce) gene regulates p53 and the mitochondrial pathway of apoptosis and is essential for mouse embryonic development. *Proc Natl Acad Sci U S A,* 102, 565-70.

REPNIK, U., STOKA, V., TURK, V. & TURK, B. 2012. Lysosomes and lysosomal cathepsins in cell death. *Biochim Biophys Acta,* 1824, 22-33.

RIEDL, S. J. & SHI, Y. 2004. Molecular mechanisms of caspase regulation during apoptosis. *Nat Rev Mol Cell Biol,* 5, 897-907.

ROTHE, M., PAN, M. G., HENZEL, W. J., AYRES, T. M. & GOEDDEL, D. V. 1995. The TNFR2-TRAF signaling complex contains two novel proteins related to baculoviral inhibitor of apoptosis proteins. *Cell,* 83, 1243-52.

ROZEN, S. & SKALETSKY, H. J. 1998. Primer3. Code available at http://www-genome.wi.mit.edu/genome_software/other/primer3.html.

ROZTOCIL, T., MATTER-SADZINSKI, L., ALLIOD, C., BALLIVET, M. & MATTER, J. M. 1997. NeuroM, a neural helix-loop-helix transcription factor, defines a new transition stage in neurogenesis. *Development,* 124, 3263-72.

SAFA, A. R., DAY, T. W. & WU, C. H. 2008. Cellular FLICE-like inhibitory protein (C-FLIP): a novel target for cancer therapy. *Curr Cancer Drug Targets,* 8, 37-46.

SAMRAJ, A. K., SOHN, D., SCHULZE-OSTHOFF, K. & SCHMITZ, I. 2007. Loss of caspase-9 reveals its essential role for caspase-2 activation and mitochondrial membrane depolarization. *Mol Biol Cell,* 18, 84-93.

SANDERS, E. J., BAUDET, M. L., PARKER, E. & HARVEY, S. 2009a. Signaling mechanisms mediating local GH action in the neural retina of the chick embryo. *Gen Comp Endocrinol,* 163, 63-9.

SANDERS, E. J., PARKER, E., ARAMBURO, C. & HARVEY, S. 2005. Retinal growth hormone is an anti-apoptotic factor in embryonic retinal ganglion cell differentiation. *Exp Eye Res,* 81, 551-60.

SANDERS, E. J., PARKER, E. & HARVEY, S. 2009b. Endogenous growth hormone in human retinal ganglion cells correlates with cell survival. *Mol Vis,* 15, 920-6.

SANDERS, E. J. & WRIDE, M. A. 1995. Programmed cell death in development. *Int Rev Cytol,* 163, 105-73.

SANTOS-CARVALHO, A., ALVARO, A. R., MARTINS, J., AMBROSIO, A. F. & CAVADAS, C. 2014. Emerging novel roles of neuropeptide Y in the retina: from neuromodulation to neuroprotection. *Prog Neurobiol,* 112, 70-9.

SANTOS-CARVALHO, A., ELVAS, F., ALVARO, A. R., AMBROSIO, A. F. & CAVADAS, C. 2013. Neuropeptide Y receptors activation protects rat retinal neural cells against necrotic and apoptotic cell death induced by glutamate. *Cell Death Dis,* 4, e636.

SATTLER, M., LIANG, H., NETTESHEIM, D., MEADOWS, R. P., HARLAN, J. E., EBERSTADT, M., YOON, H. S., SHUKER, S. B., CHANG, B. S., MINN, A. J., THOMPSON, C. B. & FESIK, S. W. 1997. Structure of Bcl-xL-Bak peptide complex: recognition between regulators of apoptosis. *Science,* 275, 983-6.

SCHOOR, O., WEINSCHENK, T., HENNENLOTTER, J., CORVIN, S., STENZL, A., RAMMENSEE, H. G. & STEVANOVIC, S. 2003. Moderate degradation does not preclude microarray analysis of small amounts of RNA. *Biotechniques,* 35, 1192-6, 1198-201.

SCHWERK, C. & SCHULZE-OSTHOFF, K. 2003. Non-apoptotic functions of caspases in cellular proliferation and differentiation. *Biochem Pharmacol,* 66, 1453-8.

SELHORST, J. B. & CHEN, Y. 2009. The optic nerve. *Semin Neurol,* 29, 29-35.

SGORBISSA, A., BENETTI, R., MARZINOTTO, S., SCHNEIDER, C. & BRANCOLINI, C. 1999. Caspase-3 and caspase-7 but not caspase-6 cleave Gas2 in vitro: implications for microfilament reorganization during apoptosis. *J Cell Sci,* 112 (Pt 23), 4475-82.

SHI, L., CHEN, G., MACDONALD, G., BERGERON, L., LI, H., MIURA, M., ROTELLO, R. J., MILLER, D. K., LI, P., SESHADRI, T., YUAN, J. & GREENBERG, A. H. 1996. Activation of an interleukin 1 converting enzyme-dependent apoptosis pathway by granzyme B. *Proc Natl Acad Sci U S A,* 93, 11002-7.

SHI, L., MAI, S., ISRAELS, S., BROWNE, K., TRAPANI, J. A. & GREENBERG, A. H. 1997. Granzyme B (GraB) autonomously crosses the cell membrane and perforin initiates apoptosis and GraB nuclear localization. *J Exp Med,* 185, 855-66.

SHI, M., VIVIAN, C. J., LEE, K. J., GE, C., MOROTOMI-YANO, K., MANZL, C., BOCK, F., SATO, S., TOMOMORI-SATO, C., ZHU, R., HAUG, J. S., SWANSON, S. K., WASHBURN, M. P., CHEN, D. J., CHEN, B. P., VILLUNGER, A., FLORENS, L. & DU, C. 2009. DNA-PKcs-PIDDosome: a nuclear caspase-2-activating complex with role in G2/M checkpoint maintenance. *Cell,* 136, 508-20.

SHOU, Y., LI, L., PRABHAKARAN, K., BOROWITZ, J. L. & ISOM, G. E. 2004. Calcineurin-mediated Bad translocation regulates cyanide-induced neuronal apoptosis. *Biochem J,* 379, 805-13.

SILKE, J. & VAUX, D. L. 2001. Two kinds of BIR-containing protein - inhibitors of apoptosis, or required for mitosis. *J Cell Sci,* 114, 1821-7.

SIMON, D. J., WEIMER, R. M., MCLAUGHLIN, T., KALLOP, D., STANGER, K., YANG, J., O'LEARY, D. D., HANNOUSH, R. N. & TESSIER-LAVIGNE, M. 2012. A caspase cascade regulating developmental axon degeneration. *J Neurosci,* 32, 17540-53.

SOKOLOWSKI, J. D., GAMAGE, K. K., HEFFRON, D. S., LEBLANC, A. C., DEPPMANN, C. D. & MANDELL, J. W. 2014. Caspase-mediated cleavage of actin and tubulin is a common feature and sensitive marker of axonal degeneration in neural development and injury. *Acta Neuropathol Commun,* 2, 16.

SONG, Z., YAO, X. & WU, M. 2003. Direct interaction between survivin and Smac/DIABLO is essential for the anti-apoptotic activity of survivin during taxol-induced apoptosis. *J Biol Chem,* 278, 23130-40.

SPALDING, K. L., DHARMARAJAN, A. M. & HARVEY, A. R. 2005. Caspase-independent retinal ganglion cell death after target ablation in the neonatal rat. *Eur J Neurosci,* 21, 33-45.

STADLER, H. S. & SOLURSH, M. 1994. Characterization of the homeobox-containing gene GH6 identifies novel regions of homeobox gene expression in the developing chick embryo. *Dev Biol,* 161, 251-62.

STAHLBERG, A., KUBISTA, M. & PFAFFL, M. 2004. Comparison of reverse transcriptases in gene expression analysis. *Clin Chem,* 50, 1678-80.

STEINLE, J. J. 2012. Retinal endothelial cell apoptosis. *Apoptosis,* 17, 1258-60.

STENNICKE, H. R., JURGENSMEIER, J. M., SHIN, H., DEVERAUX, Q., WOLF, B. B., YANG, X., ZHOU, Q., ELLERBY, H. M., ELLERBY, L. M., BREDESEN, D., GREEN, D. R., REED, J. C., FROELICH, C. J. & SALVESEN, G. S. 1998. Pro-caspase-3 is a major physiologic target of caspase-8. *J Biol Chem,* 273, 27084-90.

STERN, C. D. 2005. The chick; a great model system becomes even greater. *Dev Cell,* 8, 9-17.

SURGUCHEVA, I., WEISMAN, A. D., GOLDBERG, J. L., SHNYRA, A. & SURGUCHOV, A. 2008. Gamma-synuclein as a marker of retinal ganglion cells. *Mol Vis,* 14, 1540-8.

TANIGUCHI, Y., CHOI, P. J., LI, G. W., CHEN, H., BABU, M., HEARN, J., EMILI, A. & XIE, X. S. 2010. Quantifying E. coli proteome and transcriptome with single-molecule sensitivity in single cells. *Science,* 329, 533-8.

TAYLOR, R. C., CULLEN, S. P. & MARTIN, S. J. 2008. Apoptosis: controlled demolition at the cellular level. *Nat Rev Mol Cell Biol,* 9, 231-41.

TEZEL, G. & WAX, M. B. 1999. Inhibition of caspase activity in retinal cell apoptosis induced by various stimuli in vitro. *Invest Ophthalmol Vis Sci,* 40, 2660-7.

THAL, S. C., WYSCHKON, S., PIETER, D., ENGELHARD, K. & WERNER, C. 2008. Selection of endogenous control genes for normalization of gene expression analysis after experimental brain trauma in mice. *J Neurotrauma,* 25, 785-94.

THIEL, G. 2013. How Sox2 maintains neural stem cell identity. *Biochem J,* 450, e1-2.

TOWBIN, H., STAEHELIN, T. & GORDON, J. 1979. Electrophoretic transfer of proteins from polyacrylamide gels to nitrocellulose sheets: procedure and some applications. *Proc Natl Acad Sci U S A,* 76, 4350-4.

TOY, J., NORTON, J. S., JIBODH, S. R. & ADLER, R. 2002. Effects of homeobox genes on the differentiation of photoreceptor and nonphotoreceptor neurons. *Invest Ophthalmol Vis Sci,* 43, 3522-9.

TROUSSE, F., ESTEVE, P. & BOVOLENTA, P. 2001. Bmp4 mediates apoptotic cell death in the developing chick eye. *J Neurosci,* 21, 1292-301.

UCHIYAMA, Y. 2001. Autophagic cell death and its execution by lysosomal cathepsins. *Arch Histol Cytol,* 64, 233-46.

UNSAIN, N., HIGGINS, J. M., PARKER, K. N., JOHNSTONE, A. D. & BARKER, P. A. 2013. XIAP regulates caspase activity in degenerating axons. *Cell Rep,* 4, 751-63.

VALENCIANO, A. I., BOYA, P. & DE LA ROSA, E. J. 2009. Early neural cell death: numbers and cues from the developing neuroretina. *Int J Dev Biol,* 53, 1515-28.

VARELA-NIETO, I., DE LA ROSA, E. J., VALENCIANO, A. I. & LEON, Y. 2003. Cell death in the nervous system: lessons from insulin and insulin-like growth factors. *Mol Neurobiol,* 28, 23-50.

VARFOLOMEEV, E., BLANKENSHIP, J. W., WAYSON, S. M., FEDOROVA, A. V., KAYAGAKI, N., GARG, P., ZOBEL, K., DYNEK, J. N., ELLIOTT, L. O., WALLWEBER, H. J., FLYGARE, J. A., FAIRBROTHER, W. J., DESHAYES, K., DIXIT, V. M. & VUCIC, D. 2007. IAP antagonists induce autoubiquitination of c-IAPs, NF-kappaB activation, and TNFalpha-dependent apoptosis. *Cell,* 131, 669-81.

VAUX, D. L. & SILKE, J. 2005. IAPs, RINGs and ubiquitylation. *Nat Rev Mol Cell Biol,* 6, 287-97.

VECINO, E., HERNANDEZ, M. & GARCIA, M. 2004. Cell death in the developing vertebrate retina. *Int J Dev Biol,* 48, 965-74.

VERGARA, M. N. & CANTO-SOLER, M. V. 2012. Rediscovering the chick embryo as a model to study retinal development. *Neural Dev,* 7, 22.

VERHAGEN, A. M., EKERT, P. G., PAKUSCH, M., SILKE, J., CONNOLLY, L. M., REID, G. E., MORITZ, R. L., SIMPSON, R. J. & VAUX, D. L. 2000. Identification of DIABLO, a mammalian protein that promotes apoptosis by binding to and antagonizing IAP proteins. *Cell,* 102, 43-53.

VERHAGEN, A. M., SILKE, J., EKERT, P. G., PAKUSCH, M., KAUFMANN, H., CONNOLLY, L. M., DAY, C. L., TIKOO, A., BURKE, R., WROBEL, C., MORITZ, R. L., SIMPSON, R. J. & VAUX, D. L. 2002. HtrA2 promotes cell death through its serine protease activity and its ability to antagonize inhibitor of apoptosis proteins. *J Biol Chem,* 277, 445-54.

VIGNESWARA, V., BERRY, M., LOGAN, A. & AHMED, Z. 2013. Caspase-2 is upregulated after sciatic nerve transection and its inhibition protects dorsal root ganglion neurons from apoptosis after serum withdrawal. *PLoS One,* 8, e57861.

VITTE-MONY, I., KORNELUK, R. G. & DIAZ-MITOMA, F. 1997. Role of XIAP protein, a human member of the inhibitor of apoptosis (IAP) protein family, in phytohemagglutinin-induced apoptosis of human T cell lines. *Apoptosis,* 2, 501-9.

VOGEL, C. & MARCOTTE, E. M. 2012. Insights into the regulation of protein abundance from proteomic and transcriptomic analyses. *Nat Rev Genet,* 13, 227-32.

VON BARTHELD, C. S. & BUTOWT, R. 2000. Expression of neurotrophin-3 (NT-3) and anterograde axonal transport of endogenous NT-3 by retinal ganglion cells in chick embryos. *J Neurosci,* 20, 736-48.

WAJANT, H., PFIZENMAIER, K. & SCHEURICH, P. 2003. Tumor necrosis factor signaling. *Cell Death Differ,* 10, 45-65.

WALDBILLIG, R. J., ARNOLD, D. R., FLETCHER, R. T. & CHADER, G. J. 1991. Insulin and IGF-I binding in developing chick neural retina and pigment epithelium: a characterization of binding and structural differences. *Exp Eye Res,* 53, 13-22.

WANG, H. G., PATHAN, N., ETHELL, I. M., KRAJEWSKI, S., YAMAGUCHI, Y., SHIBASAKI, F., MCKEON, F., BOBO, T., FRANKE, T. F. & REED, J. C. 1999. Ca2+-induced apoptosis through calcineurin dephosphorylation of BAD. *Science,* 284, 339-43.

WEI, Y., FAN, T. & YU, M. 2008. Inhibitor of apoptosis proteins and apoptosis. *Acta Biochim Biophys Sin (Shanghai),* 40, 278-88.

WIESE, S., DIGBY, M. R., GUNNERSEN, J. M., GOTZ, R., PEI, G., HOLTMANN, B., LOWENTHAL, J. & SENDTNER, M. 1999. The anti-apoptotic protein ITA is essential for NGF-mediated survival of embryonic chick neurons. *Nat Neurosci,* 2, 978-83.

WILSON, K. P., BLACK, J. A., THOMSON, J. A., KIM, E. E., GRIFFITH, J. P., NAVIA, M. A., MURCKO, M. A., CHAMBERS, S. P., ALDAPE, R. A., RAYBUCK, S. A. & ET AL. 1994. Structure and mechanism of interleukin-1 beta converting enzyme. *Nature,* 370, 270-5.

WONG, H., ANDERSON, W. D., CHENG, T. & RIABOWOL, K. T. 1994. Monitoring mRNA expression by polymerase chain reaction: the "primer-dropping" method. *Anal Biochem,* 223, 251-8.

WONG, R. O. L. 2006. Retinal Development. *In:* SERNAGOR, E. (ed.) *Introduction- from eye field to eyesight.* Cambridge University Press.

WRIDE, M. A., GEATRELL, J. & GUGGENHEIM, J. A. 2006. Proteases in eye development and disease. *Birth Defects Res C Embryo Today,* 78, 90-105.

YAMASHIMA, T. & OIKAWA, S. 2009. The role of lysosomal rupture in neuronal death. *Prog Neurobiol,* 89, 343-58.

YAN, R. T. & WANG, S. Z. 1998. neuroD induces photoreceptor cell overproduction in vivo and de novo generation in vitro. *J Neurobiol,* 36, 485-96.

YANG, J., LIU, X., BHALLA, K., KIM, C. N., IBRADO, A. M., CAI, J., PENG, T. I., JONES, D. P. & WANG, X. 1997. Prevention of apoptosis by Bcl-2: release of cytochrome c from mitochondria blocked. *Science,* 275, 1129-32.

YANG, Y., FANG, S., JENSEN, J. P., WEISSMAN, A. M. & ASHWELL, J. D. 2000. Ubiquitin protein ligase activity of IAPs and their degradation in proteasomes in response to apoptotic stimuli. *Science,* 288, 874-7.

YANG, Y., HILL, J. W. & ROSENBERG, G. A. 2011. Multiple roles of metalloproteinases in neurological disorders. *Prog Mol Biol Transl Sci,* 99, 241-63.

YE, J., COULOURIS, G., ZARETSKAYA, I., CUTCUTACHE, I., ROZEN, S. & MADDEN, T. L. 2012. Primer-BLAST: a tool to design target-specific primers for polymerase chain reaction. *BMC Bioinformatics,* 13, 134.

YOSHIDA, H., KONG, Y. Y., YOSHIDA, R., ELIA, A. J., HAKEM, A., HAKEM, R., PENNINGER, J. M. & MAK, T. W. 1998. Apaf1 is required for mitochondrial pathways of apoptosis and brain development. *Cell,* 94, 739-50.

YOUNG, R. W. 1984. Cell death during differentiation of the retina in the mouse. *J Comp Neurol,* 229, 362-73.

YUAN, J., SHAHAM, S., LEDOUX, S., ELLIS, H. M. & HORVITZ, H. R. 1993. The C. elegans cell death gene ced-3 encodes a protein similar to mammalian interleukin-1 beta-converting enzyme. *Cell,* 75, 641-52.

ZHANG, X., SZABO, E., MICHALAK, M. & OPAS, M. 2007a. Endoplasmic reticulum stress during the embryonic development of the central nervous system in the mouse. *Int J Dev Neurosci,* 25, 455-63.

ZHANG, Y., PADALECKI, S. S., CHAUDHURI, A. R., DE WAAL, E., GOINS, B. A., GRUBBS, B., IKENO, Y., RICHARDSON, A., MUNDY, G. R. & HERMAN, B. 2007b. Caspase-2 deficiency enhances aging-related traits in mice. *Mech Ageing Dev,* 128, 213-21.

ZUBER, M. E., GESTRI, G., VICZIAN, A. S., BARSACCHI, G. & HARRIS, W. A. 2003. Specification of the vertebrate eye by a network of eye field transcription factors. *Development,* 130, 5155-67.

ZUBER, M. E., HARRIS, W. A. 2006. *Formation of the eye field. In: Serangor et al. (2006) Retinal Development.*

Appendices

Appendix I.

A) Ten embryonic days of this study and their correspondent recorded H & H staging

Embryonic day (E)*	4	5	6	7	8	9	10	12	14	16
Hours	96	120	144	168	192	216	240	288	336	384
H & H stage*	19-22	23-26	27-28	30-32	33-34	35	36	37-38	40-41	42-43**

* Embryos were staged upon dissection according to Hamburger and Hamilton (1992)

** Stage 46 is for the newly hatched chick.

B) Number of whole neural retinal tissue per each sample pool according to embryonic days

Embryonic day	4	5	6	7	8	9	10	12	14	16
Number of retinae	12-14	10	6	6	4	4	4	4	3	3

Appendix II.

Buffers and solutions used in this work

Procedure	Name of Buffer/ Solution	Components [Reference]	Remarks
Sample preparation	**Phosphate buffer saline (PBS), 1X**	8 g NaCl 0.2 g of KCl 1.44 g of Na_2HPO_4 0.24 g of KH_2PO_4 400 mL dH_2O, pH 7.4 Make up to 1 L	Dissection and microdissection media
	Tyrode's solution	8 g NaCl, 0.2 g KCl, 0.2 g $CaCl_2$, 0.1 g $MgCl_2$, 0.05 g NaH_2PO_4, 1 g $NaHCO_3$, 1 g Glucose, pH 6.5	
PCR	**1 and 2% agarose gel**	1 or 2% agarose gel in TBE buffer	Volume vary depending on electrophoresis system size.
Western blot (WB)	**12% Resolving gel**	5 mL buffer A 4 mL 30% polyacrylamide solution 1 mL H2O 60 µL 10% APS 20 µL TEMED	Buffer A: 45.5 g Tris base 400 mL dH_2O pH 8.8 10 mL 10% SDS Make up to 500 mL
		3.7 mL buffer B 1.5 mL 30%	Buffer B: 15.2 g Tris base

	5% Stacking gel	polyacrylamide solution 2.25 mL H2O 50 µL 10% APS 20 µL TEMED	400 mL dH_2O, pH 6.8 10 mL10% SDS Make up to 500 mL
	Laemmli loading buffer, 3X	1.88 mL Tris HCl, 1 M 3 mL glycerol 2.5 mL10% SDS 0.005% bromophenol blue 750 µL β-mercaptoethanol	
	Tris- buffer saline (PBS), 1X	27.4 mL 5M NaCl 2 .55 mL 2M KCl 25 mL 1M Tris-HCl pH7.5 Make up to 1 L with dH_2O	
	TBST, 1X	1X TBS 1% Tween20	
Immunohistochemistry (IHC)	**4% para-formaldehyde (PFA), 50 mL**	2 g PFA 0.5 mL 1M NaOH 49.5 mL 1X PBS pH 7.2 – 7.4	Fixative
	PBS-Triton (0.05%), 1L	995 mL 1X PBS 5 mL 10% Triton	Washing solution

	5% goat serum, 50 mL	2.5 mL goat serum 47.5 mL PBS-Tr 50 µL 10% sodium azide	Blocking solution
	1% goat serum, 20 mL	0.2 mL goat serum 19.8 mL PBS-Tr 20 µL 10% sodium azide	For the primary antibody dilution
H&E staining	**Scott's water**	2 g $NaHCO_3$ 20 g $MgSO_4$ 1 L tap water	Bluing agent for Hematoxylin stain
	2 X Eosin	5 g Eosin 2.5 mL acetic acid 500 mL 70% EtOH	Eosin satin

Appendix III.

A) Conventional semi-quantitative PCR conditions

	Semi-quantitative PCR	RT-qPCR
1	94° C 3 min	50° C 2 min
2	94° C 30 sec	95° C 10 min
3	(Annealing temp.)* 1 min	95° C 15 sec for 46 cycles
4	72° C 40 sec Go to 2. (for a number of cycles)*	60° C 1 min
5	72° C 10 min	-

* Specific conditions are gene specific and can be found in table 2.1.

B) Real-time quantitative PCR (RT-qPCR) conditions

	Semi-quantitative PCR	RT-qPCR
1	94° C 3 min	50° C 2 min
2	94° C 30 sec	95° C 10 min
3	(Annealing temp.)* 1 min	95° C 15 sec for 46 cycles
4	72° C 40 sec Go to 2. (for a number of cycles)*	60° C 1 min
5	72° C 10 min	-

Appendix IV.

Two-protein alignment BLAST analysis results for chicken (*Gallus gallus*) and other species for choice of primary antibodies.

IV.I β-actin

Chicken: actin, cytoplasmic 1 [*Gallus gallus*] NP_990849.1

and **human**: actin, cytoplasmic 1 [*Homo sapiens*] NP_001092.1

RID	U4Y74YA7114 (Expires on 07-13 22:25 pm)		
Query ID	gi|45382927|ref|NP_990849.1|	**Subject ID**	gi|45018851|ref|NP_001092.1|
Description	actin, cytoplasmic 1 [Gallus gallus]	**Description**	actin, cytoplasmic 1 [Homo sapiens]
Molecule type	amino acid	**Molecule type**	amino acid
Query Length	375	**Subject Length**	375
		Program	BLASTP 2.2.32+ ▷ Citation

Range 1: 1 to 375 GenPept Graphics ▼ Next Match ▲ Previous Match

Score	Expect	Method	Identities	Positives	Gaps
785 bits(2028)	0.0	Compositional matrix adjust.	375/375(100%)	375/375(100%)	0/375(0%)

```
Query  1    MDDDIAALVVDNGSGMCKAGFAGDDAPRAVFPSIVGRPRHQGVMVGMGQKDSYVGDEAQS  60
            MDDDIAALVVDNGSGMCKAGFAGDDAPRAVFPSIVGRPRHQGVMVGMGQKDSYVGDEAQS
Sbjct  1    MDDDIAALVVDNGSGMCKAGFAGDDAPRAVFPSIVGRPRHQGVMVGMGQKDSYVGDEAQS  60

Query  61   KRGILTLKYPIEHGIVTNWDDMEKIWHHTFYNELRVAPEEHPVLLTEAPLNPKANREKMT  120
            KRGILTLKYPIEHGIVTNWDDMEKIWHHTFYNELRVAPEEHPVLLTEAPLNPKANREKMT
Sbjct  61   KRGILTLKYPIEHGIVTNWDDMEKIWHHTFYNELRVAPEEHPVLLTEAPLNPKANREKMT  120

Query  121  QIMFETFNTPAMYVAIQAVLSLYASGRTTGIVMDSGDGVTHTVPIYEGYALPHAILRLDL  180
            QIMFETFNTPAMYVAIQAVLSLYASGRTTGIVMDSGDGVTHTVPIYEGYALPHAILRLDL
Sbjct  121  QIMFETFNTPAMYVAIQAVLSLYASGRTTGIVMDSGDGVTHTVPIYEGYALPHAILRLDL  180

Query  181  AGRDLTDYLMKILTERGYSFTTTAEREIVRDIKEKLCYVALDFEQEMATAASSSSLEKSY  240
            AGRDLTDYLMKILTERGYSFTTTAEREIVRDIKEKLCYVALDFEQEMATAASSSSLEKSY
Sbjct  181  AGRDLTDYLMKILTERGYSFTTTAEREIVRDIKEKLCYVALDFEQEMATAASSSSLEKSY  240

Query  241  ELPDGQVITIGNERFRCPEALFQPSFLGMESCGIHETTFNSIMKCDVDIRKDLYANTVLS  300
            ELPDGQVITIGNERFRCPEALFQPSFLGMESCGIHETTFNSIMKCDVDIRKDLYANTVLS
Sbjct  241  ELPDGQVITIGNERFRCPEALFQPSFLGMESCGIHETTFNSIMKCDVDIRKDLYANTVLS  300

Query  301  GGTTMYPGIADRMQKEITALAPSTMKIKIIAPPERKYSVWIGGSILASLSTFQQMWISKQ  360
            GGTTMYPGIADRMQKEITALAPSTMKIKIIAPPERKYSVWIGGSILASLSTFQQMWISKQ
Sbjct  301  GGTTMYPGIADRMQKEITALAPSTMKIKIIAPPERKYSVWIGGSILASLSTFQQMWISKQ  360

Query  361  EYDESGPSIVHRKCF  375
            EYDESGPSIVHRKCF
Sbjct  361  EYDESGPSIVHRKCF  375
```

IV.II XIAP

Chicken: baculoviral IAP repeat-containing protein 4 [*Gallus gallus*] NP_989919.1 and **rat**: E3 ubiquitin-protein ligase XIAP [*Rattus norvegicus*] (Norway rat) NP_071567.1

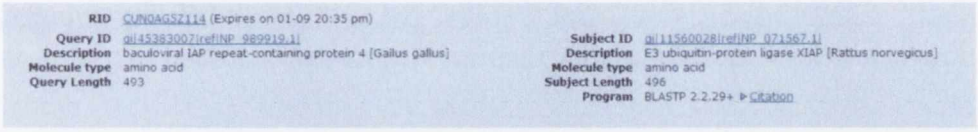

RID CUN0AGSZ114 (Expires on 01-09 20:35 pm)
Query ID gi|45383007|ref|NP_989919.1|
Description baculoviral IAP repeat-containing protein 4 [Gallus gallus]
Molecule type amino acid
Query Length 493

Subject ID gi|11560028|ref|NP_071567.1|
Description E3 ubiquitin-protein ligase XIAP [Rattus norvegicus]
Molecule type amino acid
Subject Length 496
Program BLASTP 2.2.29+ ▶ Citation

Range 1: 1 to 495 GenPept Graphics ▼ Next Match ▲ Previous Match

Score	Expect	Method	Identities	Positives	Gaps
607 bits(1564)	0.0	Compositional matrix adjust.	290/499(58%)	365/499(73%)	11/499(2%)

```
Query  1    MTCNGPDSSESGATPAIDGDQEWTQEHYRLGIFVEFPHDCPVSASALARAGFVYTGEGDK  60
            MT N  + S +      T+ D+E+ +E  RL TF  FP    PVSAS LARAGF+YTGEGD
Sbjct  1    MTFNSFEGSRTVVPADINKDEEFVEEFNRLKTFANFPSSSPVSASTLARAGFLYTGEGDT  60

Query  61   VKCFSCHVTVEGWEPGDSAIDRHKNLSPDCRFITGSAF---LENNVHPLVQSHQHRTENG  117
            V+CFSCH  V+ W+ GDSA+ RH+ +SP+CRFI G  F       +   P +Q+ Q+++EN
Sbjct  61   VQCFSCHAAVDRWQYGDSAVGRHRRISPNCRFINGFYFENGAIQSTSPGIQNGQYKSENC  120

Query  118  SSNLALPSALEDLSDVEADYLLRTRQVVDMSDTLYPKNPAMCSEEARLKSFHNWPPYGLL  177
              N     AL+  S+  ADYLLRT QVVD+SDT+YP+NPAMCSEEARLK+F NWP Y  L
Sbjct  121  VGNRN-HFALDRPSETHADYLLRTGQVVDISDTIYPRNPAMCSEEARLKTFQNWPDYAHL  179

Query  178  TPKELASAGLYYTGVGDQVACFCCGGKLKNWEPGDRAWSEHKRHFPKCFFVLGRDVGNVS  237
            +P+ELASAGLYYTG+ DQV CFCCGGKLKNWEP  RAWSEH+RHFP CFFVLGR+V   S
Sbjct  180  SPRELASAGLYYTGIDDQVQCFCCGGKLKNWEPCDRAWSEHRRHFPNCFFVLGRNVNVRS  239

Query  238  TDSICAELGRSCLNNEQHPRNPSMAEYERRIQTFLAWIYPVNKEHLAEAGFYSTGNGDHV  297
               + ++  R+  N+   PRNP+MAEY+ RI TF  W+Y VNKE LA AGFY+ G GD V
Sbjct  240  ESGVSSD--RNFPNSINSPRNPAMAEYDARIVTFGTWLYSVNKEQLARAGFYALGEGDKV  297

Query  298  VCFHCGGGLQEWKENEDPWDQHAKWFPGCKFLRDEKGLEFINNVHLRDGCRDSTIEAAE-  356
             CFHCGGGL +WK +EDPW+QHAKW+PGCK+L DEKG E+INN+HL     +S +  AE
Sbjct  298  KCFHCGGGLIDWKPSEDPWEQHAKWYPGCKYLLDEKGQEYINNIHLTHSLGESVVRIAEK  357

Query  357  ---VTILPKDDLLQNQLVQNAIHMGFSLSEIRSIMEKKLHLSGESYTSVEDLVADLISAQ  413
               VT    D + QN +VQ AI MGF+  +I+  ME+KL  SG +Y S+E L+ADL+SAQ
Sbjct  358  TPSVTKKIDDTIFQNPMVQEAIRMGFNFKDIKKTMEEKLQTSGSNYLSLEVLIADLVSAQ  417

Query  414  KENIKGEPPKESPLEQDLSIEEKLRRLQEEKLCKICMAKDISVVLIPCGHLVACKECAEA  473
            K+N + E   + S L++D+S EE+LRRLQEEKLCKICM ++I++V +PCGHLV CK+CAEA
Sbjct  418  KDNSQDESSQTS-LQKDISTEEQLRRLQEEKLCKICMDRNIAIVFVPCGHLVTCKQCAEA  476

Query  474  VNKCPLCCTNIIKRQKIFM  492
            V+KCP+CCT I  +QKIFM
Sbjct  477  VDKCPMCCTVIIFKQKIFM  495
```

IV.III Survivin

Chicken: BIRC5 baculoviral IAP repeat containing 5 [*Gallus gallus*] NP_001012318.1

and **human** : BIRC5 baculoviral IAP repeat containing 5 [*Homo sapiens*] NP_001159.2

Range 1: 3 to 139 GenPept Graphics

Score	Expect	Method	Identities	Positives	Gaps
186 bits(471)	3e-65	Compositional matrix adjust.	83/137(61%)	103/137(75%)	0/137(0%)

```
Query  5    AEMLPKEWLVYLVSTRAATFRNWPFTEGCACTPERMAAAGFVHCPSENSPDVVQCFFCLK  64
            A  LP  W  +L   R +TF+NWPF EGCACTPERMA AGF+HCP+EN PD+ QCFFC K
Sbjct  3    APTLPPAWQPFLKDHRISTFKNWPFLEGCACTPERMAEAGFIHCPTENEPDLAQCFFCFK  62

Query  65   ELEGWEPDDDPLEEHKKHSAGCAFAALQKDPSNLTVQEFLKLDKKRTKNVIKKAISQKET  124
            ELEGWEPDDDP+EEHKKHS+GCAF +++K    LT+ EFLKLD++R KN I K  + K+
Sbjct  63   ELEGWEPDDDPIEEHKKHSSGCAFLSVKKQFEELTLGEFLKLDRERAKNKIAKETNNKKK  122

Query  125  DIEDVAKGVRHAIENMG  141
            + E+ A+ VR AIE +
Sbjct  123  EFEETAEKVRRAIEQLA  139
```

V.IV Casp-3

Chicken: CASP3 caspase 3, apoptosis-related cysteine peptidase [*Gallus gallus*] NP_990056.1

Rat: Casp3 caspase 3 [*Rattus norvegicus*] NP_037054.1

Range 1: 3 to 275 GenPept Graphics

Score	Expect	Method	Identities	Positives	Gaps
386 bits(992)	2e-139	Compositional matrix adjust.	184/273(67%)	222/273(81%)	2/273(0%)

```
Query  11   SGEDVSDARSFPGSKGMNLPASKSVDSGILPDDSYRMDYPEIGVCVIINNKNFHRDIGLS  70
            + E   D++S    +   +  SKS+DSGI  D SY+MDYPE+G+C+IINNKNFH+ TG+S
Sbjct  3    NNETSVDSKSINNFETKTIHGSKSMDSGIYLDSSYKMDYPEMGLCIIINNKNFHKSTGMS  62

Query  71   SRSGTDADAASVREVFMKLGYKVKLNNDLSSRDIFKLLKNVSEEDHSKRSSFVCVLLSHG  130
            +R+GTD DAA++RE FM L Y+V+  NDL+  +I +L+ +VS+EDHSKRSSFVCV+LSHG
Sbjct  63   ARNGTDVDAANLRETFMALKYEVRNKNDLTREEIMELMDSVSKEDHSKRSSFVCVILSHG  122

Query  131  DEGLFYGIDGPLELKVLTSLFRGDKCRSLAGKPKLFFIQACRGTELDSGIEADSGPDETV  190
            DEG+ +GI+GP++LK LTS FRGD CRSL GKPKLF IQACRGTELD GIE DSG D+ +
Sbjct  123  DEGVIFGINGPVDLKKLTSFFRGDYCRSLTGKPKLFIIQACRGTELDCGIETDSGIDDDM  182

Query  191  -CQKIPVEADFLYAYSTAPGYYSWRNAAEGSWFIQSLCRMLKEHARKLELMQILTRVNRR  249
             CQKIPVEADFLYAYSTAPGYYSWRN+ +GSWFIQSLC MLK +A KLE M ILTRVNR+
Sbjct  183  ACQKIPVEADFLYAYSTAPGYYSWRNSRDGSWFIQSLCAMLKLYAHKLEFMHILTRVNRK  242

Query  250  VA-EYESCSTRQDFNAKKQIPCIVSMLTKEFYF  281
            VA E+ES S    F+AKKQIPCIVSMLTKE YF
Sbjct  243  VAIEFESFSLDATFHAKKQIPCIVSMLTKELYF  275
```

IV.V Casp-7

Chicken: CASP7 caspase 7, apoptosis-related cysteine peptidase [*Gallus gallus*]

XP_421764.3

Mouse: Casp7 caspase 7 [*Mus musculus*] (house mouse) NP_031637.1

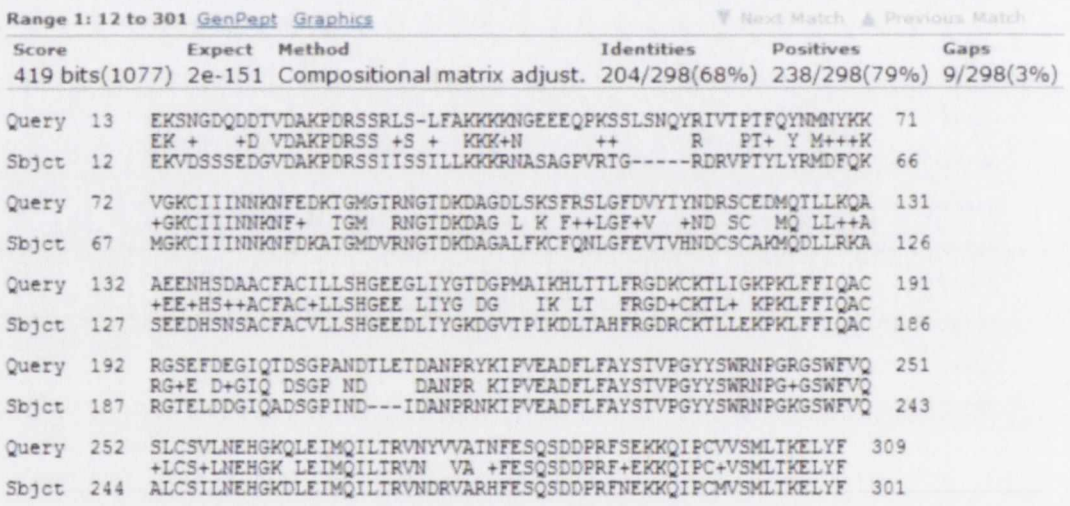

Range 1: 12 to 301 GenPept Graphics

Score	Expect	Method	Identities	Positives	Gaps
419 bits(1077)	2e-151	Compositional matrix adjust.	204/298(68%)	238/298(79%)	9/298(3%)

```
Query  13   EKSNGDQDDTVDAKPDRSSRLS-LFAKKKKKNGEEEQPKSSLSNQYRIVTPTFQYNMNYKK  71
            EK +    +D VDAKPDRSS +S +  KKK+N      ++       R   PT+ Y M+++K
Sbjct  12   EKVDSSSEDGVDAKPDRSSIISSILLKKKRNASAGPVRIG-----RDRVPTYLYRMDFQK  66

Query  72   VGKCIIINNKNFEDKTGMGTRNGIDKDAGDLSKSFRSLGFDVYTYNDRSCEDMQTLLKQA  131
            +GKCIIINNKNF+  TGM  RNGIDKDAG L K F++LGF+V  +ND SC  MQ LL++A
Sbjct  67   MGKCIIINNKNFDKATGMDVRNGIDKDAGALFKCFQNLGFEVTVHNDCSCAKMQDLLRKA  126

Query  132  AEENHSDAACFACILLSHGEEGLIYGTDGPMAIKHLTTLFRGDKCKTLIGKPKLFFIQAC  191
            +EE+HS++ACFAC+LLSHGEE LIYG DG   IK LT  FRGD+CKTL+ KPKLFFIQAC
Sbjct  127  SEEDHSNSACFACVLLSHGEEDLIYGKDGVTPIKDLTAHFRGDRCKTLLEKPKLFFIQAC  186

Query  192  RGSEFDEGIQTDSGPANDTLETDANPRYKIPVEADFLFAYSTVPGYYSWRNPGRGSWFVQ  251
            RG+E D+GIQ DSGP ND    DANPR KIPVEADFLFAYSTVPGYYSWRNPG+GSWFVQ
Sbjct  187  RGTELDDGIQADSGPIND---IDANPRNKIPVEADFLFAYSTVPGYYSWRNPGKGSWFVQ  243

Query  252  SLCSVLNEHGKQLEIMQILTRVNYVVATNFESQSDDPRFSEKKQIPCVVSMLTKELYF  309
            +LCS+LNEHGK LEIMQILTRVN  VA +FESQSDDPRF+EKKQIPC+VSMLTKELYF
Sbjct  244  ALCSILNEHGKDLEIMQILTRVNDRVARHFESQSDDPRFNEKKQIPCMVSMLTKELYF  301
```